PHYSIOLOGICAL AND SYNOPTIC-SCALE INFLUENCES ON DIURNAL HUMIDITY VARIATIONS OVER VEGETATION

by

J.C. CURRAN

Presented as a Thesis for the Degree of

Doctor of Philosophy to

the University of Edinburgh

October, 1975.

Of this fair volume which we World do name
If we the sheets and leaves could turn with care,
Of Him who it corrects, and did it frame,
We clear might read the art and wisdom rare:

But silly we, like foolish children, rest
Well pleased with colour'd vellum, leaves of gold,
Fair dangling ribbands, leaving what is best,
On the great Writer's sense ne'er taking hold;

Or if by chance we stay our minds on aught
It is some picture on the margin wrought.

W. DRUMMOND (1585-1649)

ACKNOWLEDGEMENTS

I wish to record my gratitude to:

the Head of the Meteorology Department, Dr. D.H. McIntosh, for his general guidance and pertinent advice;

my supervisor, Dr. A.S. Thom, for his patience, assistance, constructive criticism and, latterly, for his detailed corrections and ameliorations;

Dr. K.J. Weston, Dr. A.W. Daly, Dr. C.N. Duncan and Mr. J.A. Blair-Fish who all have given freely of their time and solicitude;

the Institute of Hydrology and, in particular, the staff of the Hydrometeorological Section who offered hospitality, useful discussion and data;

Mrs. R.W. Chester for her fast and accurate typing;

the U.K. Natural Environment Research Council for a studentship which financed this thesis.

DECLARATION

The thesis entitled "Physiological and synoptic-scale influences on diurnal humidity variations over vegetation" is the original work of and is composed by the undersigned.

James C. Curran, 31st October 1975

INDEX (Contd.)

INDEX (Contd.)

LIST OF SYMBOLS AND SUBSCRIPTS

Several symbols have been assigned more than one meaning so as to afford consistency between this thesis and other published works. The appropriate meaning must be chosen according to the context.

Symbols

a	convenient abbreviation for $(\Omega/2K_m)^{\frac{1}{2}}$
A	entrainment coefficient for a well-mixed atmosphere; $-H_h(t)/H_o(t)$
A'	entrainment coefficient for a poorly mixed atmosphere; $-H_h(t)/H_o((1-\psi)t - \phi)$
c	constant of proportionality; defined by Equation (5.11)
c_p	specific heat of air at constant pressure (1.01×10^3 $Jkg^{-1}K^{-1}$)
D	predictive parameter for the extent of cumulus cloud cover formation; defined by Equation (5.17)
E	water vapour flux ($kg\ m^{-2}s^{-1}$)
f(c)	an empirically derived factor which expresses the cloud-cover dependence of S(c); defined by Equations (5.4) to (5.8)
F	potential heat flux; $(\theta/T)H$
g	standard gravitational acceleration ($9.81\ ms^{-2}$)
h	height of base of inversion layer (m)
H	sensible heat flux (Wm^{-2})
k	von Kármán's constant (0.4)
K_m	eddy diffusivity of momentum (m^2s^{-1})

LIST OF SYMBOLS AND SUBSCRIPTS (Contd.)

Symbols

$\hat{K}_m$	Clarke's (1970) non-dimensional eddy diffusivity of momentum
$L_d(c)$	downward long-wave radiation flux as a function of low-cloud cover (Wm^{-2}); defined by Equation (5.2)
L_u	upward long-wave radiation flux from a black body at mean surface temperature; σT_s^4 (Wm^{-2})
m	gradient of specific humidity in boundary layer ($gkg^{-1}m^{-1}$); defined by Equation (5.11)
p	atmospheric pressure (Nm^{-2})
P	significance level of correlation
q	specific humidity (gkg^{-1})
q_s	saturation specific humidity (gkg^{-1})
r_a	aerodynamic resistance to vapour flux from forest to reference height of 20.5m (sm^{-1})
r_o	initial radius of convective bubble (m)
r_s	surface resistance of vegetative cover (sm^{-1})
R	specific gas constant for dry air (287 $Jkg^{-1}K^{-1}$)
R_n	net radiation (Wm^{-2})
s	Clarke's (1970) stability parameter
S(c)	solar radiation flux as a function of cloud cover and thickness (Wm^{-2}); expressed empirically in Equations (5.4) to (5.8)
$\overline{S}$	annual average hours per day of strong sunshine ($hr\ day^{-1}$)
sub	rate of subsidence of inversion (ms^{-1})
T	temperature (K or ^oC)
T_a	temperature at screen height (K)
T_d	dew-point temperature (^oC or ^oF)
T_s	surface temperature (K)

LIST OF SYMBOLS AND SUBSCRIPTS (Contd.)

Symbols

ε convectively produced eddy energy (Jm^{-3})

ε' rate of production of convective eddy energy (Wm^{-3}); defined by Equation (2.1)

ε_s surface emissivity

θ potential temperature (K or ^{o}C); $T(\frac{1000}{p})^{0.288}$

λ latent heat of vaporization of water ($2.47\times10^{6} Jkg^{-1}$)

ρ atmospheric density ($\rho_o \simeq 1.25\ kgm^{-3}$)

σ Stefan-Boltzmann constant ($5.67\times10^{-8}\ Wm^{-2}K^{-4}$)

ϕ lag between heat flux at the inversion and that at the ground for the initial value of the inversion height (s or hr)

ψ assumed constant rate of change with time of the total lag between the heat flux at the inversion and that at the ground, due to the assumed approximately linear change with time of the inversion height

Ω Earth's angular velocity adjusted for various lengths of day (14 hr day, $\Omega = 6.233\times10^{-5}\ rads^{-1}$; 12 hr day, $\Omega = 7.272\times10^{-5}\ rads^{-1}$; 11 hr day, $\Omega = 7.933\times10^{-5}\ rads^{-1}$; 10 hr day, $\Omega = 8.727\times10^{-5}$ rad s^{-1})

Subscripts

o denotes a value at screen height or just above a vegetative canopy

u a value just above the inversion layer

h a value just below the inversion layer

LIST OF SYMBOLS AND SUBSCRIPTS (Contd.)

Subscripts (Contd.)

x	maximum value during the day
e	denotes that the quantity originates from the entrainment process
div	denotes that the quantity results from large-scale divergence due to subsidence
MAX/MIN	with reference to diurnal changes, denotes that the change is measured between the chosen starting time and the time of absolute maximum, absolute minimum or local minimum
MAX	denotes that the change is measured between the chosen starting time and the time of absolute maximum

LIST OF PLATE AND FIGURES

LIST OF PLATE AND FIGURES (Contd.)

A transparent OVERLAY, identical to Figure (6.7), is placed in a pocket on the inside of the back cover.

LIST OF TABLES

SUMMARY

Some recent accurate data on diurnal specific humidity variations over a forest in S.E. England are related to further examples of humidity variations in the literature and their paradoxical nature is explored through a review of various diverse published explanations.

It is here suggested that, on some occasions, the unexpected drop in specific humidity during the middle of the day results from the entrainment process at a subsidence inversion. Presently accepted entrainment theory is questioned on one of its basic assumptions and an alternative theory is proposed and tested. Acceptable results having been obtained, an independent estimate is made of the value of the entrainment coefficient and the result is found to agree well with the concensus of previously obtained values.

The new theory permits the derivation of an analytical predictive equation for diurnal humidity variations over a vegetated surface under anti-cyclonic conditions. When the equation is tested against the real data from the forest in S.E. England, it is found to resolve the apparent paradox.

For use in conjunction with this predictive equation, a method is described for predicting the daily maximum net radiation. This is made possible through the formulation of a theory of cumulus cloud formation which provides a way of forecasting, from easily obtainable parameters, the extent to which such cloud will develop. The theory is tested and the results are found to be encouraging.

SUMMARY (Contd.)

Subsequently, entrainment theory is extended, on an annual average basis, to both cyclonic and anti-cyclonic conditions and, thereby, annual average diurnal changes of temperature and humidity are related to annual average Bowen ratio by eliminating the effect of deep mixing in the lower troposphere. Mean Bowen ratios throughout Europe are thereby derived; a map is constructed; and the values related to various physiographical influences.

In conclusion, a number of suggestions are made for further investigation and experimentation in order to verify several controversial postulates which are fundamental to much of this thesis.

CHAPTER 1

INTRODUCTION

Studies of the atmospheric planetary boundary layer are assuming increasing importance, not only because it is the part of the atmosphere within which all plants and animals exist and with which they interact, but also because the dynamics of the whole atmospheric system is closely coupled to the heat, water vapour and momentum fluxes passing through this layer.

The present work discusses the development of the boundary layer and its interaction with vegetation through consideration of temporal changes in specific humidity. This particular quantity is employed since it acts as a useful tracer and is also a fundamental influence on the rate of evaporation from natural surfaces and hence, in itself, is an important parameter in hydrological studies.

Under conditions of positive net radiation a vegetative cover acts as a source of latent heat as well as of sensible heat. The sensible heat flux (occasionally aided by radiative flux convergence) raises the temperature of the atmospheric boundary layer and, like-wise, it might be expected that the latent heat flux would increase the specific humidity of the boundary layer even though the vegetation exerts a physiological control over the rate of evaporation and, thereby, over the size of the increase. On any particular day, of course, synoptic-scale advection may mask these effects.

The work of this thesis initially was prompted by the observation of the apparent paradox that, on an unexpectedly

large number of occasions over Thetford Forest in Norfolk, the specific humidity passed through an absolute or local minimum at some time during daylight hours, whereas, predictably, the temperature rose to a maximum usually at some time in mid-afternoon.

1.1 Data from Thetford Forest

Thetford Forest extends to an area of over 70 square kilometres of level countryside and is planted, at a density of 800 trees per hectare, with Scots and Corsican pine. Near the centre of the forest the Institute of Hydrology operates a meteorological and biological experiment to investigate in detail the local water-cycle. A major part of the experimental equipment comprises two instrumented towers and a computerised data storage system.

Sensitive wind, temperature and humidity sensors are positioned at eleven levels within and above the forest canopy which is now at an average height of 17m. Plate (1) shows one instrument tower with aspirated temperature and humidity sensors mounted at heights of 12.8m, 16.8m, 18.1m, 19.7m, 22.1m, 25.4m and 30.2m; additionally a radiation sensor is placed at 20.5m. Since the towers are at a distance of at least 1½ km from any discontinuity in the forest cover then, according to Pasquill (1972), profiles of temperature, specific humidity and wind speed for heights of up to 15m above the trees will be free from distortion due to advection from surrounding regions with different land use and different surface roughness.

The very accurate temperature and humidity data from forty days in 1972 herein presented are obtained from

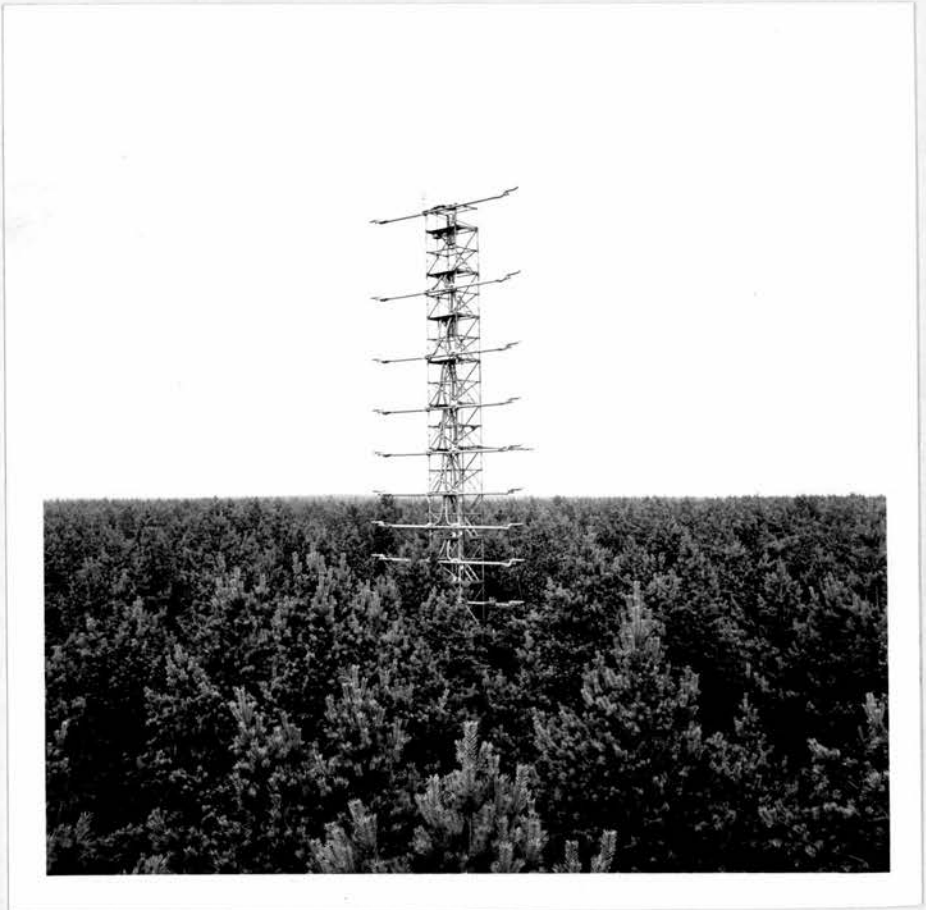

Plate (1) Instrument tower in Thetford Forest

(photograph by courtesy of the Institute of Hydrology).

twenty-minute averages of these parameters subsequently averaged over the top four levels on the upwind side of the instrument tower. The flux data are computed from the profiles, again as twenty-minute averages, using the Bowen ratio method as described by Rider and Robinson (1951). Temperature measurements are probably accurate to $\pm$ 0.01°C, specific humidity measurements to $\pm$ 0.005 gkg^{-1} but the fluxes themselves to no better than $\pm$ 25°/o on average.

Of the forty days, all show a maximum of temperature which occurs between 10.50 and 16.30 GMT, the average time of maximum temperature being 13.55 GMT with a standard deviation of $\pm$ 1.7 hr. On the other hand, only eight of the forty days exhibit a straightforward maximum of specific humidity, the remaining thirty-two exhibiting either an absolute or a local minimum of specific humidity at some time during the day. The times of occurrence of these minima and maxima lie between 9.50 and 18.10 GMT with a mean value of 13.25 GMT and standard deviation of $\pm$ 2.1 hr. So, in contrast to temperature, specific humidity appears to behave unpredictably not only in its diurnal trend but also in the time at which it passes through a turning point.

As expected, the diurnal increase in temperature is found to be quite closely related to the sensible heat flux from the forest canopy. Figure (1.1) illustrates that, in general, the greater the integrated sensible heat flux (between the time when the available energy of the forest canopy becomes positive and the time of maximum temperature) then the greater is the corresponding change in temperature. (Available energy is defined by Stewart and Thom (1973) as net radiation minus the sum of various loss terms, the most

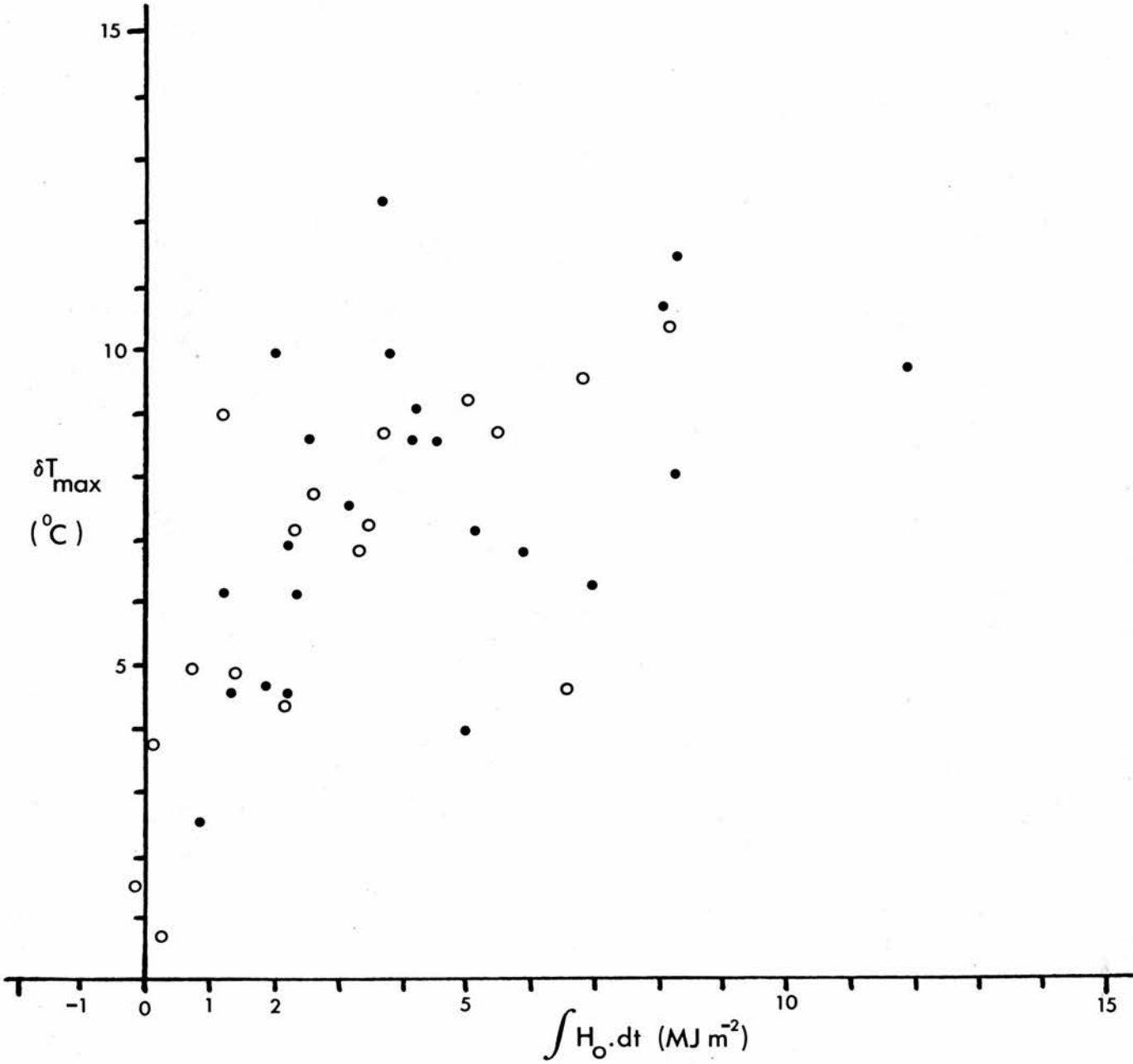

Figure (1.1) Change in temperature versus integrated sensible heat flux, where both are for period between time when available energy = 0 and time when temperature is at maximum.

o strong advection possible

• strong advection unlikely

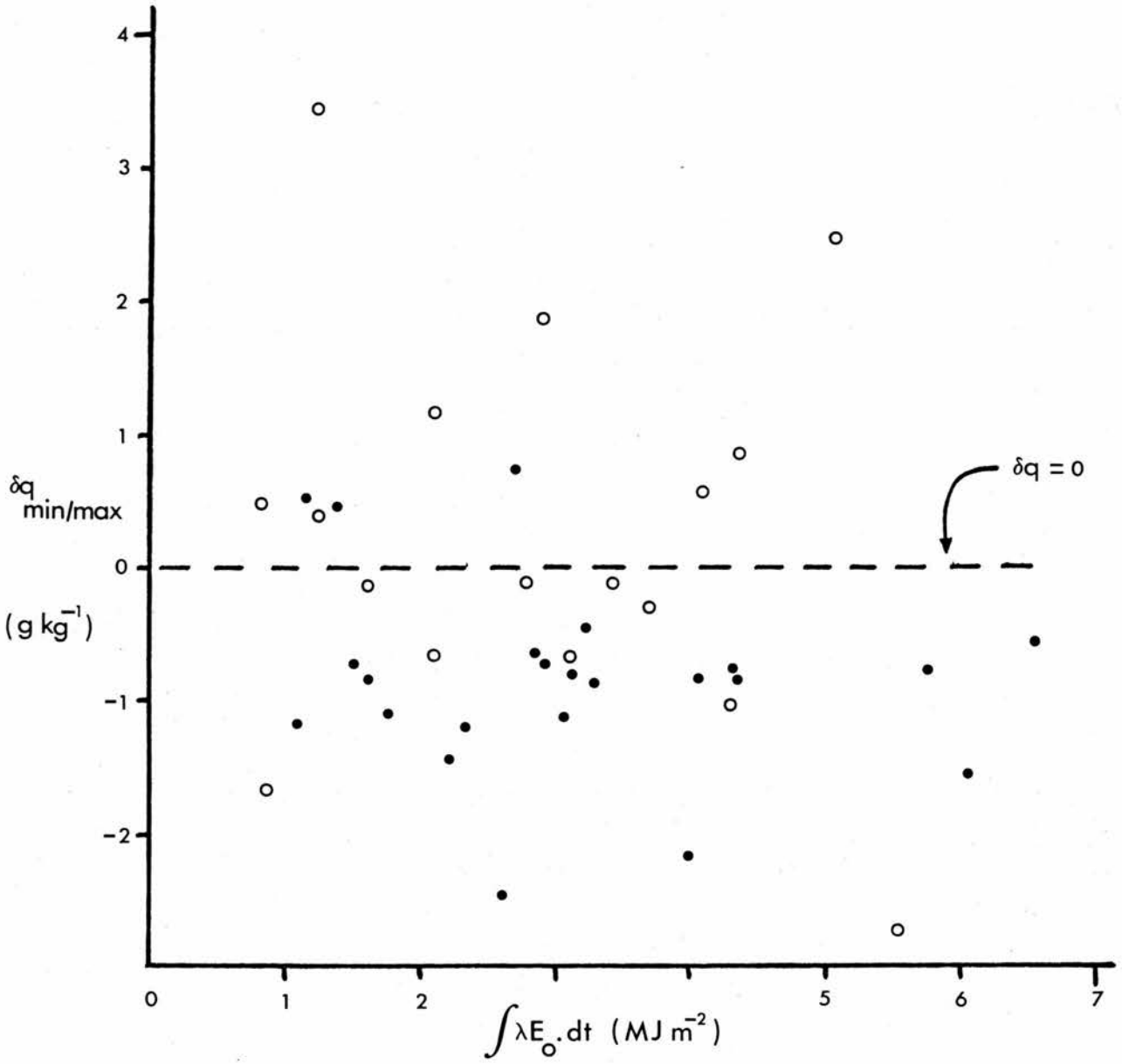

Figure (1.2) Change in specific humidity versus integrated latent heat flux, where both are for period between time when available energy = 0 and time when specific humidity is at absolute minimum, local minimum or absolute maximum.

o strong advection possible

• strong advection unlikely

significant of which are the fluxes of energy into the ground and into storage in the vegetative cover).

In contrast, a similar graph for specific humidity, Figure (1.2), reveals no such distinct trend. The change in specific humidity between the time when available energy is zero and the time of occurrence of absolute maximum, absolute minimum or local minimum of specific humidity appears to bear no relation whatsoever to the latent heat flux from the forest integrated over the same period.

No relationship is evident even when an attempt is made to exclude those days during which advection may have played a major rôle. On the graphs, two plotting symbols are used to distinguish between those days which, according to the Daily Weather Reports of the U.K. Meteorological Office, have the slightest possibility of producing any frontal activity at Thetford Forest and those days which are comparatively advection-free. In the advection-free situations, diurnal temperature change remains closely related to the integrated sensible heat flux, as expected, but the specific humidity change remains unrelated to the integrated latent heat flux.

The same results are found when considering the changes in temperature and specific humidity between the time when the available energy is zero and a chosen standard time of 13.30 GMT. For this case, of the forty days, only one exhibits a small decrease in temperature whereas twenty-seven show a decrease in specific humidity. Figure (1.3) illustrates that, with or without major synoptic advection, the changes in these two parameters appear to be entirely unrelated.

Finally, in Figure (1.4), the inverse of the ratio

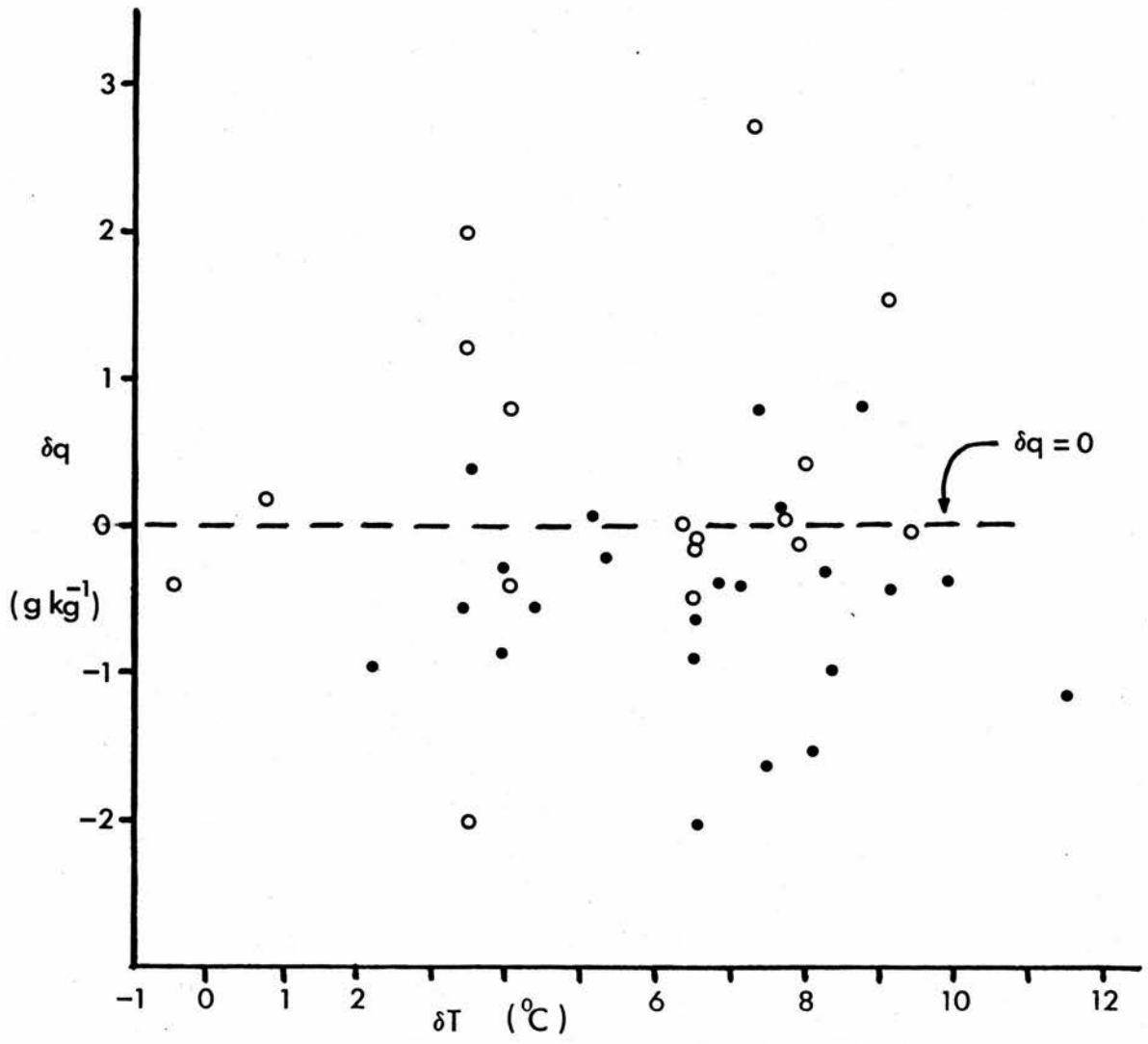

Figure (1.3) Change in specific humidity versus change in temperature, both for period between time when available energy = 0 and time of 13.30 GMT.

o strong advection possible

• strong advection unlikely.

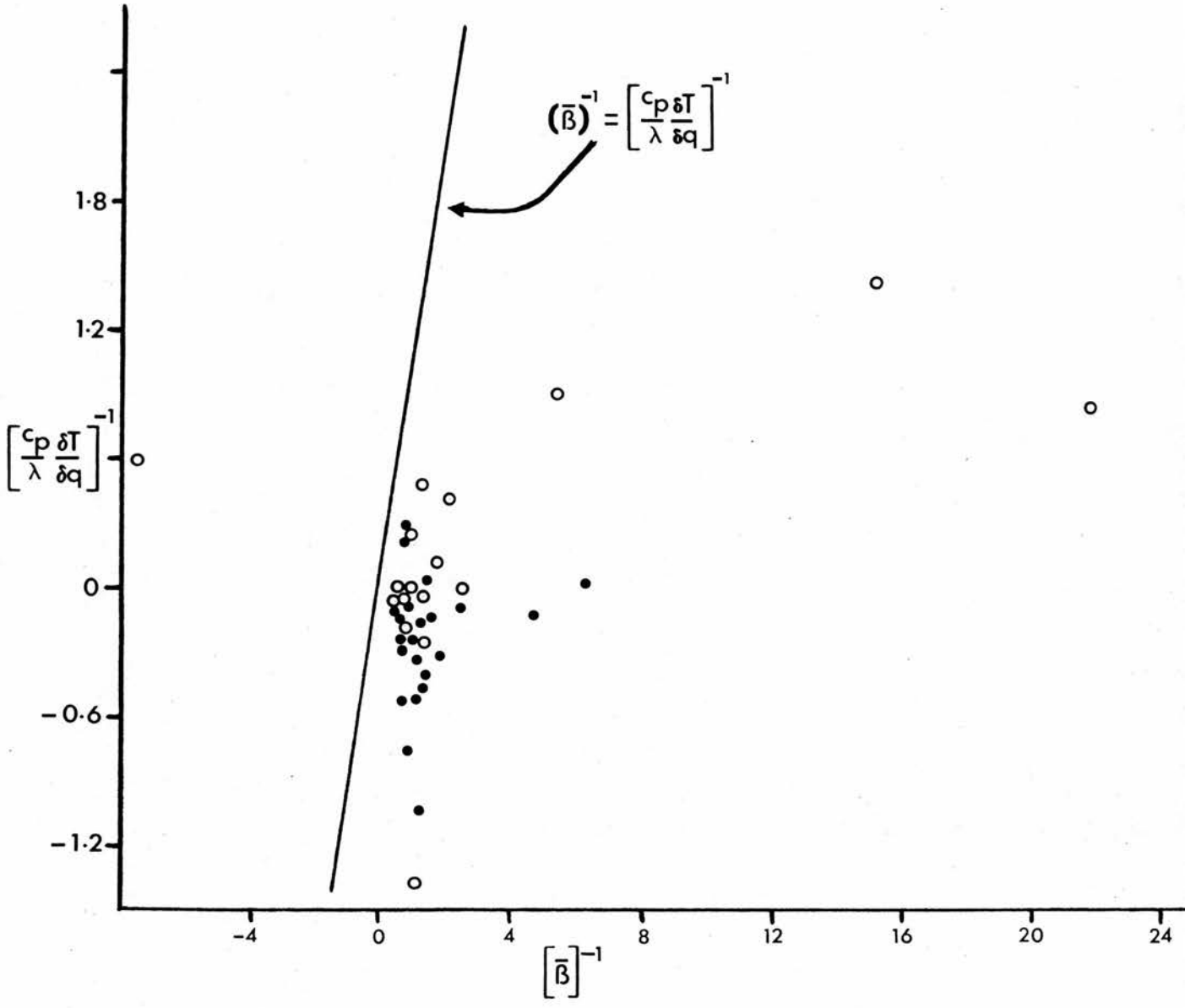

Figure (1.4) Inverse of mean Bowen ratio versus inverse of $(\frac{c_p}{\lambda}\frac{\delta T}{\delta q})$, both for period between time when available energy = 0 and time of 13.30 GMT.

o strong advection possible

• strong advection unlikely.

$\frac{c_p}{\lambda} \cdot \frac{\delta T}{\delta q}$ is plotted against the inverse of the mean Bowen ratio ($\bar{\beta}$) for the period up to 13.30 GMT (the inverses are used merely for convenience); the mean Bowen ratio is calculated from twenty-minute average values determined throughout the day from the profiles of temperature and humidity. (See List of Symbols for definitions.) If β has a constant value during the day then, for a closed, well-mixed forest/atmosphere system, the value of $\frac{c_p}{\lambda} \cdot \frac{\delta T}{\delta q}$ would be expected to be identical to that value. However, it is clear not only that there is no equality between the two parameters but also that there seems to be little consistent inter-dependence. All the points lie to the right of the line $(\bar{\beta})^{-1} = (\frac{c_p}{\lambda} \cdot \frac{\delta T}{\delta q})^{-1}$ which implies, for a given Bowen ratio, either that the diurnal change in temperature is consistently too great or that the diurnal change in specific humidity is consistently too small.

In summary, the temperature over Thetford Forest is well-behaved, attaining, in early afternoon, a maximum value which is dependent upon the magnitude of the sensible heat flux from the forest to the atmospheric boundary layer. However, the specific humidity above the forest appears to behave in a way entirely independent of the latent heat flux from the forest. More often than not the specific humidity actually drops to a greater or lesser extent at some time during the daylight period.

1.2 Data from other sources

This apparently paradoxical behaviour is not a newly observed phenomenon. Tunnell (1958) investigated the diurnal change in vapour pressure using world climatological data. He discovered that early (i.e. mid-morning) maxima of vapour pressure (implying a subsequent decrease during the middle part of the day) are common in continental (extra-tropical) and desert climates. This is in contrast to the equatorial continental climate type where, throughout the year, the vapour pressure has a minimum value at about 4.00h and a maximum value at about 16.00h. This latter behaviour is in the expected sense for a well-mixed, advection-free, vegetation/atmosphere system and it is departures from this behaviour, as exemplified by the continental (extra-tropical) climates, that must be explained in the first instance.

Tunnell (1958) regards the anomalous behaviour as the result of a four stage process;

1) a rise of vapour pressure after sunrise when dew and, later, soil moisture are evaporated,
2) a fall towards mid-day, due to either excessive vertical transport of moisture by convection or to a fall in available soil moisture,
3) a rise towards sunset associated with the decrease of convection,
4) a slow decrease of vapour pressure towards sunrise caused by the downward transport and deposition of moisture, associated with the nocturnal cooling of the lower layers of the atmosphere.

Best et al. (1952) make use of the same arguments to explain the observed diurnal variations from 879 days of accurate data from S. England. For all days a minimum of absolute humidity is discovered near dawn, whereafter it rises to a maximum at about 12.00h for clear or overcast days in winter although very much earlier, at 7.00h or 8.00h, for clear or overcast days in summer. After this early maximum in summer, the absolute humidity steadily decreases until sunset on clear days but, for overcast days, falls to a minimum at 11.00h and then rises to another and greater maximum at 17.00h. To explain this behaviour the above arguments are supplemented by proposing that in the mid-day period the maximum in ground-source vapour flux more than compensates for the loss of atmospheric water vapour due to increased turbulence and so the vapour pressure rises. Any secondary maxima later in the day are assumed to be due to vapour diffusing downwards from a humidity inversion above as condensation takes place at the ground.

Local minima of vapour pressure are also distinguishable in the climatological data published, for example in the "Climatological Atlas of the British Isles", compiled by the U.K. Meteorological Office (H.M.S.O.). Kew recordings reveal distinct mid-part of the day local minima or flattenings of vapour pressure for four of the six months presented and also for the annual average. Aberdeen exhibits the same behaviour to a lesser degree whereas Eskdalemuir and Valentia show a diurnal variation which, in shape, is more similar to that found in regions of equatorial continental climate and needs no explanation here. Figure (1.5) compares diurnal variations

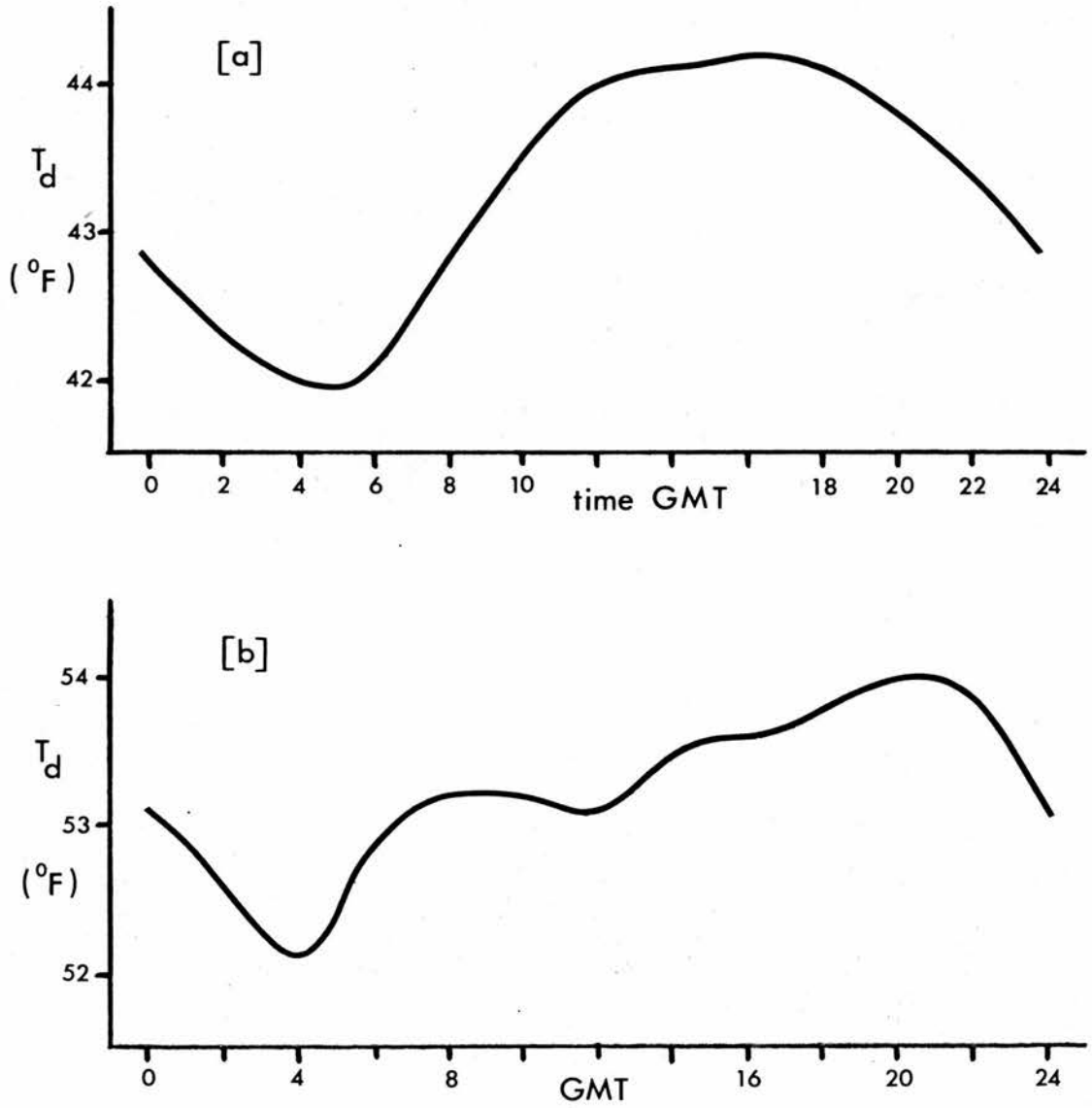

Figure (1.5) Diurnal variation of dew point at Kew; (a) annual average, (b) July average (Data from Bilham (1938)).

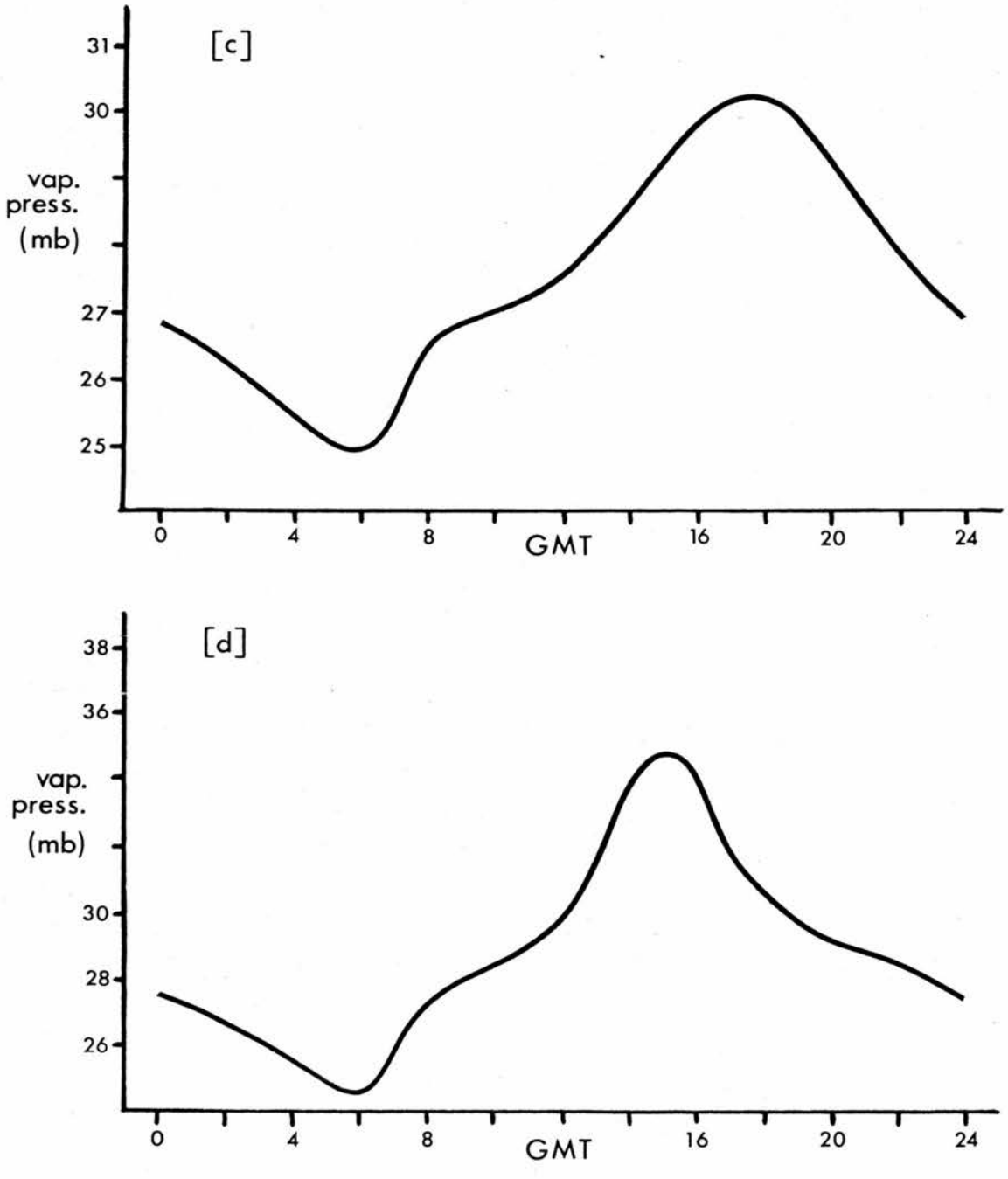

Figure (1.5) Diurnal variation of vapour pressure at Eala; (c) annual average, (d) April average (data from Vandenplas (1947, 1949)).

of vapour pressure at Eala (18°15'E, 0°03'N), a station deep in the Equatorial Forest, with those of dew point at Kew. In both cases the variation is presented as an annual average and as an average for a "summer" month.

The "Climatological Atlas of the British Isles" also reproduces the temperature and humidity variations recorded during the daylight hours at Kew on 10th July 1934 when the humidity dropped to an exceptionally low level. On this day a strong anti-cyclone was almost stationary over the North Sea and winds were blowing from Belgium to S.E. England although, interestingly, dew points in Belgium were higher on the afternoon and evening of 9th July than were those measured throughout S.E. England on that day and on 10th July. The case is reviewed by Bilham (1938) who suggests that the decrease in humidity was caused by the descent of a dry stratum of air from higher levels to the ground surface. Read (1934) additionally suggests that convectional movement may have mixed the damper surface layers with drier air at higher levels.

Geiger (1966) reviews the data of Best et al. (1952) and also presents data from three dry August days in Finland when a double maximum and a local minimum of vapour pressure were apparent during the day. He also invokes the argument of a delicate balance between the ground-source vapour flux and turbulent transport upwards as was employed by Tunnell (1958) and by Best et al. (1952).

However, a completely different explanation is offered by James (1957) who visualises the process as one in which turbulence diffuses water vapour upwards through the boundary

layer and eventually stores it within the inversion layer which, under anti-cyclonic conditions, acts as a lid to the boundary layer. His calculations for a test-case indicate that this process will result in a net increase in the mixing-ratio of the boundary layer during the day. This is a forecast which is borne out, on average, for clear summer days (i.e. days with a capping anti-cyclonic inversion) according to the data of Best et al. (1952).

There are a great many references in the literature to occurrences of low humidity in Britain and almost as many explanations of why they occur. Smith (1958) proposes that low humidities observed in Scotland on 10th June 1956 were caused by the descent of an anti-cyclonic inversion to ground-level. However, at the same time, this inversion was clearly distinguishable at some height above the Moray Firth, so he further suggests that low humidities at some places were the result of the down-mixing effect ahead of a penetrating sea-breeze front.

Green (1965) explains a large collection of such cases of low humidity either by subsidence of extremely dry layers of air from above or by the föhn effect. The same explanations are given by Hawke (1946) and Green et al. (1964). However, Green (1956) suggests that atmospheric overturning may be important in bringing down dry air from above and Hawke (1944) lays emphasis on the geographical source and track of air as it moves towards the British Isles. One significant point which requires explanation is that all of these occurrences of low humidity were recorded during the middle part of the day and if they are all merely a result of synoptic sub-sidence alone then it is equally likely that they would occur

at night.

1.3 Intentions of Thesis

As discussed above, several diverse and contradictory theories have been propounded to explain sundry observed patterns of diurnal humidity variation. It is the general intention of this thesis to clear away much of this qualitative and schematic thinking and to present a unified approach in an explanation of the observations. Initially this will be done on a local and diurnal scale and subsequently on a regional and climatological scale.

On the diurnal scale and under anti-cyclonic conditions, it was originally intended to include in a physical model of the humidity-controlling processes over vegetation both the synoptic-scale influence, through classical-style entrainment at the inversion, and the physiological influence, through the varying stomatal resistance of the vegetative cover. Firstly, however, it soon became clear that the classical theory of entrainment makes some assumptions that are perhaps unwarranted and a new theory is formulated (Chapter 2) and subsequently tested (Chapter 3); secondly, it became apparent that the physiological influence plays a rather minor rôle on a diurnal scale and its effect is approximated.

It was always intended that numerical methods should be avoided and analytical solutions to the physical model be found such that they might easily be used predictively in the field. The new entrainment theory and the approximation of the physiological influence permit this and hence an analytical predictive equation for the diurnal variation of specific humidity is derived and tested against data from seven fine

days at Thetford Forest (Chapter 4). The results of such a predictive equation must be modified if, at some time during the day, cumulus cloud develops, thereby reducing the net radiation at ground-level; therefore a new parameter is theoretically derived which can predict the extent to which cumulus cloud-cover will develop during any particular day (Chapter 5). It is hoped that this parameter, itself, may become a useful predictive tool.

In conclusion, climatological data of the diurnal changes in temperature and in dew-point from all parts of the world are used in an extended entrainment theory to make predictions of regional and annual Bowen ratios and, in this way, a map is produced of Bowen ratios in Europe. From the outset it was expected that the physiological control over evaporation (and, hence, also over Bowen ratio) on a regional and climatological scale would be related to various physiographical influences such as geology and soil type and this is discussed in some detail (Chapter 6). In addition this last chapter finally realises the original motivating intention of the thesis which is to explain the commonly observed and apparently paradoxical behaviour of humidity at Thetford Forest.

CHAPTER 2

ENTRAINMENT THEORY

In Chapter 1 it was seen that the specific humidity at the bottom of the boundary layer will drop during the day under certain anti-cyclonic conditions - occasionally in quite a dramatic way. On the other hand, at Thetford Forest, it was observed to drop very often and even under cyclonic conditions. Since a synoptically cyclonic situation is often complicated by strong advection and, at present, little is understood of the boundary layer mixing process, the next four chapters will deal in particular with the diurnal development of the anti-cyclonic, inversion-capped boundary layer. The cyclonic cases will be dealt with later, on an annual average basis so as to eliminate the grosser effects of advection on diurnal changes.

2.1 Physical Process of Entrainment

2.1(a) Earlier theories of entrainment

Under anti-cyclonic conditions, persistent large-scale subsidence within the middle troposphere must always produce an inversion layer somewhere within the lower troposphere, usually in the region of 1000m above the ground. This inversion layer, across which the potential temperature may increase by as much as $10^{o}C$ and the specific humidity decrease by as much as 5 gkg^{-1}, is usually of the order of 100m deep.

Under clear-sky conditions direct radiative heating of the ground produces a large sensible heat flux. Richardson (1920) showed that associated with any sensible heat flux is a rate of production of eddy-energy given by

$$\varepsilon' = gH/c_pT \quad \text{or} \quad gF/c_p\theta \qquad (2.1)$$

So, when the ground acts as a source of sensible heat energy for the boundary layer it also acts as a source of turbulent eddy-energy. Note that the energy of turbulence will be about four orders of magnitude less than the energy associated with the sensible heat flux.

The founding-father of entrainment theory, Ball (1960), assumed that there is no viscous dissipation of thermally generated turbulent kinetic energy in the planetary boundary layer. Since the turbulent energy content of the boundary layer does not continuously increase, he postulated that it must be consumed, at a rate equal to that of its production, by entraining heat downwards at the inversion at a rate equal to the driving heat flux upwards at the ground. In order to parameterise this process, Ball defined an "entrainment coefficient" (A) as the negative of the ratio of the entrained sensible heat flux at the inversion to the driving ground-source sensible heat flux and accordingly Ball assumed the entrainment coefficient to be of value unity.

In this way, then, the eddy-energy produced by buoyancy forces at the bottom of the boundary layer is used up in working against buoyancy forces at the top of the boundary layer as warm air from above the inversion level is mixed down into the boundary layer below. This transport of warm air results in a rise of the inversion level.

Implicit in this argument is the additional assumption that the boundary layer is well mixed, which requires that the response at the inversion level to a stimulus at the ground is immediate; clearly, with a boundary layer some hundreds

of metres deep, this is not so. Although more recent workers have abandoned the assumption of a total absence of viscous dissipation, they have retained the concept of a well-mixed boundary layer. Historically the development of entrainment theory has been through the works of Lenschow and Johnson (1968), Lilly (1968), Carson (1973), Carson and Smith (1973), Betts (1973), Tennekes (1973), Readings et al. (1973), Deardorff (1974a) and Cattle and Weston (1975) who have assumed or measured, on a variety of occasions and at various times of day, values of the entrainment coefficient ranging all the way from zero to unity, but with a concensus of opinion for an average daytime value in the region of 0.25.

This chapter presents an original theory of entrainment which dispenses with the idealisation of a perfectly mixed boundary layer, introduces a new limiting factor to the rate of entrainment and thereby explains and removes one of the difficulties inherent in all other entrainment theories. Since this new theory was developed it has been further supported by evidence which is discussed in § 3.1(b).

2.1(b) A new theory of entrainment

In a convective situation, warm air bubbles or plumes rise from the ground surface towards the inversion and in so doing they form a turbulent wake. Some of this turbulent energy is dissipated immediately in expanding the rising bubble by entrainment across its surface, while the remainder of the energy is imparted to the surrounding atmosphere and diffuses outwards. If the diurnal heat flux at the ground is sinusoidal there will be a resultant sinusoidal production of

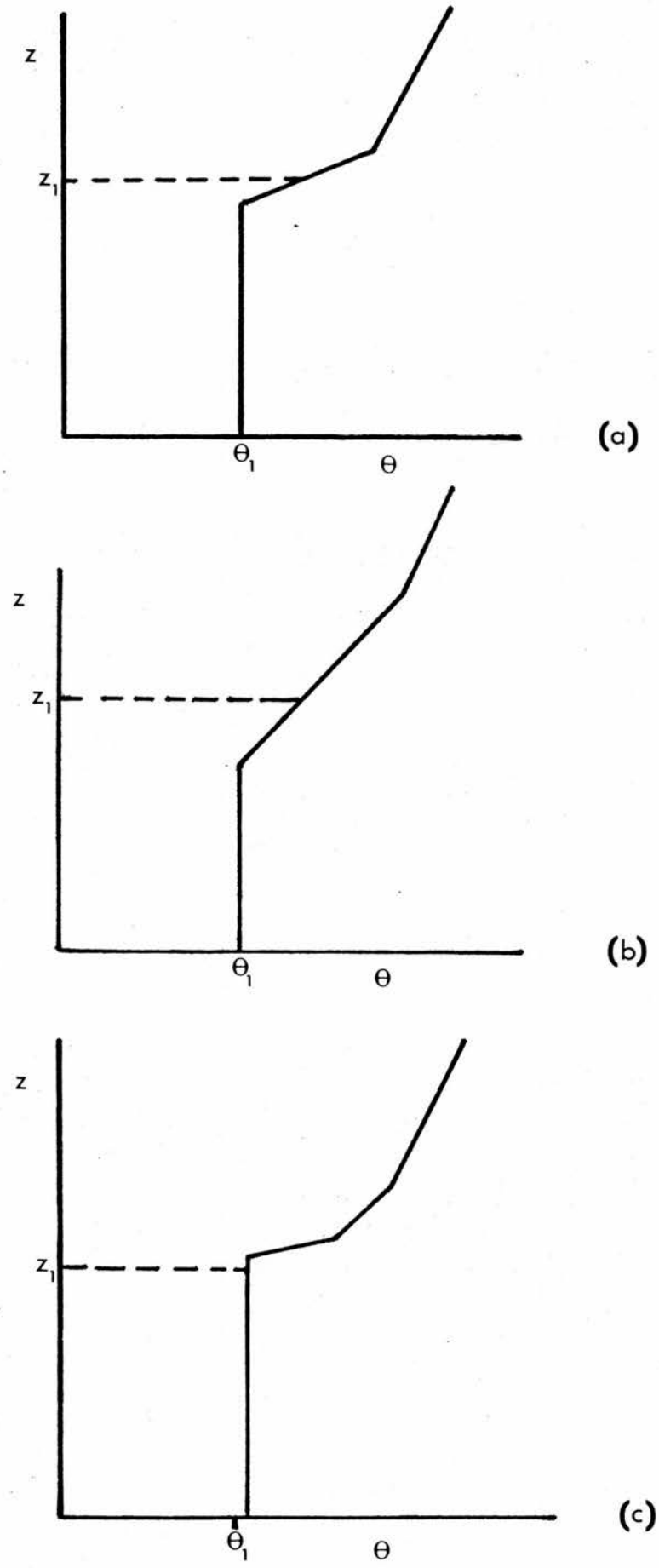

Figure (2.1) Three stages in development of inversion layer during entrainment; (a) initial, (b) intermediate, (c) final.

eddy energy throughout the boundary layer. If the layer is 500m deep then the convective bubbles will rise through it in a matter of minutes, whereas the turbulence left in their wake will, on average, have to diffuse 250m to reach the inversion. This process will take considerably longer than a few minutes.

The new model of entrainment proposes that bombardment of the inversion layer by the quickly rising thermal imparts turbulence to it either through the production of Kelvin-Helmholtz billows or through the turbulent breakdown of all or part of the thermal itself. This method of entrainment has since been proposed by Rayment and Readings (1974). The eddy-energy of the inversion layer is then expended against buoyancy forces by bringing warm air downwards into the inversion layer from above and cold air upwards from below. Thus the inversion layer expands upwards and downwards and the shallow layer of Figure (2.1(a)) becomes the deeper layer of Figure (2.1(b)). Neither has the inversion height been raised nor has heat been added to the bulk of the boundary layer. In fact, no amount of turbulence introduced at the inversion level will produce the observed effects of entrainment; it will only tend to destroy the shallow inversion layer altogether and replace it by an extended positive gradient of potential temperature.

To complete the entrainment process the lower end of the now thickened inversion layer has to be eroded from below by the entraining action of thermally produced turbulence diffusing upwards from the bulk of the boundary layer. This mixes heat down into the boundary layer and re-establishes a

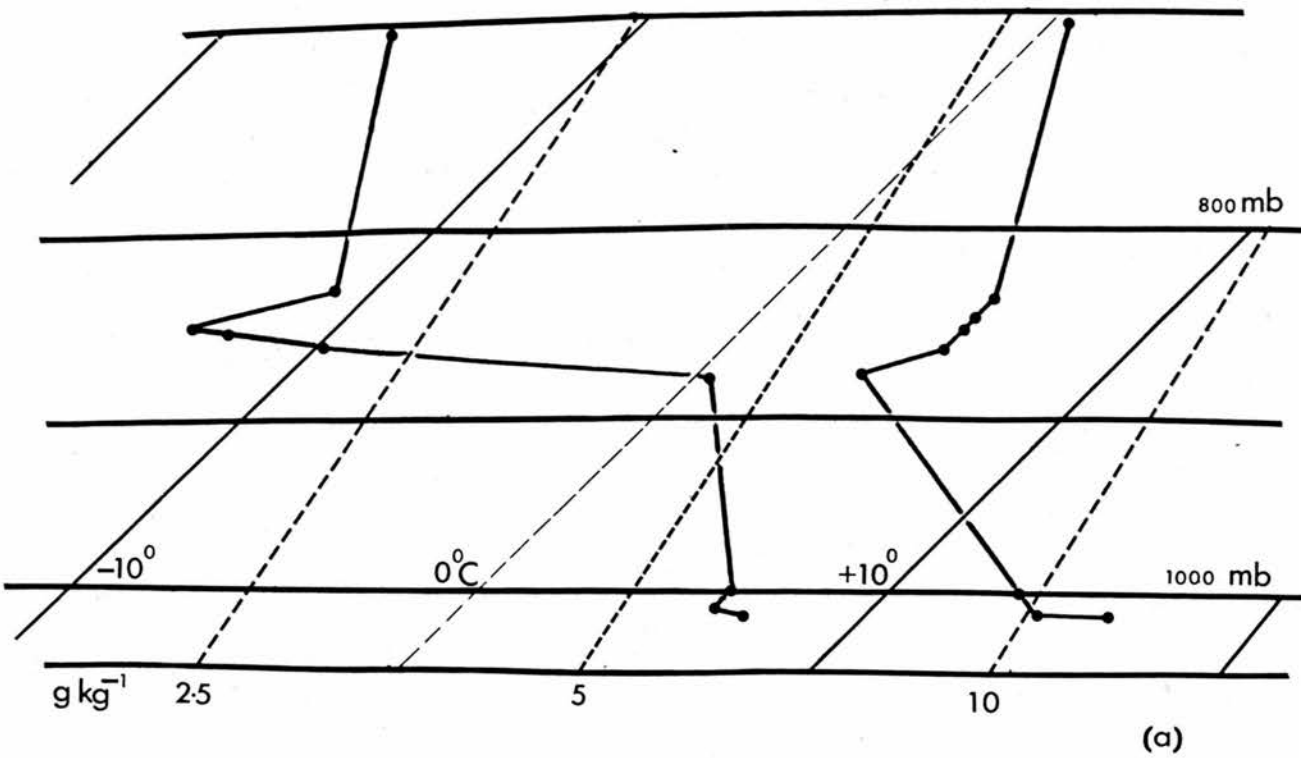

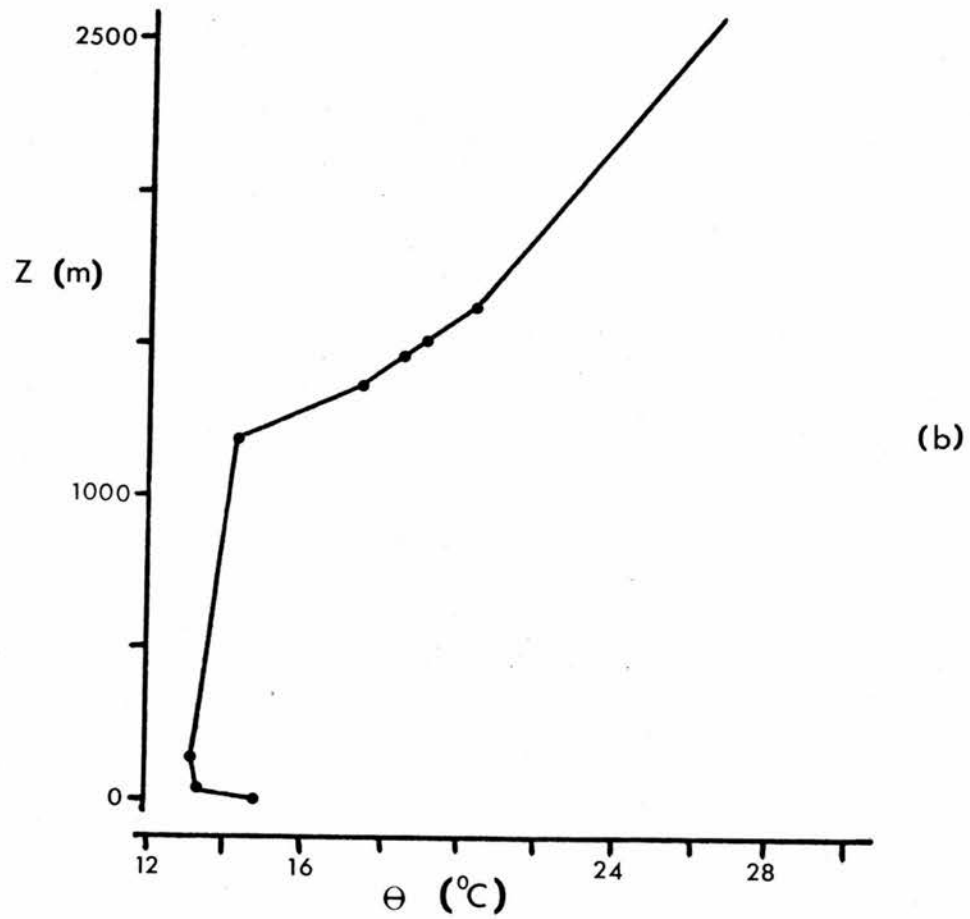

Figure (2.2) (a) Tøgram of 12.00h ascent at Crawley on 16th Sept. 1971.

(b) Equivalent temperature profile plotted as θ versus z.

shallow inversion layer, but now at a greater height. A temperature profile similar to that of Figure (2.1(c)) may be attained and, incidentally, it is not uncommon to observe forms approximating to this from radio-sonde data during the middle of the day under anti-cyclonic conditions (e.g. Figure (2.2)).

The downward heat flux just below the inversion and the rate at which the inversion rises are seen to depend fundamentally upon the rate of diffusion of thermally generated turbulence in the boundary layer. Subsequent to the formulation of this theory, Deardorff (1974b) has shown that there is a large upwards diffusion of turbulent eddy energy between the ground and the inversion level and that this is the only source which compensates the losses due to dissipation and the negative heat flux just below the inversion.

The following sections demonstrate that the finite diffusion time of eddy energy in an imperfectly mixed boundary layer results in a diurnal variation of the entrainment coefficient (A). A new coefficient (A') is consequently defined to include this effect.

2.2 The Rôle of Eddy Diffusion

2.2(a) Diffusion Equation

If the fairly constant and relatively small amount of wind-induced eddy energy is justifiably neglected in calm anti-cyclonic conditions then, at any height, the diurnal variation of thermally produced eddy energy is controlled by a diffusion process which, if similar to that of momentum, may be represented by the equation

$$\frac{\partial \varepsilon}{\partial t} = K_m \frac{\partial^2 \varepsilon}{\partial z^2} \quad . \qquad (2.2)$$

For a sinusoidal heat flux, Equation (2.2) is subject to the conditions:

(1) at the source (say $z = 0$): $\varepsilon = \varepsilon_x \sin \Omega t$

(2) at great height ($z = \infty$): $\varepsilon = 0$.

The solution of Equation (2.2) is then

$$\varepsilon = \varepsilon_x \exp(-az)\sin(\Omega t - az)$$

where $a = (\Omega/2K_m)^{1/2}$.

So, for a diffusion path length of 250m from the assumed eddy energy source (viz. § 2.1(b), the maximum eddy energy occurs at a time given by

$$\Omega t - 250a = \pi/2$$

which is a time later than that for the maximum at the source by the amount

$$\phi = 250a/\Omega = 250/(2K_m\Omega)^{1/2} \qquad (2.3)$$

Since the dissipation of the thermally produced eddy energy of the boundary layer is the operating mechanism for entrainment then this also gives an estimate of the lag of the entrained heat flux behind the driving ground-source heat flux for the arbitrary boundary layer depth of 500m.

2.2(b) Eddy Diffusivity

Clarke (1970) found from a total of forty-two atmospheric soundings that, in conditions of deep convection, the non-dimensional eddy diffusivity, $\hat{K}_m$, had a mean value close to 0.025 over a considerable depth of the boundary layer; for

the same occasions the stability parameter, sk^2, had the mean value of -139.

Using the definitions of $\hat{K}_m$ and s, knowing their mean values and assuming a surface temperature of 293°K and a surface heat flux of 400 Wm^{-2}, it is possible to eliminate the unknown friction velocity, U_*, and to solve for K_m, the value thus obtained being 21 m^2s^{-1}, coincidental with the value found using Clarke's (1970) data for cases of shallow convection. So, irrespective of inversion height, such a value appears to be a reasonable estimate of K_m.

From Equation (2.3) the lag is now calculated to be

$$\phi = 250/(2 \times 21 \times 7.29 \times 10^{-5})^{\frac{1}{2}} \text{ s} \simeq 1\tfrac{1}{4} \text{ hr.} \qquad (2.4)$$

This may well be an overestimate of the lag since more turbulence will be produced above a height of 250m by a rising, accelerating and expanding warm air bubble than will be produced below. The value of K_m and its assumed independence of time and of height are approximations which make the above derived value of ϕ additionally uncertain.

2.3 Results of New Theory

2.3(a) A New Entrainment Coefficient, A'

The observations quoted by Carson (1973) demonstrate that the inversion level rises at an approximately linear rate throughout the day, provided that the entrainment process predominates over dynamical effects such as large-scale anticyclonic subsidence. Hence an additional, linearly increasing time lag, ψt, should be included. The total phase shift between the two fluxes becomes $\Omega(\psi t + \phi)$ which requires

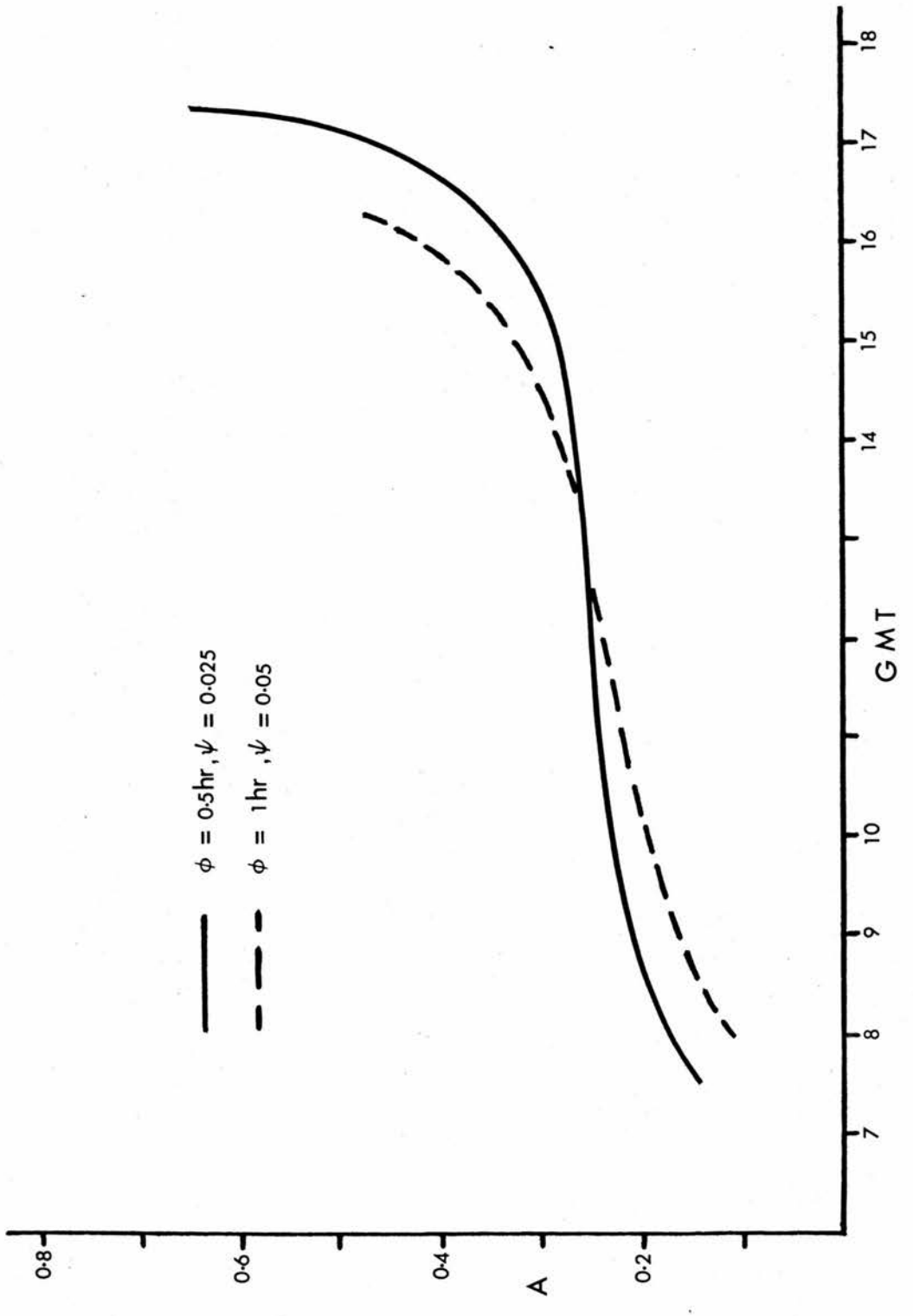

Figure (2.3) Value that A must assume throughout day to allow for diffusion time of eddy energy, given that A' = 0.25.

that a new entrainment coefficient, A', be defined such that, for a sinusoidal heat flux,

$$A' = -(H_{hx}\sin \Omega t)/(H_{ox}\sin \Omega((1 - \psi)t - \phi)) \quad . \qquad (2.5)$$

2.3(b) Comparison of A and A'

The presently accepted definition of the entrainment coefficient, A, results in the inter-relationship

$$A = A' \sin\Omega((1 - \psi)t - \phi)/\sin \Omega t \quad . \qquad (2.6)$$

If a constant value is assigned to the parameter A', then there is a resultant diurnal variation of the coefficient A.

The analysis of § 2.2(b) suggests that, for a boundary layer 500m deep, an initial lag of half an hour between the driving, ground-source sensible heat flux and the entrained heat flux may reasonably be assumed. For example, Figure (2.3) shows a graph of A against time of day for assumed values of A', ϕ and ψ of 0.25, ½hr and 0.025 respectively. Thus the value of $(\psi t + \phi)$ is assumed to increase from half an hour at sunrise to almost 50 mins at sunset, which corresponds to the inversion level rising from 500m to 800m during the day. These values are compatible with a lag of approximately one hour found experimentally by Rayment and Readings (1974) during the middle part of the day under a similar inversion. Shown for comparison on Figure (2.3) is the case of A', ϕ and ψ having values of 0.25, 1 hr and 0.05 respectively.

The graph indicates that A, which is defined using the unrealistic concept of a highly turbulent and perfectly mixed

boundary layer, must increase throughout the day owing to the finite response time of the real atmosphere. This behaviour agrees well with the diurnal change in A which other workers, empirically, have found necessary to employ. For instance, Carson (1973) developed a multi-phase model in which A was assigned different values during different periods of the day, its afternoon value being much greater than its morning value. Similarly, the measurements of Rayment and Readings (1974) suggest that the entrainment coefficient increases from morning to afternoon, whilst Deardorff (1974a) shows that, during the afternoon period (12.00h to 16.00h), the value of A remains relatively constant.

Interestingly, the theories and dimensional arguments of Carson and Smith (1973) result in a predicted diurnal variation of A similar to that of Figure (2.3), although for very different reasons. They suggest that the value of A depends upon the ground-source sensible heat flux, the change in potential temperature across the inversion and the wind shear across it, all of which are time-dependent. The rate of entrainment in the present theory is postulated to be limited by the rate of diffusion of turbulence in the boundary layer and not by the rate of expansion of the inversion layer as in all preceding theories, and so it is unlikely that A' would depend upon the precise nature of the inversion. However, it is possible that A' does depend upon several factors such as magnitude of heat flux, height of the inversion and boundary-layer stability. In the remainder of this thesis such complications will be ignored and A' will be assumed constant with a value of 0.25.

CHAPTER 3

TWO TESTS OF ENTRAINMENT THEORY

3.1 Test of Limiting Process

The new theory of entrainment propounded in Chapter 2 is, to a certain extent, controversial. Its point of departure from all other theories may be regarded as its assumption that the rate at which mass is entrained into the planetary boundary layer from above the inversion is limited by the rate at which turbulent energy from within the boundary layer diffuses upwards and erodes the bottom of the inversion layer. This is in contradiction to other theories which, tacitly or otherwise, assume that the rate of mass entrainment is limited by the entrainment process within the inversion layer, which tends to thicken it, and that there is at all times more than sufficient turbulence diffusing upwards from the boundary layer to carry away the entrained heat. Which then is correct? Does the process which tends to change Figure (2.1(a)) into Figure (2.1(b)) dominate over the process which changes Figure (2.1(b)) into Figure (2.1(c)), or vice versa?

These diagrams suggest a test by which the limiting process may be detected. If entrainment into the inversion layer itself, either by Kelvin-Helmholtz billow production or the turbulent breakdown of an impinging thermal, is the limiting process then erosion of the bottom of the inversion layer will proceed at a faster rate than that at which the layer is expanding; hence, on average, the inversion layer will become thinner during a convective period. On the other hand, if,

as suggested in Chapter 2, the limiting process is that of erosion of the bottom of the inversion layer then entrainment into the inversion layer itself will continue at a disproportionately high rate and the inversion layer will thicken.

3.1(a) Data on Inversion Thickness

Accurate measurements of the diurnal development of an inversion layer during a convective period are rare, since it has, in the past, not been considered as a relevant study. However, temperature profiles presented by Lenschow and Johnson (1968) show the inversion thickness increasing from 167m at 10.10 CST to 222m at 13.00 CST on 8th June 1964; a slight increase is perhaps also detectable between 8.40 CST and 11.40 CST on 10th June 1964. In a non-advective situation the data of Cattle and Weston (1975) imply that the inversion layer of 24th March 1972 over S. England increased in thickness by 3 mb (about 30m) between 10.30 GMT and 13.30 GMT, and on 16th June 1972 by 9 mb (about 90m) between 10.30 GMT and 14.30 GMT. It is noteworthy that five out of the seven temperature profiles published in that paper have a shape similar to that of Figure (2.1(c)). Unfortunately, the bottom and top of the inversion layer in the data of Deardorff (1974a) are rather ill-defined, although it appears that there may be a thinning between 12.00h and 15.00h and a thickening between 15.00h and 18.00h. The best published data from which inversion thicknesses may be extracted are by Rayment and Readings (1974) for the 14th May 1971 at Malvern. Table (3.1) is taken from their profiles of temperature at the given times.

TIME (GMT)	Δp thickness of inversion (mb)
7.36	7
8.59	17
10.38	13
11.36	19
12.39	difficulty in interpretation
13.34	27
14.58	25

TABLE (3.1) Inversion thickness at given times, taken from the data of Rayment and Readings (1974) for 14th May 1971 at Malvern.

It is clear that, although there is some fluctuation, a distinct thickening towards afternoon occurs, at which time the inversion layer reaches a maximum thickness of about 250m. Readings et al. (1973) show that, for this particular inversion, the Richardson number ($= \frac{g \Delta z \Delta \theta}{\theta (\Delta u)^2}$) attains its critical value of $\frac{1}{4}$ only when the inversion thickness is 12-16m. In other words, the inversion has to be stretched over the summit of an impinging thermal plume until it reaches this small thickness before turbulent breakdown occurs through Kelvin-Helmholtz billow production. If this is the mechanism then, clearly, there is considerable overshoot in turbulence production and resulting entrainment since the average inversion thickness does not appear to return to a value just above that for a critical Richardson number but increases up to about 250m.

The fairly accurate measurements quoted above all indicate that a typical mid-day inversion has a thickness of about 20mb which implies that the standard U.K. Meteorological Office radio-sonde is quite capable of revealing some inversion structure. However, radio-sonde data must be treated with some caution since only one sounding is made at one particular place at one time and this may not be representative of the average structure of the inversion. The times of ascent (00.00, 12.00 and 24.00h) are not ideal for this particular study since the mid-night ascent may not correspond closely to a dawn or dusk ascent, if such were available, and consequently advection may play a more influential rôle. Additionally, it is notoriously difficult to define with any accuracy the precise top and bottom of a subsidence inversion.

Table (3.2) presents the change of inversion thickness

TABLE (3.2) CHANGE OF INVERSION LAYER THICKNESS (?? denotes difficulty in interpretation)

Date	Place	Δp (mb) (00.00 GMT)	Δp (mb) (12.00 GMT)	Δp(mb) (24.00)	Change in (mb) inversion thickness 00.00-12.00	12.00-24.00	00.00-24.00
2/5/71	Crawley	17	30	75	+13	+45	+58
2/6/71	Crawley	60	??	15	??	??	??
3/6/71	Crawley	15	21	12	+6	-9	-3
7/7/71	Crawley	15	15	42	0	+27	+27
8/7/71	Crawley	42	33	55	-9	+22	+13
15/9/71	Crawley	10	18	33	+8	+15	+23
16/9/71	Crawley	33	41	50	+8	+9	+17
16/6/70	Crawley	28	13	29	-15	+16	+1
17/6/70	Crawley	29	35	??	+6	??	??
24/5/70	Crawley	51	60	17	+9	-43	-34
18/5/70	Crawley	??	54	14	??	-40	??
20/5/70	Crawley	??	9	??	??	??	??
3/6/70	Crawley	??	41	57	??	+16	??
4/6/70	Crawley	57	90	??	+33	??	??
11/8/70	Crawley	15	18	28	+3	+10	+13
26/8/70	Crawley	20	19	20	-1	+1	0
28/8/70	Crawley	22	78	18	+56	-60	-4
5/7/71	Crawley	??	??	??	??	??	??
11/6/69	Aughton	24	26	31	+2	+5	+7

TABLE (3.2) (Contd.)

Date	Place	Δp(mb) (00.00 GMT)	Δp(mb) (12.00 GMT)	Δp (24.00)	Change in (mb) inversion thickness 00.00-12.00	12.00-24.00	00.00-24.00
11/7/71	Crawley	21	28	43	+7	+15	+22
3/5/71	Crawley	75	16	??	-59	??	??
11/6/69	Crawley	50	74	20	+24	-54	-30
4/6/71	Crawley	12	36	17	+24	-19	+5
14/6/73	Crawley	50	75	62	+25	-13	+12
4/7/73	Crawley	??	24	23	??	-1	??
30/6/73	Crawley	17	26	14	+9	-12	-3
5/6/73	Crawley	15	28	57	+13	+29	+42
7/7/73	Crawley	18	??	36	??	??	+18
16/8/71	Crawley	33	26	29	-7	+3	-4
6/6/70	Crawley	??	12	25	??	+13	??
8/6/73	Crawley	40	51	20	+9	-31	-22
26/7/73	Crawley	??	19	17	??	-2	??
13/7/71	Crawley	??	22	44	??	+22	??
9/6/73	Crawley	20	46	90	+26	+44	+70
8/6/69	Crawley	41	54	49	+13	-5	+8
9/6/69	Crawley	49	61	??	+12	??	??
14/6/69	Crawley	26	??	??	??	??	??
13/7/69	Crawley	13	19	43	+6	+24	+30
17/7/69	Crawley	23	40	19	+17	-21	-4

TABLE (3.2) (Contd.)

Date	Place	Δp (mb) (00.00 GMT)	Δp (mb) (12.00 GMT)	Δp (mb) (24.00GMT)	Change in (mb) inversion thickness 00.00-12.00	12.00-24.00	00.00-24.00
25/7/69	Crawley	52	58	69	+6	+11	+17
30/7/69	Crawley	20	55	??	+35	??	??
7/8/69	Crawley	35	14	25	-21	+11	-10
28/5/68	Crawley	70	75	121	+5	+46	+51
29/5/68	Crawley	121	120	78	-1	-42	-43
9/6/68	Crawley	35	52	36	+17	-16	+1
10/6/68	Crawley	36	187	17	+151	-170	-19
12/6/68	Crawley	26	36	20	+10	-16	-6
30/6/68	Crawley	?	49	?	??	??	??
18/7/68	Crawley	18	58	25	+40	-33	+7
5/8/68	Crawley	15	21	56	+6	+35	+41
22/8/68	Crawley	?	30	26	??	-4	??
23/8/68	Crawley	26	72	35	+46	-37	+9
24/8/68	Crawley	35	29	??	-6	??	??
25/8/68	Crawley	??	??	19	??	??	??
26/8/68	Crawley	19	13	17	-6	+4	-2
27/8/68	Crawley	17	22	??	+5	??	??

	Period of Time (GMT)		
	00.00-12.00	12.00-24.00	00.00-24.00
Number of days for which the inversion thickened	32	22	22
Number of days for which the inversion thinned	9	20	13
Number of days for which the inversion thickness remained unchanged	1	0	1
Number of days with difficulty in interpretation of data	14	14	20
Mean change of inversion thickness	+12.5mb.	-4.9mb.	+8.6mb.

TABLE (3.3) SUMMARISED RESULTS OF TABLE (3.2).

between mid-night and mid-day, mid-day and mid-night and also for the whole 24-hour period for fifty-five fairly cloudless summer days (all days with ≤ 3 oktas cloud cover during the mid-day period). Thirty-three of the days are those used in the tests of §3.2, Chapter 4 and Chapter 5 where the individual selection procedures are described. It is sufficient here to say that they have in no way been specially selected for this test. The Daily Weather Reports of the U.K. Meteorological Office for the months of May, June, July, August and September of the years of 1968 and 1969 were also scrutinised to find days of 3 oktas or less cloud cover at Gatwick under anti-cyclonic conditions. This resulted in an additional twenty-two test days. The radio-sonde station of Crawley, situated close to Gatwick, is always used since it is the only British upper air station which is remote from an extensive water surface and therefore is likely to experience well-developed convection on sunny, summer days. Aughton is also used on 11th June 1969 since the analysis of §3.2 shows it to be downwind of a long land fetch.

The results are summarised in Table (3.3) and reveal that, indeed, the inversion layer substantially thickens between 00.00h and 12.00h (a t-test gives a 99°/o confidence level to the true mean for this period being different from zero). However the amount of thickening is greatly reduced or even becomes a thinning for the period 12.00h - 24.00h which is again to be expected since, as indicated in Figure (2.3), for a given constant value of A' the rate of entrainment into the boundary layer and out of the inversion layer becomes greater in the afternoon. For the whole 24-hour period, as well as

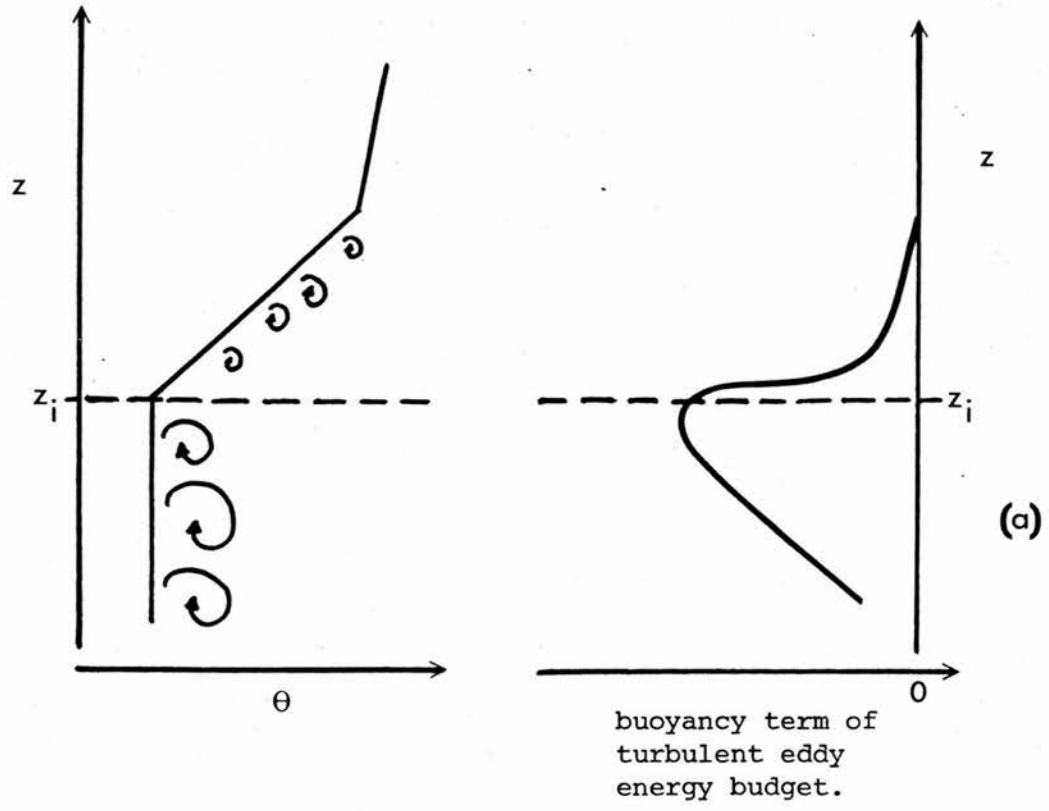

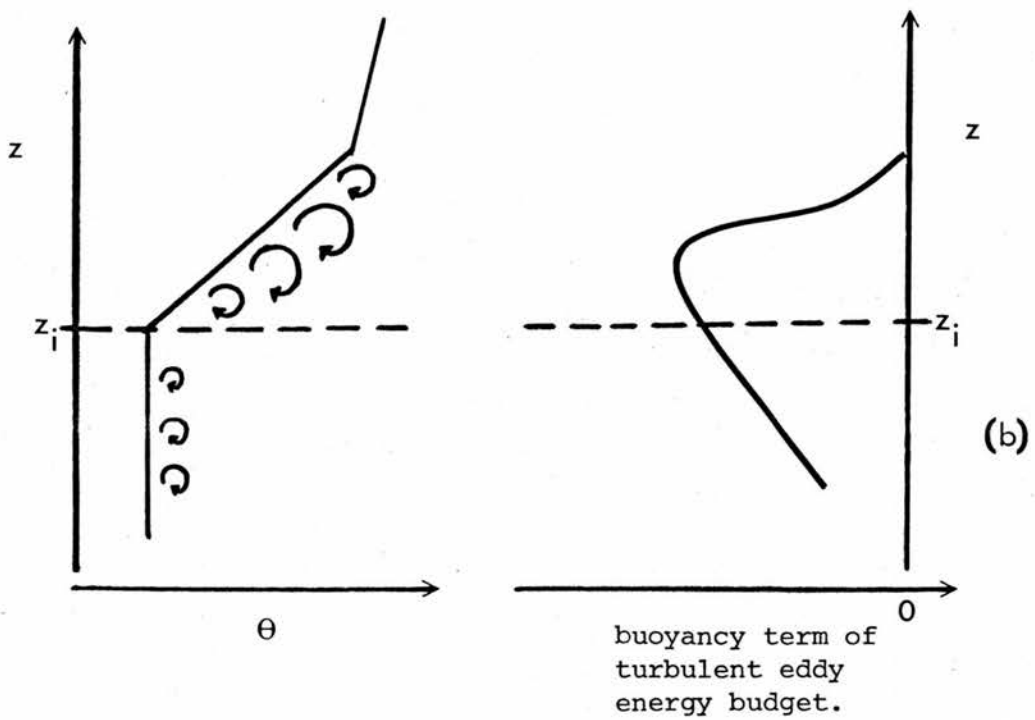

Figure (3.1) Schematic representation of absorption of turbulent eddy energy in working against buoyancy forces for
(a) entrainment process limited by Kelvin-Helmholtz billow production,
(b) entrainment process limited by diffusion of boundary layer turbulence.

the morning, it is apparent that diffusion of boundary layer turbulence is the limiting process to the rate of entrainment.

3.1(b) Further Evidence

There is a great deal of circumstantial evidence which is easily explained by this new theory of entrainment, such as the common occurrence of temperature profiles like Figure (2.1(c)); the need for Rayment and Readings (1974) to include a lag between the driving and entrained heat fluxes; the need for multi-phase entrainment models to include a diurnal increase in the parameter A; and the large upwards diffusion of eddy energy throughout the boundary layer as calculated by Deardorff (1974b). Finally, Deardorff (1974b) also shows that the dissipation of eddy energy against buoyancy forces reaches a maximum value just above the bottom of the inversion layer. This is further supporting evidence for the case of diffusion of turbulence as being the limiting process. Figure (3.1) demonstrates this point diagrammatically. Assuming that a convective period starts with a finite thickness of inversion layer and that subsequently there is a more than sufficient supply of boundary-layer turbulence to carry away the heat entrained into the inversion layer from above, then the boundary layer turbulence will additionally erode away the inversion itself and the turbulence dissipated against buoyancy forces will be greater just below the inversion bottom than above it. This is shown schematically in Figure (3.1(a)). On the other hand, if boundary layer turbulence is not sufficient to keep pace with the heat being entrained into the inversion layer then the dissipation against buoyancy forces will be less

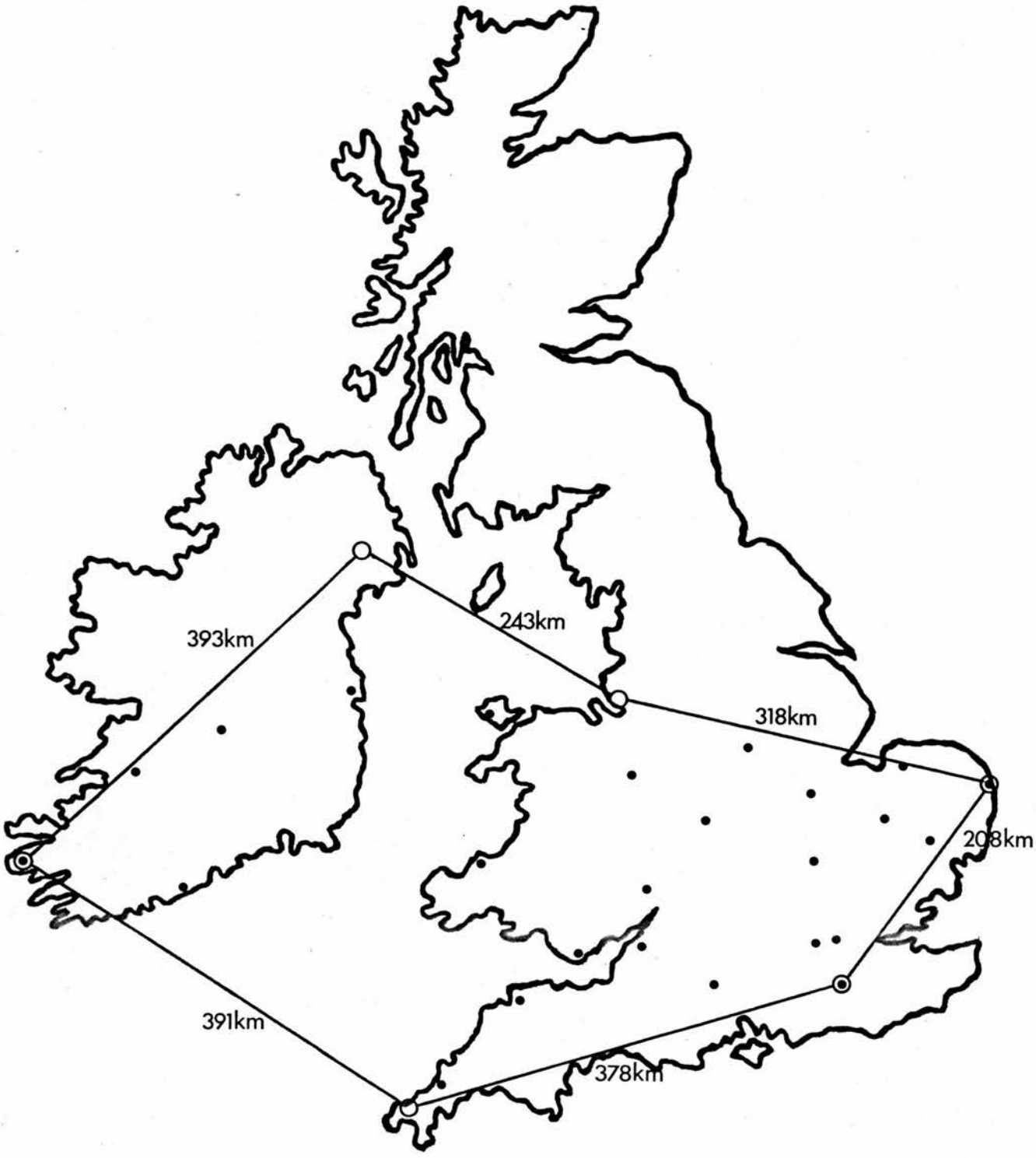

Figure (3.2) Polygon used in calculation of §3.2

O radio-sonde stations,

• stations reporting cloud cover.

below the inversion bottom than just above it, since the inversion layer will be expanding. This is shown in Figure (3.1(b)), which is similar in shape to the profile calculated by Deardorff (1974b).

3.2 A Synoptic-scale Budget of Vapour Flux

This second test is applicable to all theories of entrainment and is devised to check the assumption that the inversion acts as a one-way valve, allowing mass to be entrained downwards across it but not allowing anything to pass upwards. At the same time, the test provides an estimate of the entrainment coefficient.

The 5th - 12th June 1969 was a particularly settled anticyclonic period. On the 11th June, S. England lay between two high pressure centres, one lying off the N.E. coast of England and the other off the W. coast of Ireland. The anti-cyclone was mature and beginning slowly to decline.

Figure (3.2) shows the radio-sonde stations used in this test and also the weather stations giving reports of cloud cover. The radio-sonde data for the 12.00 GMT ascents at the six stations were used to compute the total balance of water vapour flux in or out of the volume of atmosphere lying above the immediate top of the inversion layer and below the tropopause for the polygon shown in Figure (3.2). For this computation the troposphere above the inversion was divided into more or less homogenous layers. This entailed using seven layers at Valentia, five at Hemsby, eight at Aughton, eleven at Long Kesh, six at Crawley and six at Camborne. Using the average values of wind speed, wind direction, density and

specific humidity for these layers, the fluxes of vapour in or out of the volume may be determined for each layer and finally the sum of these fluxes gives the net balance of vapour flux for the whole volume. 256 individual measurements of wind speed, wind direction, temperature and humidity were used in the calculation and random errors should, hopefully, cancel out.

3.2(a) Results of Calculation

The summation of convergence into and divergence out of the above-inversion volume through the vertical sides gives a net vapour mass flux per unit plan area of -0.18×10^{-5} $kgm^{-2}s^{-1}$.

A weighted average of mixing ratio is taken at each of the six stations for layers of 100 mb or less above the inversion and below the tropopause at the time of 24.00h, 10th June 1969 and of 24.00h, 11th June 1969. Then, a knowledge of the pressure at the top of the inversion layer for each station permits the calculation of the total mass of above-inversion water vapour per unit plan area.

A weighted average is then taken of these values to compute the average mass per unit area of above-inversion water vapour for the whole volume at these two times. The results are 6.53 kgm^{-2} and 5.48 kgm^{-2} respectively; that is, the atmosphere above the inversion becomes significantly drier. This amount of drying would require an average divergence of water vapour out of the volume of 1.22×10^{-5} $kgm^{-2}s^{-1}$, which, with the calculated outward flux of 0.18×10^{-5} $kgm^{-2}s^{-1}$ at 12.00h, 11th June 1969, implies a net downwards vapour flux across the inversion of 1.03×10^{-5} $kgm^{-2}s^{-1}$ throughout the day; the inversion is shown effectively to act as a one-way valve.

3.2(b) Estimation of Entrainment Coefficient

A weighted average of the six values of mixing ratio at the top of the inversion layer at 12.00h results in an average value for the area of 2.52 gkg^{-1} and if the downward water vapour mass flux across the inversion at 12.00h is 1.03×10^{-5} kg $m^{-2}s^{-1}$, then the total mass flux of air is $1.03 \times 10^{-5}/2.52 \times 10^{-3}$ or 4.10×10^{-3} $kgm^{-2}s^{-1}$.

The weighted average of potential temperature change across the inversion layer for the six stations gives a representative value for the whole area of $+4.3^{o}C$. Hence, the net average entrained heat flux for the whole 24 hr period is

$$c_p \overline{\Delta\theta}(4.10 \times 10^{-3}) = 17.8 \text{ Wm}^{-2} .$$

For a 16 hr. period of sunlight, the average would have to be 26.7 Wm^{-2} to produce the same effect and if the entrained heat flux is roughly sinusoidal in nature then it would require a maximum, approximately mid-day, value of $\frac{\pi}{2}(26.7) = 41.9$ Wm^{-2}.

On 11th June 1969 the stations shown in Figure (3.2) reported an average cloud cover of 2 oktas, 1 okta and < 1 okta at 6.00h, 12.00h and 18.00h respectively. Assuming an average cover throughout the day of 1 okta and using the appropriate diagrams of Smith et al. (1972), the methods discussed in §5.1 suggest that, on such a day in Central England, the available energy for a vegetated surface with an albedo of 0.25 is about 440 Wm^{-2} at mid-day. However, 38°/o of the area shown in Figure (3.2) comprises sea-surface which, even under conditions of large net radiation, does not increase

its temperature and does not produce any significant convection; thus, the effective maximum available energy per unit area of the whole surface should be reduced to 273 Wm^{-2}.

Cattle and Weston (1975) have shown that, after a settled summer anti-cyclonic period over S. England, the regional Bowen ratio has a value of approximately 2. (This figure may be regarded as an upper limit since one of their two measurements was made after a dry spell in early spring, when the average regional leaf area index would be lower than in summer, and the other measurement, made in summer, was less certain but indicated a lower value closer to 1.5.) Since 11th June 1969 was preceded by seven dry days throughout the area, it may be assumed that $\beta = 2$ is typical of the land surfaces in England, Wales and Ireland and thus, of a maximum available energy of 273 Wm^{-2}, only 182 Wm^{-2} will be removed as a turbulent sensible heat flux capable of producing entrainment at the inversion.

Comparison of this flux with the magnitude of the entrained heat flux calculated earlier implies that the near-mid-day entrainment coefficient has a value of $41.9|182 = 0.23$ (if a Bowen ratio of unity is assumed then the coefficient increases to 0.31).

The value estimated by this method is very close to that quoted in Chapter 2 and is further justification for the use of the value of 0.25 in the remainder of this thesis.

CHAPTER 4

DIURNAL VARIATION OF HUMIDITY OVER VEGETATION UNDER ANTI-CYCLONIC CONDITIONS

4.1 Introduction

It was never intended in this thesis to become involved in detailed numerical modelling. From the outset it has been considered more profitable to concentrate on a set of assumptions and on a model which would provide an analytical solution which was both easily understandable and readily applicable; inevitably, this approach has resulted in a sacrifice of rigour and accurary.

Chapter 2 presents a theory of entrainment which, for the first time, results in a diurnal variation of the entrainment coefficient (A) which is expressible in analytical form, as in Equation (2.6). This removes the first and major obstacle in attempting to model the boundary layer, since previous models have included a discontinuous change in A at various times of day and have thereby demanded the application of numerical integration methods.

4.2 Model of Boundary Layer Process

4.2(a) Diurnal Variation of Inversion Height

The theory of Chapter 2 allows for the finite diffusion time of thermally generated eddy-energy in the boundary layer and predicts that the heat flux just below the inversion at any time is

$$H_h(t) = -A.H_o(t) \quad , \qquad (4.1)$$

where A is defined by Equation (2.6). The assumption is now made that

$$H_o(t) = H_{ox} \sin \Omega t, \qquad (4.2)$$

where the Earth's angular velocity, Ω, is adjusted to account for the varying length of day with season (see List of Symbols).

Using the nomenclature of Carson (1973), the rate at which volume of air is entrained into the boundary layer per unit area, $w_e(t)$, is defined by

$$F_h(t) = -\rho_h c_p w_e(t) \Delta\theta \simeq H_h(t) \qquad (4.3)$$

where the approximation is very good as F_h and H_h are equal to within about $0.01^o/o$.

The rate at which mass is entrained into the boundary layer per unit area is $\rho_h g\, w_e(t)$ and hence, over a period of time t_o to t, the increase in mass per unit area of the boundary layer due to entrainment is $\int_{t_0}^{t} \rho_h g\, w_e(t).dt$ and the resulting increase in depth of the boundary layer is $\frac{R\overline{T}}{g\overline{p}} \int_{t_0}^{t} \rho_h g\, w_e(t).dt$, where $\overline{T}$ and $\overline{p}$ are the average temperature (^oK) and pressure (Nm^{-2}) of the boundary layer. If the initial depth of the boundary layer is $h(t_o)$ and there is a constant rate of subsidence, sub, then, at any time t, the height of the inversion is

$$h(t) = h(t_o) - sub(t-t_o) + \frac{R\overline{T}}{g\overline{p}} \int_{t_0}^{t} \rho_h g\, w_e(t).dt \,. \qquad (4.4)$$

The solution of this equation is complicated by the inversion-height dependence of $\overline{T}$ and $\overline{p}$. For inversion heights between 500m and 2000m, the error introduced into the entrainment term by using the values of T_o and p_o, instead of $\overline{T}$ and $\overline{p}$, ranges between $+1.5^o/o$ and $+7^o/o$. If the values $(T_o - 5^oK)$ and $(p_o - 5 \times 10^3 Nm^{-2})$ are used, then the error lies between $-1.5^o/o$ and $+3.5^o/o$ and is zero when $h \simeq 1000m$. This level of error is tolerable when it is

remembered that, in Equation (4.4), the entrainment term and $h(t_o)$ are likely to be similar in magnitude and hence the error in $h(t)$ is not likely to exceed $2^o/o$ at any time.

Substitution of Equations (4.1), (4.2) and (4.3) into Equation (4.4) and subsequent integration gives

$$h(t) = h(t_o) - \text{sub}(t-t_o) + \frac{R(T_o-5)A'H_{ox}}{c_p(p_o-5\times10^3)\Delta\theta\Omega(1-\psi)} \times \{\cos\Omega((1-\psi)t_o-\phi) - \cos\Omega((1-\psi)t-\phi)\}, \quad (4.5)$$

where T_o has a time dependence and may change its value by anything up to $8^o/o$ during the day; its diurnal variation is assumed to be

$$T_o(t) = T_o(t_o) + \left[T_{ox}-T_o(t_o)\right] \sin\Omega((1-\psi)^2 t-(2-\psi)\phi) . \quad (4.6)$$

This complicated form is employed for two reasons; firstly, the time dependency is identical to that of the entrainment term in the vapour flux balance described in § 4.2(d) and, secondly, it represents the shape of the diurnal temperature change quite accurately, as shown in the test cases of §4.3(c).

Substitution of Equation (4.6) into Equation (4.5) leads to the final form of the inversion height equation,

$$h(t) = h(t_o) - \text{sub}(t-t_o) + \frac{RA'H_{ox}\left[T_o(t_o)-5+(T_{ox}-T_o(t_o))\sin\Omega((1-\psi)^2 t-(2-\psi)\phi)\right]}{c_p\Delta\theta(p_o-5\times10^3)\Omega(1-\psi)} \times \{\cos\Omega((1-\psi)t_o-\phi) - \cos\Omega(1-\psi)t-\phi)\} . \quad (4.7)$$

4.2(b) Latent Heat Balance of the Boundary Layer

The latent heat balance of a column of unit cross-sectional area extending from the ground to the bottom of the inversion layer has only three flux terms; one is the vapour flux downwards from the inversion resulting from the entrainment process (a), one is the vapour flux upwards from the vegetative cover (b) and the last is the vapour flux outwards across the vertical sides of the column (c). This last term results from frictionally induced cross-isobar flow and, to a greater or lesser extent, is associated with dynamical subsidence.

(a) Expressed in a form similar to that of Equation (4.3), the latent heat flux just below the inversion is

$$\lambda E_h(t) = \rho_h \lambda q_u \, w_e(t) \qquad (4.8)$$

which, with Equations (4.1), (4.2) and (4.3), implies that

$$\lambda E_h(t) = \frac{\lambda}{c_p} \cdot \frac{q_u}{\Delta\theta} \cdot A' . H_{ox} \sin\Omega((1-\psi)t-\phi). \qquad (4.9)$$

(b) Monteith (1965) expresses the latent heat flux from a vegetative cover as

$$\lambda E_o(t) = \frac{\Delta . R_n + \frac{\rho_o c_p}{r_a} (vpd)}{\Delta + \gamma(1 + \frac{r_s}{r_a})} , \qquad (4.10)$$

where (vpd) = vapour pressure deficit.

The present study is of a coniferous forest under dry, anti-cyclonic conditions, for which case r_s is large (typically 120 sm^{-1} at mid-day) compared to r_a (typically 6 sm^{-1}) and the vapour pressure deficit is fairly large (typically 1000 Nm^{-2} at mid-day), thus

permitting an approximation, which is true to within 20°/o, that the latent heat flux is

$$\lambda E_o(t) = \frac{\rho_o c_p (vpd)}{\gamma r_s} = \frac{\rho_o c_p p_o}{0.622 \gamma r_s} (shd), \qquad (4.11)$$

where (shd) = specific humidity deficit = $q_s(T_o) - q_o$. (4.12)

A computerised fitting of orthogonal polynomials of increasing degree to a set of data of q_s and T determined that the second order polynomial,

$$q_s(T) = (1485.7 - 10.96T + 0.02027.T^2) gkg^{-1}, \qquad (4.13)$$

is accurate to better than ± 2°/o over the range of temperature 278°K to 298°K.

Substitution of Equations (4.12), (4.13) and (4.6) into Equation (4.11) implies that

$$\lambda E_o(t) =$$

$$\frac{\rho_o c_p p_o . 10^{-3}}{0.622 \gamma r_s} \Big[1485.7 - 10.96 (T_o(t_o) - (T_{ox} - T_o(t_o)) \sin\Omega ((1-\psi)^2 t - (2-\psi)\phi)$$

$$+ 0.02027 (T_o(t_o) + (T_{ox} - T_o(t_o)) \sin\Omega ((1-\psi)^2 t - (2-\psi)\phi))^2 - q_o(t)\Big] . \qquad (4.14)$$

(c) The vapour flux divergence out of the column due to subsidence is given simply by

$$\lambda E_{div}(t) \simeq - \bar{\rho} \lambda q_o(t)sub \ , \qquad (4.15)$$

where $\bar{\rho}$ is the average density of the boundary layer.

4.2(c) Physiological Influence Through r_s

The vapour flux described by Equation (4.11) is partly controlled by the value of the canopy or surface resistance, r_s, which is closely related to the average stomatal resistance of the vegetative cover. The Hydrometeorological Section of the Institute of Hydrology has found that, for 60 dry days, the average surface resistance of Thetford Forest increases almost linearly with time from 95 sm^{-1} at 7.30 GMT to 123 sm^{-1} at 12.30 GMT and thereafter increases more rapidly to 240 sm^{-1} by 17.30 GMT. This increase in surface resistance is probably due to an accumulating soil water stress and naturally tends to decrease the magnitude of the ground-source vapour flux; however, this effect cannot, by itself, ever account for an actual drop in humidity, as is often observed over the forest during the day. For this reason the varying physiological control throughout the day may be regarded as less important than the synoptic influence of the entrainment process.

A monotonically increasing value of r_s during the day is by no means universal; Szeicz et al. (1973) discover that on four out of five days there is a minimum of leaf resistance during the middle of the day, whereas an erratic increase in resistance occurs throughout the fifth day which is one of some water stress; McNaughton and Black (1973) find that the canopy resistance of a Douglas Fir forest is fairly constant with time for three out of four days and on the fourth rises from 50 sm^{-1} at 6.00 PST to 150 sm^{-1} at 1600 PST. The behaviour of Thetford Forest is consequently not typical of all vegetative covers and is perhaps a result only of the species

of tree and of the very porous and friable sandy soil of the region, which results in a build-up of soil water stress during the day.

Finally, and most importantly, if a linear increase with time of r_s is included in Equation (4.11), then it becomes impossible to solve Equation (4.17) analytically and the employment of numerical methods becomes essential.

For these three reasons the physiological control over humidity is approximated in this chapter by ascribing to r_s an appropriate constant value which, in the test of §4.3(c), is taken as the measured mid-day value of each of the seven test days.

4.2(d) Diurnal Variation of Specific Humidity near the Ground

A small volume of air just above the vegetative cover will have a balance of latent heat slightly different from that of a column as described in §4.2(b). Chapter 2 emphasised that the boundary layer is not perfectly mixed but has a finite resistivity and thus the vapour flux which is entrained into the boundary layer from the inversion layer will produce its effect at the ground some time later. The phase shift between the entrained flux and the driving ground-source flux at any time has been expressed in Equation (2.5) as $\Omega(\psi t + \phi)$. When the sensible heat flux at the ground (H_o) has a magnitude corresponding to the time t, the heat flux at the inversion has a magnitude determined by H_o at the time $(t-\psi t-\phi)$. Similarly, when the entrained heat flux, at the inversion has a magnitude corresponding to the time t', a small volume of air at ground-level is responding to the heat flux which was

entrained at time $(t'-\psi t'-\phi)$; if $t' = t-\psi t-\phi$, then the volume is responding to the entrained flux whose magnitude is determined by the ground-source heat flux at time $((1-\psi)^2 t - (2-\psi)\phi)$.

Hence, for the small volume at ground level, Equation (4.9) becomes

$$\lambda E_{oe}(t) = \frac{\lambda}{c_p} \cdot \frac{q_u}{\Delta\theta} \cdot A' \cdot H_{ox} \sin\Omega((1-\psi)^2 t - (2-\psi)\phi). \quad (4.16)$$

If the small volume is defined as one n^{th} part of the whole column, then summing the three terms in the latent heat flux balance, (Equations (4.14), (4.15) and (4.16)), integrating over the period of time t_o to t and equating this to the change in internal latent heat of the volume over the same period results in the equation

$$\frac{1}{n} \int_{t_0}^{t} \left[\lambda E_o(t) + \lambda E_{oe}(t) + \lambda E_{o\ div}(t)\right] .dt = \frac{1}{n} \rho_o \lambda \left[q_o(t)h(t) - q_o(t_o)h(t_o)\right], \quad (4.17)$$

which, unfortunately, does not have an analytical solution.

This is due to the feedback terms represented by the appearance of $q_o(t)$ in $\lambda E_o(t)$ and $\lambda E_{o\ div}(t)$ of Equations (4.14) and (4.15) respectively. The only way to resolve this problem, other than by numerical methods, is to approximate the terms by substituting the constant value $q_o(t_o)$ in place of $q_o(t)$; in effect, this removes the dependence of the ground-source latent heat flux on the diurnal variation of the ambient specific humidity which, typically, may lead to an error of 7°/o in this flux at mid-day, and it also removes the dependence of the divergent latent heat flux on the specific humidity and, thereby,

may introduce an error of about 13°/o at mid-day. This latter error is less important since the divergent flux is small. The neglect of feedback terms in the latent heat flux balance may, typically, result in an inaccuracy of 7°/o at mid-day which, with the error mentioned in § 4.2(b) may give an overall error in the flux balance of about 20°/o at mid-day; if q_o falls during the day then this error is in the sense of an underestimate of the net vapour flux into the boundary layer.

The diurnal variation of specific humidity near the ground may now be determined from Equations (4.14), (4.15), (4.16) and (4.17), with the above assumption, to be

$$
\begin{aligned}
q_o(t) = \frac{1}{h(t)}\Bigg[& q_o(t_o)\{h(t_o)-\mathrm{sub}(t-t_o)\} \\
& + \frac{q_u A' H_{ox}}{\rho_o c_p \Delta\theta\Omega(1-\psi)^2}\{\cos\Omega((1-\psi)^2 t_o-(2-\psi)\phi) \\
& \qquad - \cos\Omega((1-\psi)^2 t-(2-\psi)\phi)\} \\
& + \frac{p_o c_p .10^{-3}}{0.622\gamma\lambda r_s}\Big\{(t-t_o)(1485.7-10.96T_o(t_o)+0.02027T_o^2(t_o) \\
& \qquad -q_o(t_o).10^3) \\
& + \frac{T_{ox}-T_o(t_o)}{\Omega(1-\psi)^2}(10.96-0.04054T_o(t_o))(\cos\Omega((1-\psi)^2 t-(2-\psi)\phi) \\
& \qquad -\cos\Omega((1-\psi)^2 t_o-(2-\psi)\phi)) \\
& + \frac{0.02027(T_{ox}-T_o(t_o))^2}{2(1-\psi)^2}\Big[(t-t_o)(1-\psi)^2 \\
& \qquad + \frac{\sin 2\Omega((1-\psi)^2 t_o-(2-\psi)\phi)-\sin 2\Omega((1-\psi)^2 t-(2-\psi)\phi)}{2\Omega}\Big]\Big\}\Bigg]
\end{aligned}
\tag{4.18}
$$

where $h(t)$ is given by Equation (4.7).

4.3 Test of Model

4.3(a) Test Data

The validity of the Equations (4.7) and (4.18) is tested by using data from seven fairly cloudless days (≤ 3 oktas cover) in 1971. The behaviour of Thetford Forest on these days is described in detail by Stewart and Thom (1973) who provide information on the diurnal variation of available energy, ground-source latent heat flux and canopy resistance; thus are provided the values of H_{ox} (assumed to be the maximum available energy minus the maximum latent heat flux) and of r_s (assumed to be constant at its measured mid-day value). The Institute of Hydrology has kindly provided data from which can be calculated hourly average values of temperature and specific humidity averaged over the top four upwind levels of the instrument tower (Plate(1)); thus are provided the values of $T_o(t_o)$, T_{ox} and $q_o(t_o)$ and the measured diurnal variation of specific humidity with which to compare the calculated value. Data on the inversion are extracted from the Daily Aerological Record of the U.K. Meteorological Office; the values of q_u and $\Delta\theta$ are taken as the average values for the 00.00h, 12.00h and 24.00h ascents at Crawley and at Hemsby and the height of the bottom of the inversion layer, again as an average for the two stations, is determined at 00.00h, 12.00h and 24.00h on each day. Unfortunately, for only two of the seven test cases (3rd June 1971 and 7th July 1971) does the tethered balloon at Cardington provide soundings giving information on the inversion structure during the middle part of the day and so this information is only used as corroborative evidence for the validity of the Crawley and Hemsby data.

The Daily Weather Report of the U.K. Meteorological Office is the source for p_o which is the 12.00h value at Honington. In accordance with the values of §2.3(b), ϕ and ψ are chosen to correspond respectively to the initial height of and to the change in height of the inversion layer.

4.3(b) Method of Calculation

The sources listed in §4.3(a) provide values of H_{ox}, r_s, $T_o(t_o)$, T_{ox}, $q_o(t_o)$, q_u, $\Delta\theta$ and p_o. The choice of ϕ and ψ determines the choice of t_o so that none of the trigonometric functions in Equations (4.7) and (4.18) will be negative. Equation (4.7) is then evaluated and the unknown value of "sub" (typically $+4 \times 10^{-3} ms^{-1}$) is adjusted until the predicted behaviour of the inversion height agrees fairly well with the three measured heights at 00.00h, 12.00h and 24.00h; for this calculation, it is assumed that the inversion level descends linearly, at the rate specified by "sub", between midnight and dawn and between the following sunset and midnight. Once the value of "sub" has been established, sufficient information is available for Equation (4.18) to predict the diurnal variation of specific humidity and, thereafter, a comparison may be made with the measured variation.

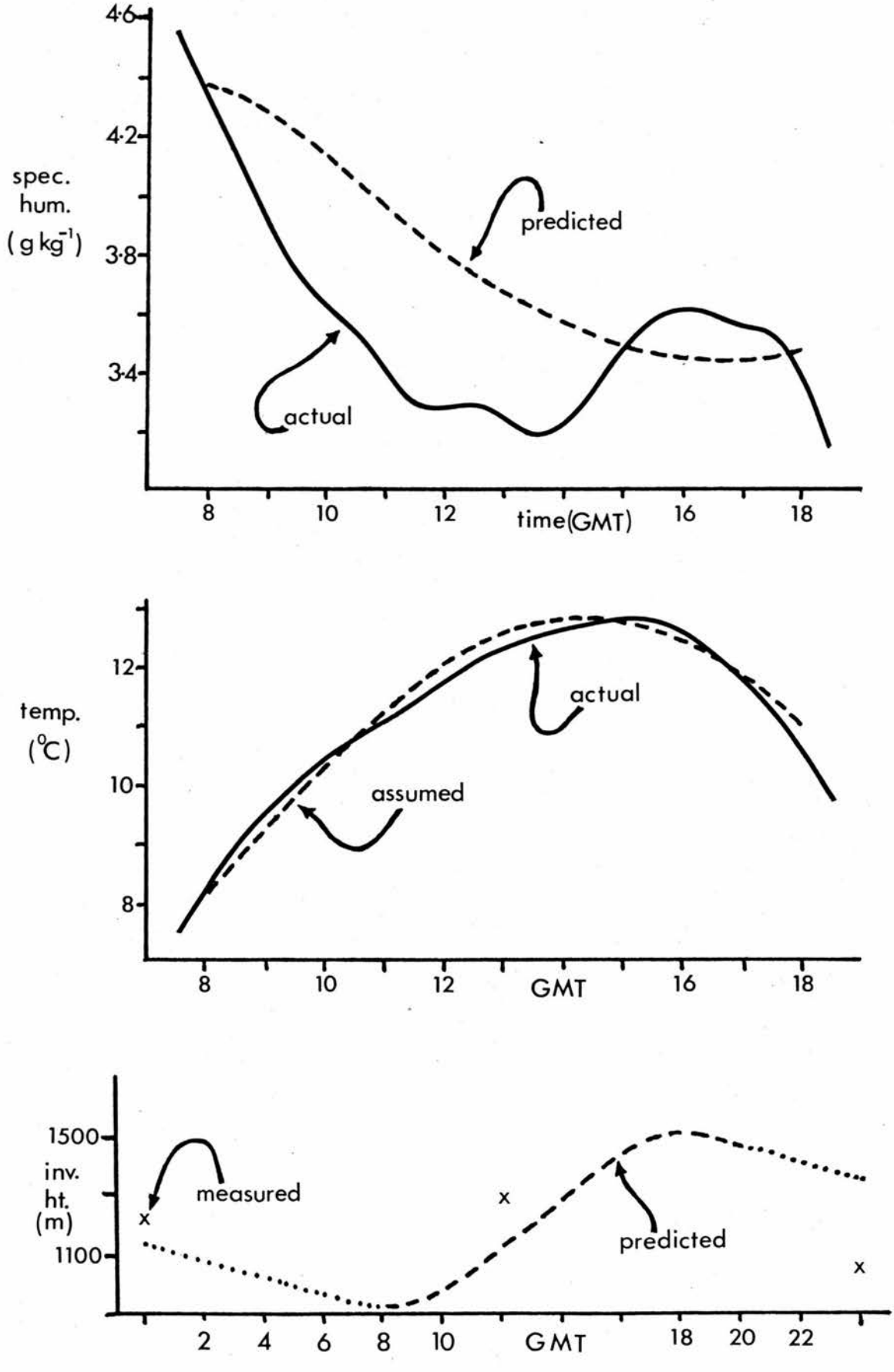

Figure (4.1) 2nd May 1971.

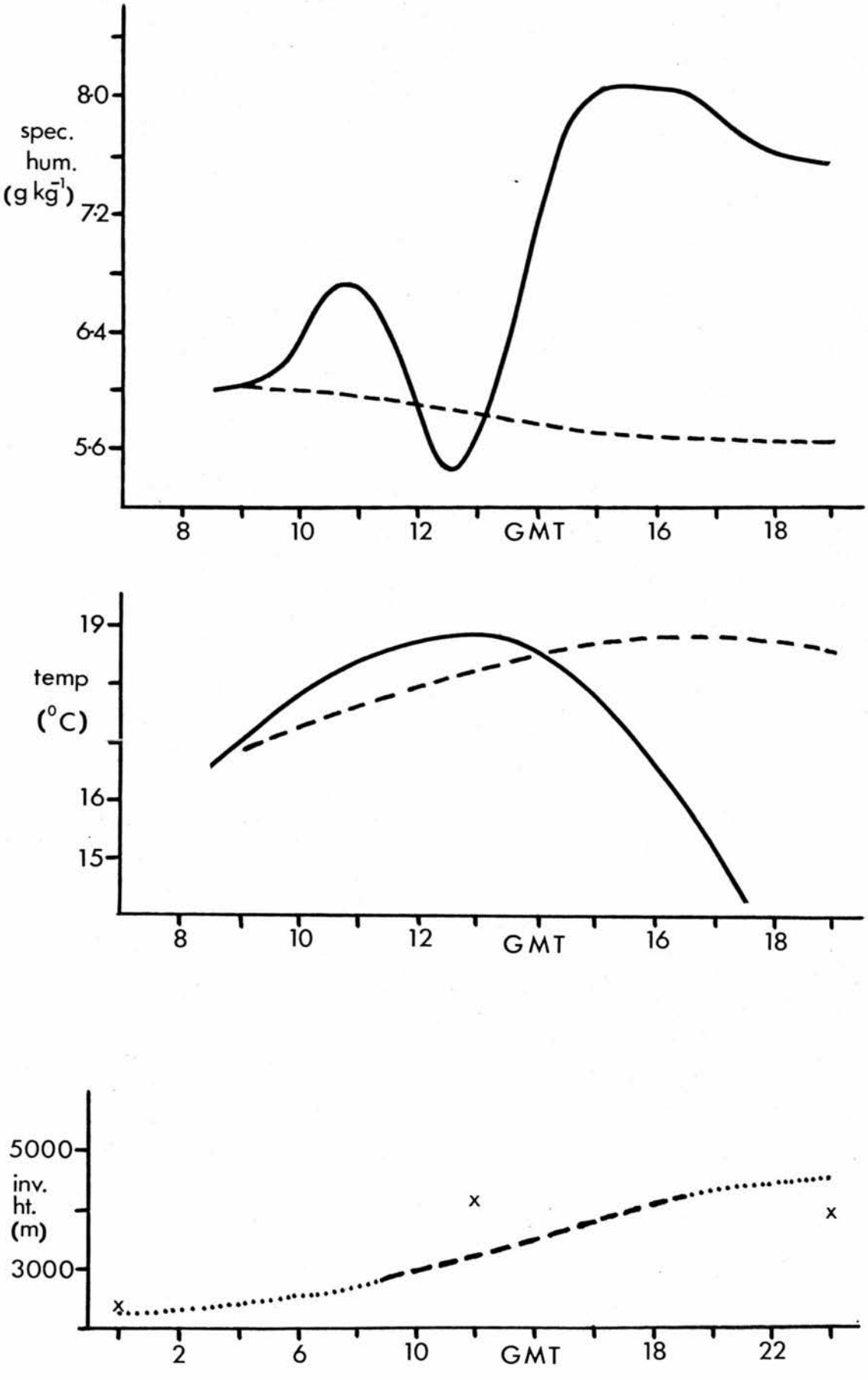

Figure (4.2) 2nd June 1971.

4.3(c) Test Cases

2nd May, 1971, Figure (4.1). The parameters for use in Equations (4.7) and (4.18) are:

$h(t_o)$	= 930m	t_o	= 2hr	$\Delta\theta$	= 3^oC
$q_o(t_o)$	= 4.4 gkg^{-1}	sub	= $+7\times10^{-3}ms^{-1}$	ψ	= 0.025
q_u	= 1.5 gkg^{-1}	H_{ox}	= 460 Wm^{-2}	ϕ	= 1hr
r_s	= 120 sm^{-1}	p_o	= 102000 Nm^{-2}	$T_o(t_o)$	= 281.25^oK
T_{ox}	= 285.8^oK	A'	= 0.25	Ω	= 7.272×10^{-5}rad s^{-1}

This case immediately confirms that the specific humidity can drop during the day despite a large latent heat flux from the ground which, on this day, reached a maximum value of 180 Wm^{-2}.

2nd June, 1971, Figure (4.2). The parameters are:

$h(t_o)$	= 2900m	t_o	= 4hr	$\Delta\theta$	= 4.4^oC
$q_o(t_o)$	= 6.0 gkg^{-1}	sub	= $-18\times10^{-3}ms^{-1}$	ψ	= 0.05
q_u	= 2.0 gkg^{-1}	H_{ox}	= 480 Wm^{-2}	ϕ	= 2 hr
r_s	= 170 sm^{-1}	p_o	= 100800 Nm^{-2}	$T_o(t_o)$	= 290.01^oK
T_{ox}	= 291.82^oK	A'	= 0.25	Ω	= $6.233\times10^{-5}rads^{-1}$

(The negative value of "sub" used here is in an attempt to allow for the change in inversion height during the day presumably due to advection.)

Clearly, on this day, Thetford experienced substantial advection which is revealed by the dramatic increase in specific humidity and by the decrease in temperature after 12.30 GMT.

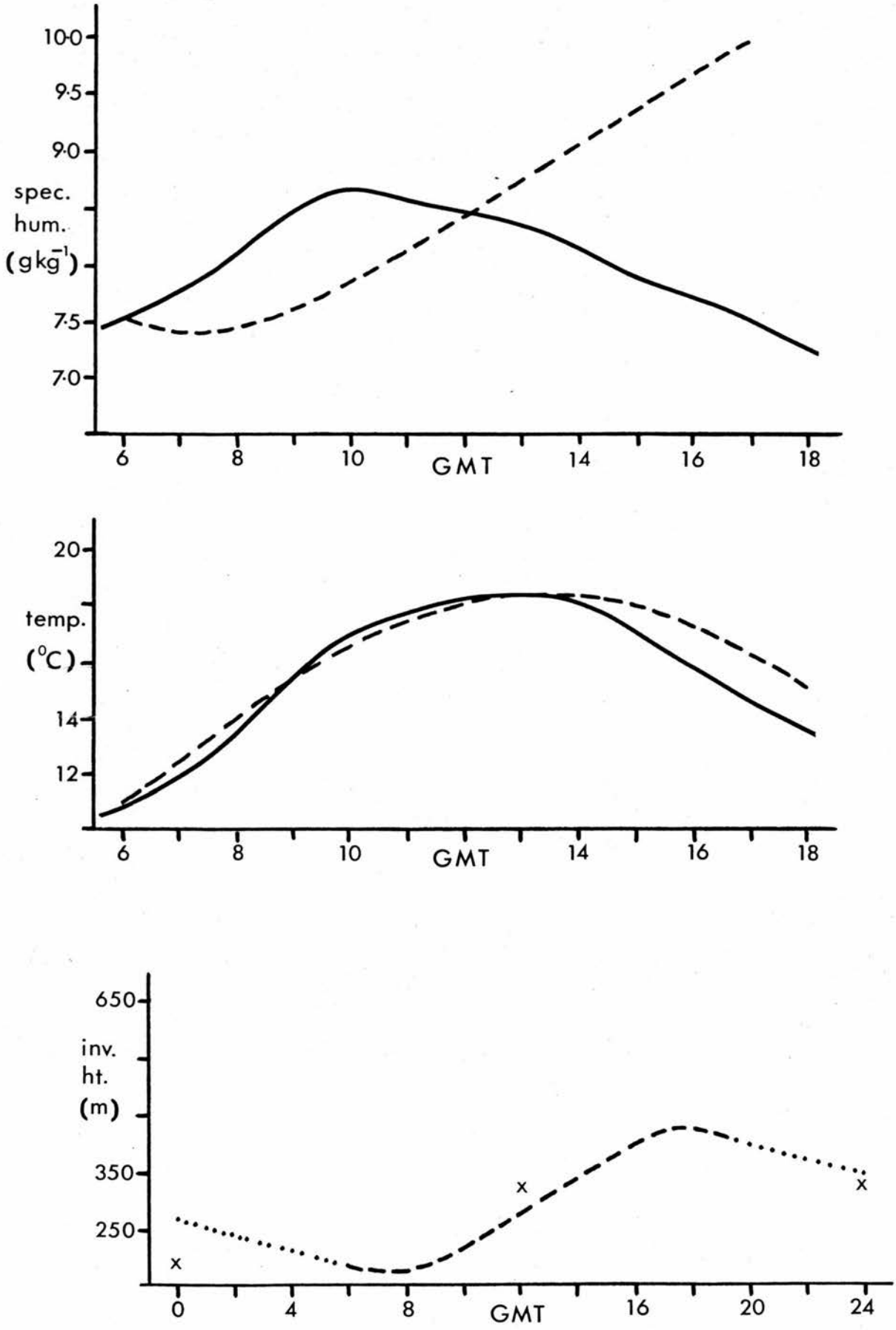

Figure (4.3) 3rd June 1971.

Similar changes were recorded at the nearby meteorological station of Honington but not further inland at Cardington. Further, the radio-sonde ascents at Hemsby, in particular, reveal a very complicated vertical structure which may be due to the advection across the North Sea of the continental boundary layer and, for this reason, it is difficult to parameterise the entrainment process with any confidence.

Smith (1974) notes that, even against a 10 kt wind, a sea-breeze front managed to penetrate inland as far as Thetford by 18.00 GMT on 14th June 1973. In the case studied here, the wind was generally easterly and blowing at about 10 kt and, therefore, it is possible that a sea-breeze front passed over Thetford Forest at about 13.00 GMT. Anyway, advection after that time appears to invalidate what may otherwise have been a reasonable forecast.

3rd June, 1971, Figure (4.3) The parameters are:

$h(t_o)$	= 180m	t_o	= 1 hr	$\Delta\theta$	= 7.9°C
$q_o(t_o)$	= 7.5 gkg^{-1}	sub	= $+4\times10^{-3} ms^{-1}$	ψ	= 0.025
q_u	= 8.0 gkg^{-1}	H_{ox}	= 500 Wm^{-2}	ϕ	= 0.5 hr
r_s	= 140 sm^{-1}	p_o	= 101500Nm^{-2}	$T_o(t_o)$	= 284.06°K
T_{ox}	= 291.5°K	A'	= 0.25	Ω	= $6.233\times10^{-5} rads^{-1}$

As on the previous day, the vertical structure of the atmosphere was very complicated. For a day with such a low inversion and almost clear skies, the diurnal temperature rise was very small because of a north-easterly wind blowing at greater than 10 kt and so advection again played an

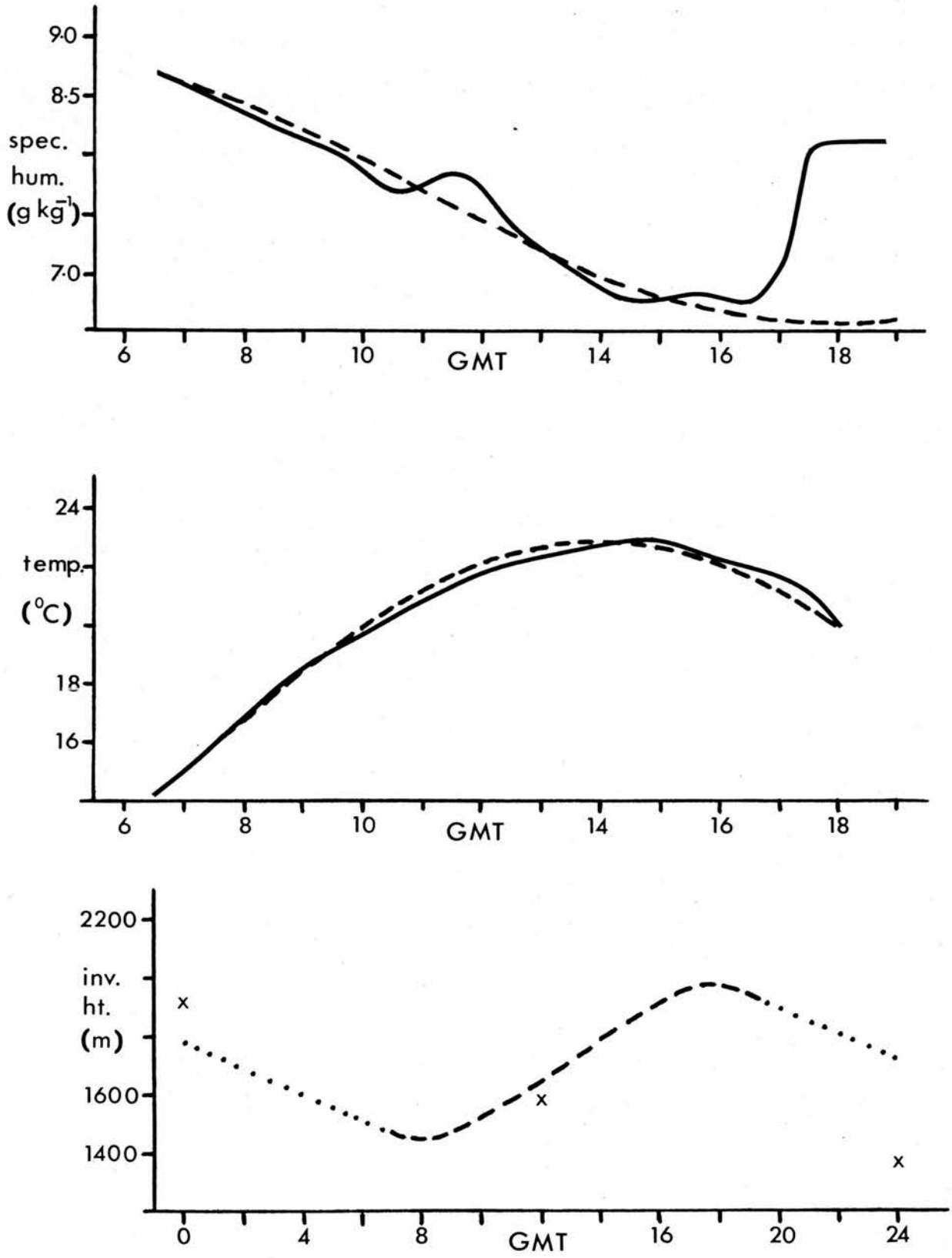

Figure (4.4) 7th July 1971.

influential role on this day. However, of the seven test cases, this is the only one for which a significant rise of specific humidity is forecast and, except for the obviously advective case of Figure (4.2), it is the only day on which the specific humidity does increase.

7th July 1971, Figure (4.4) The parameters are:

$h(t_o)$	= 1470m	t_o	= 2 hr	$\Delta\theta$	= 2.6°C
$q_o(t_o)$	= 8.6 gkg^{-1}	sub	= $+12\times10^{-3}ms^{-1}$	ψ	= 0
q_u	= 2.7 gkg^{-1}	H_{ox}	= 400 Wm^{-2}	ϕ	= 1 hr
r_s	= 140 sm^{-1}	p_o	= 102500Nm^{-2}	$T_o(t_o)$	= 288.18°K
T_{ox}	= 295.8°K	A'	= 0.25	Ω	= $6.233\times10^{-5}rads^{-1}$

This was a day of light (7kt) north-easterly wind and of a distinct inversion at all times at both Hemsby and Crawley. The temperature record at Thetford reveals no evidence of advection and so it is not surprising that the agreement between forecast and actual specific humidity is better on this day than on any of the other six test cases.

The rise in humidity at 17.00 GMT was probably due to the build-up of vapour under the beginnings of a low-level radiation inversion.

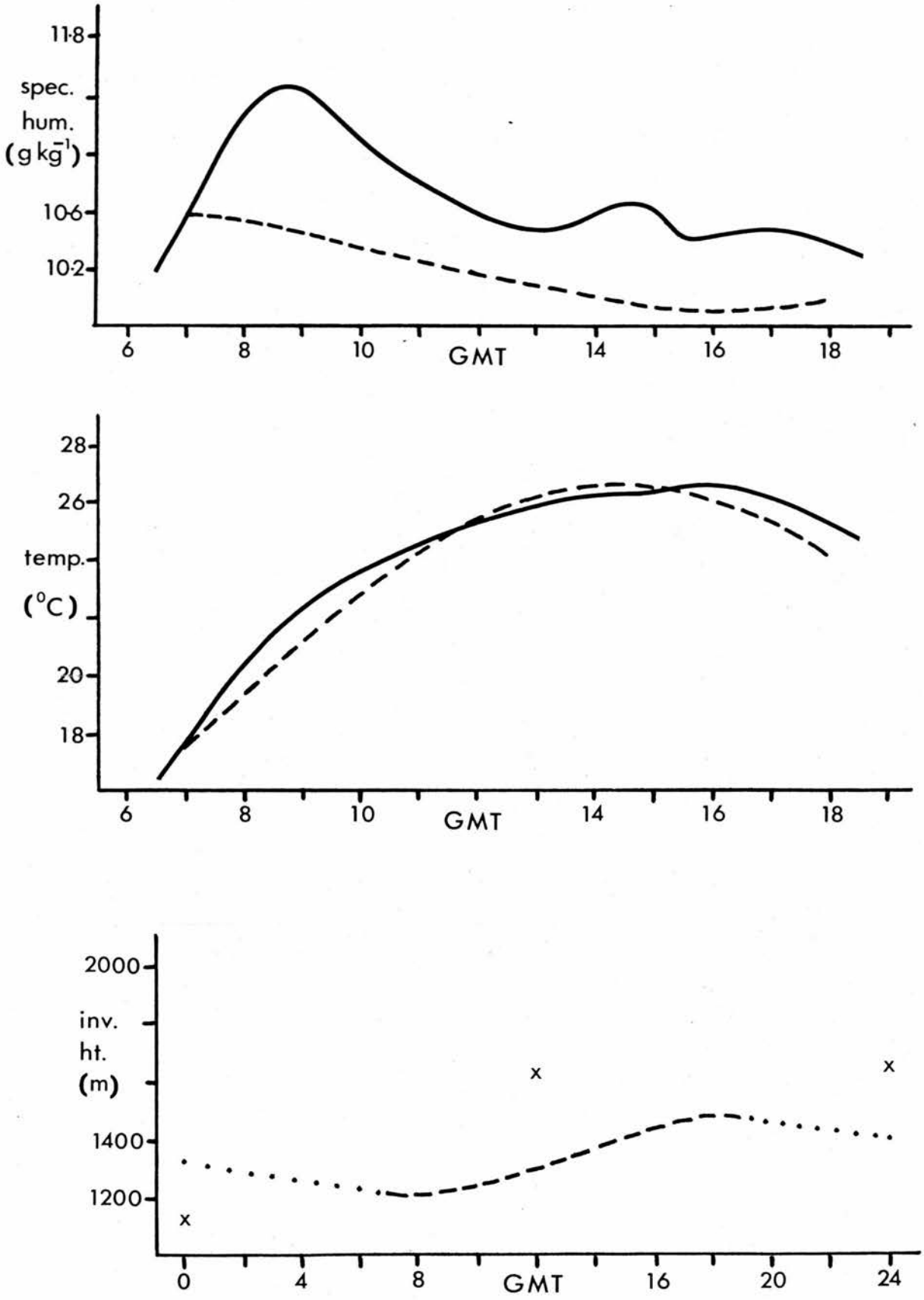

Figure (4.5) 8th July 1971.

8th July 1971, Figure (4.5) The parameters are:

$h(t_o)$	= 1220m	t_o	= 2 hr	$\Delta\theta$	= 5.7°C
$q_o(t_o)$	= 10.6 gkg^{-1}	sub	= $+4.0\times10^{-3} ms^{-1}$	Ψ	= 0.025
q_u	= 2.7 gkg^{-1}	H_{ox}	= 360 Wm^{-2}	ϕ	= 1 hr
r_s	= 130 sm^{-1}	p_o	= 101500Nm^{-2}	$T_o(t_o)$	= 290.64°K
T_{ox}	= 299.6°K	A'	= 0.25	Ω	= $6.233\times10^{-5} rads^{-1}$

This was another day of light winds blowing from the south-east and of a distinct inversion at all times at Hemsby and Crawley. The temperature and dew-point records from Thetford Forest, Honington and Cardington all show that the air was saturated at dawn and the 00.00h ascents at Hemsby and at Crawley reveal a strong low-level radiation inversion. Thus at 7.00 GMT the specific humidity just above Thetford Forest was lower than the average for the layer up to the subsidence inversion because of dew formation overnight. Hence, the value of $q_o(t_o)$ used in Equation (4.18) is really an unrepresentative one, and, perhaps with justification, t_o could be modified subjectively to correspond to the time at which the radiation inversion has been dissipated. Apart from this effect the forecast is correct in its trend.

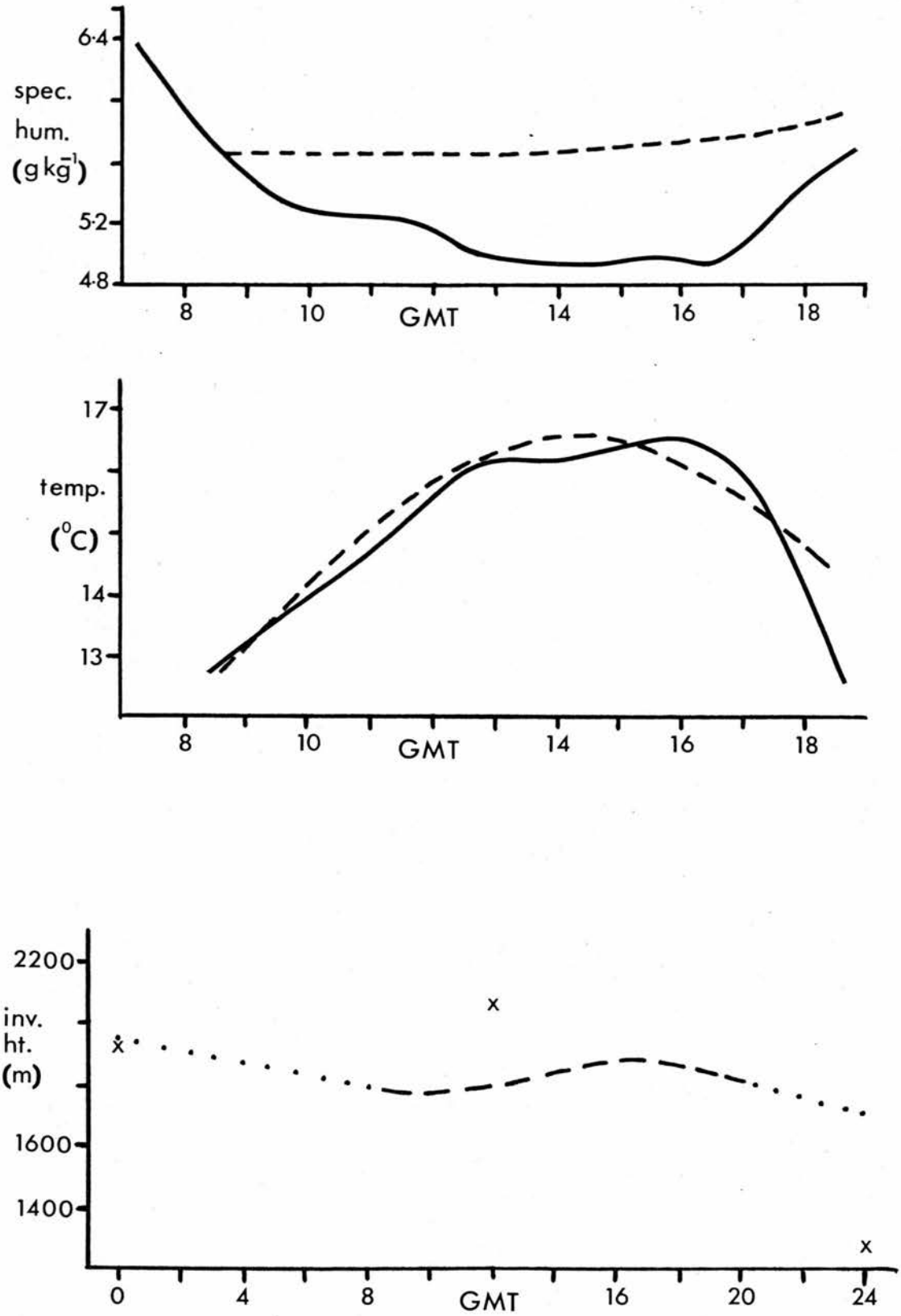

Figure (4.6) 15th September 1971.

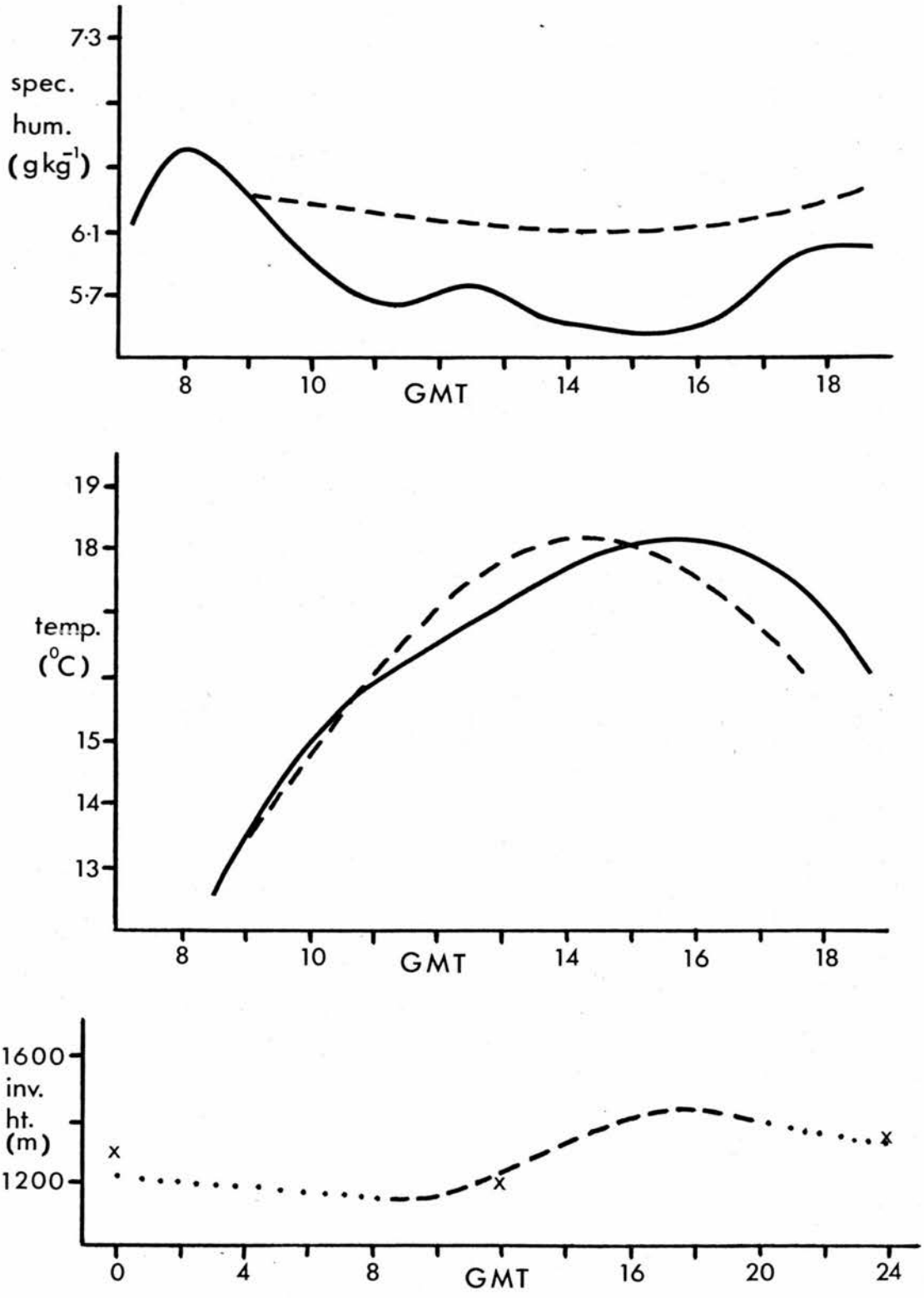

Figure (4.7) 16th September 1971.

15th September 1971, Figure (4.6) The parameters are:

$h(t_o)$ = 1790m	t_o = 2hr	$\Delta\theta$ = 4.9°C
$q_o(t_o)$ = 5.7 gkg^{-1}	sub = $+5.8\times10^{-3} ms^{-1}$	ψ = 0.025
q_u = 2.0 gkg^{-1}	H_{ox} = 270 Wm^{-2}	ϕ = 1 hr
r_s = 120 sm^{-1}	p_o = 102000Nm^{-2}	$T_o(t_o)$= 285.7°K
T_{ox} = 289.6°K	A' = 0.25	$\Omega = 7.933\times10^{-5} rads^{-1}$

Again this was a day of light north-easterly winds with a 3 oktas cloud cover developing in the afternoon. Other than the slight fluctuations in the temperature record perhaps indicating advection, there is no physical reason to explain the difference between the predicted and observed trend in specific humidity.

16th September 1971, Figure (4.7) The parameters are:

$h(t_o)$ = 1150m	t_o = 2hr	$\Delta\theta$ = 4.5°C
$q_o(t_o)$ = 6.3 gkg^{-1}	sub = $+1.4\times10^{-3} ms^{-1}$	ψ = 0.025
q_u = 2.3 gkg^{-1}	H_{ox} = 310 Wm^{-2}	ϕ = 1 hr
r_s = 140 sm^{-1}	p_o = 102500Nm^{-2}	$T_o(t_o)$= 286.5°K
T_{ox} = 291.1°K	A' = 0.25	$\Omega = 8.727\times10^{-5} rads^{-1}$

Very light southerly winds permitted the formation of an overnight radiation inversion and subsequent dew-fall, as for 8th July 1971. Unfortunately, the time t_o is such that the value of specific humidity just above the forest is then high due to the accumulation of vapour underneath this inversion,

and the predicted specific humidity then remains higher than the actual throughout the day. However, the prediction of trend is again good.

4.4 Predictive Value of Model

The seven test cases indicate that, in the absence of advection, the non-numerical model of the humidity-controlling processes in an inversion-capped boundary layer is valuable in predicting the major trend of humidity variation during the day and, in the absence of a nocturnal inversion, can provide an accurate forecast of the absolute values of humidity throughout the day.

Equations (4.7) and (4.18) may be used in a purely predictive sense if the maximum values of temperature and of sensible heat flux during the day can be estimated. Chapter 5 describes a convenient theory by which can be predicted the extent to which cumulus cloud will develop during the day: traditional methods may then be used to determine the maximum net radiation during that day. Equation (4.11) may be used to estimate the maximum latent heat flux by assuming the constancy during the day of the initial value of specific humidity, $q_o(t_o)$, and assuming a maximum daily temperature which, in turn, may be estimated by the method of Johnston (1958). Finally, the maximum sensible heat flux may be taken as the difference between the maximum values of net radiation and of latent heat flux.

CHAPTER 5

A PREDICTOR OF CUMULUS CLOUD COVER

5.1 Dependence of Net Radiation on Cloud Cover

In the previous chapter an equation was derived for the prediction of specific humidity over a vegetated surface during the day (Equation (4.18)). One of the variables in the equation is the daily maximum value of available energy which is very nearly equal to that of net radiation. The net radiation depends on many factors such as time of day, time of year, surface albedo and emissivity, surface temperature, temperature and humidity structure of the atmosphere, turbidity of the atmosphere and amount and depth of cloud cover. Monteith (1973) reviews several empirical equations for the estimation of net radiation. He states that

$$R_n = (1 - \alpha_s)S(c) + \varepsilon_s(L_d(c) - L_u), \qquad (5.1)$$

where for low clouds

$$L_d(c) = \sigma Ta^4 \left[1.20-171/\sigma T_a^4\right]\left[1 + 0.2c^2\right], \qquad (5.2)$$

and $$L_u = \sigma T_s^4 . \qquad (5.3)$$

Lumb (1964) derives empirical equations for estimating the solar radiation over the N. Atlantic under various cloud conditions,

$$S(c) = 1350\, f(c) \sin\beta \quad (Wm^{-2}) \qquad (5.4)$$

$\leq$ 2 oktas cu : $f(c) = 0.61 + 0.20 \sin\beta$ (5.5)

3-5 oktas cu: $f(c) = 0.38 + 0.34 \sin\beta$ (5.6)

7-8 oktas s-c: $f(c) = 0.17 + 0.30 \sin\beta$ (5.7)

thick s-c or st : $f(c) = 0.08 + 0.11 \sin\beta$ (5.8)

Monteith (1973) indicates that, for a grass surface, $\alpha_s = 0.23$ and it would be reasonable to assume that $\varepsilon_s = 95^o/o$ (see Sellers (1965)). If an air temperature of 293°K is assumed and surface temperatures of 297°K, 297°K, 293°K, 293°K respectively assumed under the four cloud conditions of Equations (5.5) to (5.8) and if a solar elevation, β, of 58½°, corresponding to mid-day, mid-summer in the British Isles (55°N), is assumed then Table (5.1) can be constructed using Equations (5.1) to (5.8).

Table (5.1)

Cloud Cover	S(c) Wm^{-2}	L_u Wm^{-2}	$L_d(c)$ Wm^{-2}	$L_d(c)-L_u$ Wm^{-2}	R_n Wm^{-2}
⩽ 2 oktas cu	898.4	441.2	331.5	-109.7	587.5
3-5 oktas cu	771.0	441.2	347.0	- 94.2	504.2
7-8 oktas s-c	490.1	417.9	388.5	- 29.4	349.5
thick s-c or st	200.0	417.9	396.5	- 21.4	133.7

Clearly the net radiation, and hence the available energy, of the grass surface depends very much on the extent and depth of cloud cover. The values of S(c) in Table (5.1) agree quite closely with those which can be calculated from the solar radiation versus time of year diagram and accompanying cloud cover conversion factors used by Smith et al. (1972). Their diagram may be used as an alternative to the Equations (5.4) to (5.8). There are problems in using Equation (5.3) in an estimate of net radiation since, in general, it is difficult to estimate a surface temperature. Monteith (1973) suggests

that under clear-sky conditions it is reasonable to assume that, for a surface at air temperature,

$$L_u - L_d(0) = (107 - T_a{}^{\circ}C)\,Wm^{-2} \qquad (5.9)$$

and so a net loss of 100 Wm^{-2} is a good average figure for the long wave radiative loss from the surface under cloudless conditions. It is also reasonable to reduce this value, proportionately with increase in cloud cover, to about 20 Wm^{-2} for thick strato-cumulus. These approximations may be used in place of Equations (5.2) and (5.3).

Whether the above approximations are used or Equations (5.2) and (5.3), and whether the diagram of Smith et al. (1972) is used or Equations (5.4) to (5.8), it remains essential to forecast the mid-day cloud-cover in order to forecast the mid-day net radiation by Equation (5.1). Under anti-cyclonic conditions this entails the forecasting of the extent of cumulus or strato-cumulus development during the day. The remainder of this chapter develops a theory which results in a predictive method.

5.2 Theory of Cumulus Cloud Formation

Using observations made from an aircraft during a spiral climb from surface to cloud base, Warner (1963) reported the existence of a lapse of specific humidity in the planetary boundary layer below an inversion and a cloud layer. This is compatible with assumptions made in Chapters 2 and 4 where the planetary boundary layer is not regarded as being "well-mixed" and the finite diffusion time of turbulent energy is considered to be important. Supporting evidence for Warner's claim is found in the results of James (1957) although, as stated in the review article of Cornford (1966) anomalies in some of the

accumulated data on the humidity structure of the boundary layer below an inversion warrant further experimentation. The discrete nature of free convection demands a high degree of areal and temporal averaging at several levels below an inversion in order to identify with certainty the presence of a small lapse of specific humidity.

5.2(a) Entrainment across the Inversion

For an inversion-capped boundary layer the entrainment process may be parameterised in the usual way by employing the entrainment coefficients A' or A. Since the following calculations are all made at mid-day then $A \simeq A'$ and, as before, it will be assumed that, at this time, both have the value of 0.25.

The entrainment process introduces warm, dry air into the top of the boundary layer. This addition acts as a source of heat but as a sink of water vapour. For this air to be dampened to the average specific humidity of the boundary layer requires, just below the inversion, an upward flux of vapour of magnitude

$$\lambda E_h = \rho_h \lambda \Delta q \, w_e = - A \frac{\lambda}{c_p} \frac{\Delta q}{\Delta \theta} H_o \quad . \qquad (5.10)$$

This theory postulates that the boundary layer is not perfectly mixed but has a small, finite resistivity and, in the same way as a current through an electrical resistance maintains a potential gradient along that resistance, so the fluxes of water vapour into the boundary layer at the bottom and effectively out of the boundary layer at the top maintain a gradient of specific humitity throughout the layer; hence,

the gradient is proportional to the sum of the flux of Equation (5.10) and the vapour flux upward from the ground and is also inversely proportional to the depth of the boundary layer. The gradient may then be expressed as

$$m = -\frac{c}{h} H_o \left(\frac{1}{\beta} - A \frac{\lambda}{c_p} \frac{\Delta q}{\Delta \theta}\right) , \qquad (5.11)$$

where c is the constant of proportionality.

5.2(b) Entrainment across a Bubble Surface

As a convective bubble rises from the ground, turbulence in the air and in its own wake will cause entrainment across its surface. If the bubble rises into progressively drier air then the bubble itself will gradually become drier. Warner (1963) derives the following equation for the specific humidity of air in a convective bubble at any height:

$$q = q_o + \frac{3}{4} mz - \frac{m r_o}{4a} \left(1 - \left(\frac{r_o}{r_o + az}\right)^3\right) \qquad (5.12)$$

where q_o and r_o are the bubble's initial specific humidity and radius. The constant a has been experimentally determined by Turner (1963) to lie between 0.2 and 0.3.

Differentiation of Equation (5.12) with respect to r_o gives

$$\frac{\partial q}{\partial r_o} = -\frac{m}{a}\left(\frac{1}{4} + \left(\frac{r_o}{r_o + az}\right)^3 \left[\frac{3}{4}\left(\frac{r_o}{r_o + az}\right) - 1\right]\right) \qquad (5.13)$$

which, for a negative gradient m, is always greater than zero for positive or negative values of r_o (although, of course, the latter are physically unrealistic). The important result is that, at any given height, larger bubbles will always have a higher specific humidity than smaller bubbles.

5.2(c) Process of Cloud Formation

It is postulated that the extent of cloud cover depends upon the initial radius of the smallest bubble which is still saturated at the inversion after rising through the boundary layer.

In clear sky conditions, convection from the ground becomes organised into a pattern of large and discrete rising thermals. It is envisaged that if conditions are right for these thermals to form clouds then the result is a sparse cover, perhaps of about 1 okta. The shadow effect of these clouds on the ground produces great temporal variability in net radiation at any location and thereby in sensible heat flux. It is postulated that this process begins to destroy the large-scale convective organisation and so more but smaller thermals predominate. If these thermals are still large enough to be saturated below the inversion then further cloud formation will occur and the cover will increase. A steady-state will be attained when thermals leave the ground with an initial radius which allows them just to be saturated at the inversion. A thermal of smaller initial radius than this will reach the inversion unsaturated and cloud evaporation will occur. If the deduced steady-state initial radius is zero then strato-cumulus results. Larger steady-state radii indicate lesser cloud cover.

5.3 Test of Theory

5.3(a) Test Data

The Daily Weather Reports of the U.K. Meteorological Office for the summer months (May, June, July and August) of the years 1970, 1971 and 1973 were scrutinised for front-free

anti-cyclonic days in S.E. England. From these were selected days of cloud type 1, 2, 4 or 8 and cloud cover of 1; 3, 4 or 5; 6, 7 or 8 oktas reported at Gatwick (the code numbers of cloud type refer to various structures and formations of cumulus and strato-cumulus clouds and are explained in detail in "Instructions for the Preparation of Weather Maps", Meteorological Office (H.M.S.O.)). The cloud cover is selected and grouped in this way to give three groups which are of different average cloud cover, which are of roughly the same sample size and which, if possible, are non-contiguous. This process resulted in a total of 69 days for which Tøgrams were drawn using the 12.00 GMT radio-sonde ascent at Crawley. Fifteen days were found to have rather indistinct inversions which were difficult to interpret and, of the remaining fifty-four days, it was discovered that on four days the reported cloud-base height at Gatwick differed from the calculated inversion height at Crawley by 1300m or more. Thus 19 days were rejected and the preceding theory is tested using the remaining fifty days which are split into three groups; days with 6 oktas or more of cloud cover reported, days with 3-5 oktas and days with 1 okta.

5.3(b) Evaluation of c

For saturation of a bubble at the inversion it is necessary that

$$q_o + \tfrac{3}{4}mh - \frac{mr_o}{4a}\left(1 - \left(\frac{r_o}{r_o+ah}\right)^3\right) \geq q_{sh} \qquad (5.14)$$

where q_{sh} is the saturation specific humidity of air just below the inversion and is assumed to be a close approximation to the saturation specific humidity of air in the bubble at

that height. If the initial radius is to be zero then Equation (5.11) and Equation (5.14) require that

$$c \leq -4(q_{sh} - q_o)/3H_o \left(\frac{1}{\beta} - A \frac{\lambda}{c_p} \frac{\Delta q}{\Delta \theta}\right) \qquad (5.15)$$

This expression is evaluated using the twelve days with ≥ 6 oktas of cloud cover at Gatwick. Fortunately the appearance of Δq and $\Delta \theta$ as a ratio makes the result relatively insensitive to the often necessarily subjective choice of the positions of the bottom and top of the inversion layer. The value of A is assumed to be 0.25; β is assigned the constant value of 2 which is a reasonable estimate of the mid-day value for dry anti-cyclonic conditions in S.E. England and is supported by the measurements of Cattle and Weston (1975); H_o is taken to be its clear sky value for this Bowen ratio and the time of year; q_o refers to the value at screen height which Kaimal (1974) finds to be close to the base of the small convective plumes of the atmospheric surface layer which, according to Scorer and Ludlam (1953) then aggregate to form the penetrative, boundary layer thermal.

The average value obtained is

$$c \leq 14.7 \times 10^{-6} . \qquad (5.16)$$

This figure is likely to be an underestimate owing to the over-large value of H_o (its clear sky value) assumed on each of the days. On the other hand, since the strato-cumulus cloud layer is of finite depth then the convective bubbles must be saturated at some height lower than that of the inversion. This can be allowed for by assigning to c a value smaller than that of Equation (5.16). For the following test c is taken as 10^{-5}.

This value of c inserted in Equation (5.11) does give a magnitude of gradient which agrees reasonably well with those quoted by Warner (1963). For example, on 11th Oct. 1965, the calculated value of m is -12×10^{-4} gkg^{-1}m^{-1} whereas the measured value is -7.9×10^{-4} gkg^{-1}m^{-1}.

5.3(c) Separation of Days with Different Cloud Cover, Method 1

For saturation to occur at the inversion, Equation (5.14) may be turned into an equality and from this equation a parameter D may be defined such that

$$D = 4a\left(\frac{3}{4} + \frac{q_o}{mh} - \frac{q_{sh}}{mh}\right) = \frac{r_o}{h}\left(1 - \left(\frac{r_o}{r_o + ah}\right)^3\right) \qquad (5.17)$$

using Equation (5.11) to eliminate m gives

$$D = 4a\left(\frac{3}{4} + \left[(q_{sh} - q_o)/cH_o\left(\frac{1}{\beta} - A\,\frac{\lambda}{c_p}\,\frac{\Delta q}{\Delta \theta}\right)\right]\right) \qquad (5.18)$$

This parameter depends rather weakly on the inversion height h and on the subjectively acquired inversion strength data since, again, Δq and $\Delta\theta$ appear as a ratio. However, the parameter itself is closely related to r_o. Equation (5.17) can, of course, be solved for r_o either graphically or by computer.

In the following test of the three groups of days β is again assumed to be 2 on all occasions, H_o again assigned its clear sky value on all occasions, and a and A both taken to be 0.25. The statistical significance of the separation between the three groups achieved by the parameter D depends little on what constant value of β is chosen. However, it is worsened by assuming equal values of H_o for

TABLE (5.2) - VALUES OF D FOR DAYS IN 1970, 1971 AND 1973, CALCULATED BY EQUATION (5.18).

Date	Cloud cover at 12.00h at Gatwick (oktas)	Inv. height from Crawley ascent at 12.00h (m)	Cloud base reported at 12.00h at Gatwick (m)	D	Mean D ± st. error of mean
27 May 1970	5	1009	1080	0.3	
6 June 1970	3	984	840	0.3	
14 June 1970	4	1066	1050	0.3	
20 June 1970	4	682	960	0.3	
25 June 1970	4	1399	900	0.5	
1 Aug. 1970	4	1291	1140	0.1	
9 Aug. 1970	4	880	750	0.2	
12 Aug. 1970	5	1376	1050	0.4	
4 July 1971	5	1637	1350	-0.3	0.21
13 July 1971	3	1083	1200	0.5	±0.06
16 Aug. 1971	3	1689	960	-0.1	
1 June 1973	4	1070	960	0.2	
8 June 1973	3	1414	1200	0.3	
9 June 1973	3	1364	1140	0.4	
3 July 1973	4	1523	1350	-0.1	
8 July 1973	4	1959	1200	-0.3	
26 July 1973	3	665	840	0.4	
27 July 1973	5	1145	1080	0.4	

TABLE (5.2) (Contd.)

Date	Cloud cover at 12.00h at Gatwick (oktas)	Inv. height from Crawley ascent at 12.00h (m)	Cloud base reported at 12.00h at Gatwick (m)	D	Mean D ± st. error of mean
22 May 1970	7	1723	1350	-0.2	
30 May 1970	6	1940	1350	-0.7	
31 May 1970	8	1524	1080	-0.6	
2 June 1970	7	2137	1500	-0.6	
17 July 1970	7	1994	2100	-0.2	
13 May 1971	8	376	450	0.2	-0.36
18 July 1971	7	1948	1050	-0.4	±0.10
20 July 1971	6	1613	1800	0.2	
15 Aug. 1971	7	2027	1350	-0.7	
4 June 1973	7	2068	1500	-0.5	
30 July 1973	7	817	1200	-0.2	
8 Aug. 1973	7	2089	1800	-0.8	
18 May 1970	1	1038	1200	0.6	
20 May 1970	1	1142	900	0.1	
24 May 1970	1	1353	1080	0.4	
3 June 1970	1	1469	1500	0.5	
4 June 1970	1	1570	1140	0.5	
16 June 1970	1	715	750	0.2	

TABLE (5.2) (Contd.)

Date	Cloud cover at 12.00h at Gatwick (oktas)	Inv. height from Crawley ascent at 12.00h (m)	Cloud base reported at 12.00h at Gatwick (m)	D	Mean D ±st. error of mean
17 June 1970	1	1346	840	0.4	
11 Aug. 1970	1	1080	900	0.8	
26 Aug. 1970	1	636	780	0.4	
28 Aug. 1970	1	1391	900	-0.4	0.52
3 May 1971	1	1288	1050	1.1	±0.10
3 June 1971	1	380	750	1.0	
4 June 1971	1	527	750	0.9	
5 July 1971	1	569	750	0.9	
8 July 1971	1	1634	1350	-0.5	
11 July 1971	1	914	1050	0.6	
5 June 1973	1	1544	1500	0.9	
14 June 1973	1	1367	1440	0.9	
30 June 1973	1	1076	840	0.3	
7 July 1973	1	704	750	0.8	

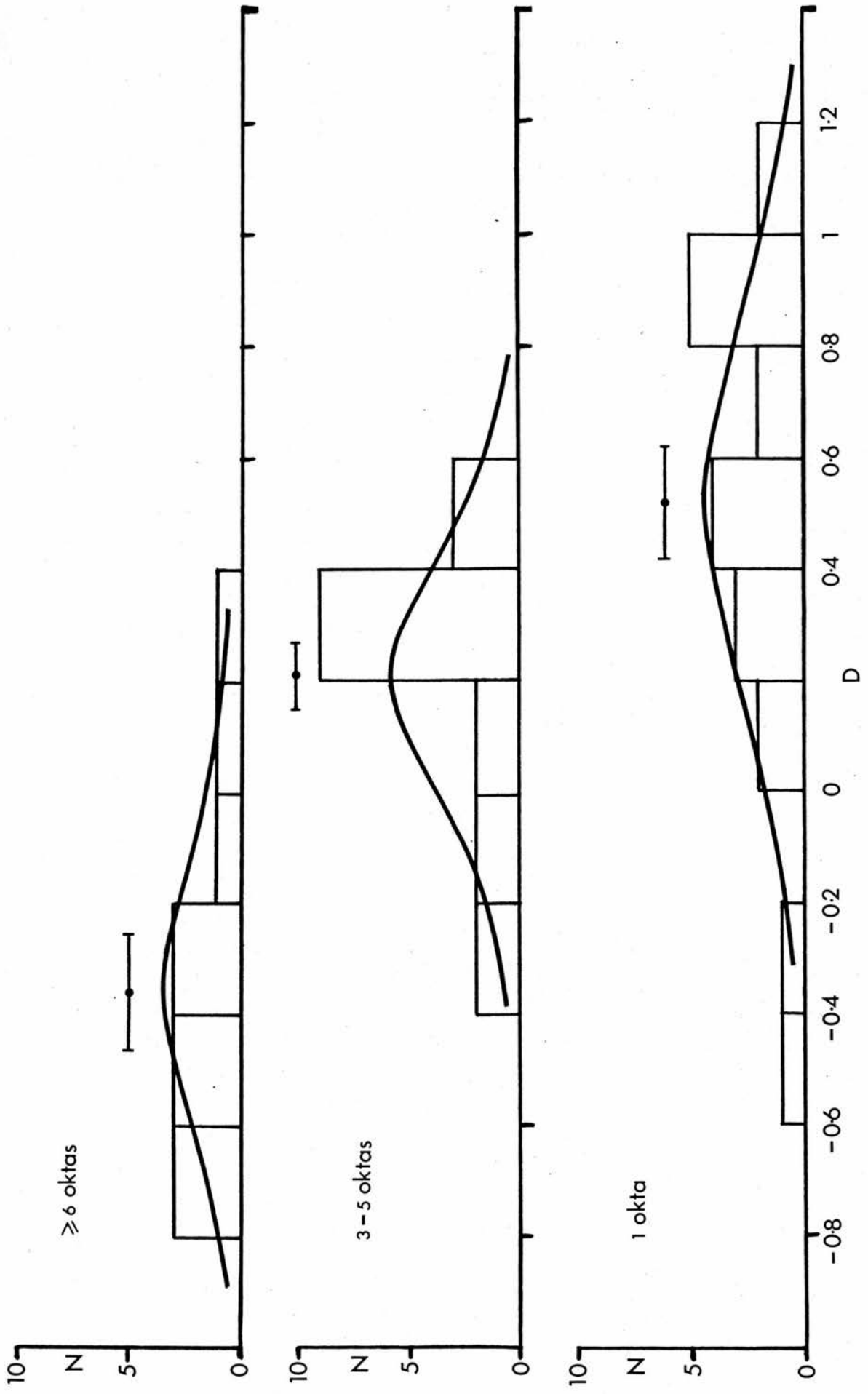

Figure (5.1) Number distribution, N, of D-values for three cloud cover groups. Also shown are bars indicating standard errors of means and normal distributions of equal area and standard deviation to the samples.

all extents of cloud cover since this underestimates the difference in the specific humidity gradients.

Calculated values of D are shown in Table (5.2) and displayed graphically in Figure (5.1). The major source of random error in D is the uncertainty in the radio-sonde measurements, partly due to instrumental limitations and partly to the possibility of a single ascent at Crawley being unrepresentative of the average structure of the boundary layer at Gatwick.

Assuming that the variances of D within the three groups are identical and unknown, a t-test may be applied to pairs of the groups with the following results; there is a much greater than 99.95°/o probability that the D-values for 1 okta and for ≥ 6 oktas cloud cover days are selected from two completely different populations; similarly there is a greater than 99.95°/o probability that days of 3-5 oktas and of > 6 oktas have a different mean D-value; and there is a 99.4°/o probability that 1 okta and 3-5 oktas differ in their mean values of D.

The mean values of D and of inversion height for the three groups may be used in Equation (5.17) to calculate the mean initial radii. These are 0, 290m and 1350m respectively for days of extensive cloud cover, part cloud cover and little cloud (accepting that negative values of r_o are physically impossible).

5.3(d) Method 2

Using Equation (5.17) and Equation (5.11) and making the substitution

$$\Delta q = q_u - (q_o + mh) \qquad (5.19)$$

	MEAN D	STANDARD ERROR
CLOUD 1	-0.19	0.05
COVER 3-5	0.22	0.05
(oktas) $\geq$ 6	0.54	0.12

TABLE (5.3) - VALUES OF D FOR THE THREE CLOUD COVER GROUPS, CALCULATED BY EQUATION (5.20).

leads to an expression for D which does not contain the measured value q_h, namely

$$D = 4\alpha \left[\frac{3}{4} + \frac{c_p\Delta\theta + cA\lambda H_o}{cc_p\Delta\theta\left(\frac{1}{\beta} - A\frac{\lambda}{c_p}\frac{q_u - q_o}{\Delta\theta}\right)} (q_{sh} - q_o) \right] \qquad (5.20)$$

where q_{sh} is the value of q_s at T_h. The values of D determined by this expression are presented in Table (5.3).

The evaluation of D by Equation (5.18) requires the insertion of a value for Δq which is derived from measurements of q_u and q_h, whereas Equation (5.20) requires measurements of q_u and q_o. The performance of the standard U.K. Meteorological Office radio-sonde is such that the measurement of q_o is likely to be much more accurate than that of q_h and hence Equation (5.20) is inherently less prone to random errors in data than is Equation (5.18). Indeed the elimination of the measured value q_h reduces the standard errors in the means of all the groups without greatly changing the mean values of D, except in the case of $\geq$ 6 oktas when the over-large assumed value of H_o for these days produces an inaccurate estimate of m and hence of q_h. The separation between days of 3-5 oktas and days of 1 okta cloud cover is increased to 99.7°/o certainty.

5.3(e) Method 3

If a dry adiabatic lapse rate is assumed in the boundary layer then the measured value T_h may be eliminated from Equation (5.20) to give

$$D = 4\alpha \left[\frac{3}{4} + \frac{c_p(\theta_u - \theta_o) + cA\lambda H_o}{cc_pH_o(\theta_u - \theta_o)\left(\frac{1}{\beta} - A\frac{\lambda}{c_p}\frac{q_u - q_o}{\theta_u - \theta_o}\right)} (q_{sh} - q_o) \right] \qquad (5.21)$$

	MEAN D	STANDARD ERROR
CLOUD 1	-0.39	0.13
COVER 3-5	0.74	0.12
(<u>oktas</u>) ≥ 6	0.26	0.12

TABLE (5.4) - VALUES OF D FOR THE THREE CLOUD COVER GROUPS, CALCULATED BY EQUATION (5.21).

where q_{sh} is the value at $\theta_o \left(\frac{1000}{p_h}\right)^{-0.288}$.

This expression can be evaluated knowing only temperature and humidity at the ground and above the inversion and also the height of the inversion itself. The values of D determined in this way are shown in Table (5.4). The standard errors are found to be larger in all cases and the mean value of D to be substantially changed for days of 1 okta cover. This is due to the inappropriateness of an assumed adiabatic lapse rate on days of such large ground-source and entrained heat fluxes. Nevertheless, the certainty of distinction between 1 okta and 3-5 oktas increases to 99.8°/o.

5.3(f) The Initial Radius, r_o

The values of r_o, corresponding to the above mean values of D and of inversion height, are large and perhaps are overestimates since the preceding theory has assumed that convective bubbles are internally well mixed. McCarthy (1974) has shown that, in fact, thermals are inhomogeneous and have a maximum of temperature, and hence also of specific humidity, at their centres. This implies that a bubble, small enough for the preceding theory to predict unsaturation at the inversion, may remain damp enough near its core for saturation and cloud formation to occur. This shortcoming of the theory does not, however, detract from the usefulness of the parameter D.

5.4 Predictive Value of Theory

The analysis presented here imparts some validity to the simple theory employed which incorporates entrainment across the inversion layer and across the surface of a rising

convective bubble. The postulate of cloud cover being dependent upon the smallest initial radius of convective bubbles which are still saturated at the inversion leads to the formulation of an easily determined parameter D and, even with the relatively poor data used here, the value of D is shown to distinguish very significantly between the three cloud cover groups used in the test.

This parameter may then be used predictively if future values of q_{sh}, Δq, $\Delta\theta$ and q_o are estimated for use in Equation (5.18); or if future values of q_{sh}, q_u, $\Delta\theta$ and q_o are estimated for use in Equation (5.20); or values of q_o, q_u, θ_u and h for use in Equation (5.21). It is noteworthy that the results of Equation (5.18) are not significantly affected if q_{sh} is calculated from the inversion height and the surface air temperature, on the assumption of a dry adiabatic lapse rate. Similar treatment of Equation (5.20) yields results close to those of Equation (5.21).

The theory of Chapter 4 results in predictive equations for both q_o and h, assuming a maximum daily temperature and a maximum value of available energy. Now the cloud cover predictor, D, evaluated, for example, by Equation (5.18) with the dawn value of q_o, can be used in conjunction with the equations of §5.1 to predict the maximum available energy during the day and then the method of §4.4 permits the prediction of mid-day values of q_o and h. The calculation may then be iterated using successively better estimates of the mid-day values of q_o and h until a sufficient degree of accuracy is obtained. However, it is unlikely that, in most cases, iteration will be necessary since the values of

	INVERSION HEIGHT (m)		
	500	1500	2500
CLOUD 1	0.63	0.47	0.37
COVER 4	0.38	0.18	0.11
(oktas)8	<0	<0	<0

TABLE (5.5) - VALUES OF D AGAINST CLOUD COVER AND INVERSION HEIGHT, FOR USE WITH EQUATION (5.18) AND EQUATION (5.20).

q_o and h do not change greatly during the day.

With the assumption that the mean initial radii calculated in §5.3(c) are typical of their respective cloud cover groups, values of D may be determined for a range of inversion heights. These values are shown in Table (5.5). Conversely, once the value of D is found from Equation (5.18) or Equation (5.20) and the inversion height is known for a particular day then Table (5.5) may be consulted and the likely cloud cover determined. A similar table may be constructed for use with Equation (5.21).

CHAPTER 6

AVERAGE DIURNAL CHANGES OF HUMIDITY AND TEMPERATURE AND THEIR RELATION TO THE BOWEN RATIO

In Chapter 1 a simple-minded approach to the problem of diurnal changes of temperature and of humidity indicates that the ratio $\frac{c_p}{\lambda} \cdot \frac{\delta T}{\delta q}$ (or equivalently $\frac{\gamma}{\Delta} \cdot \frac{\delta T}{\delta T_d}$) ought perhaps to be equal to, or at least be closely related to, the local Bowen ratio. However, Figure (1.4) reveals that, for the Thetford data at least, this is not so. It is further suggested in Chapter 1 that the absence of correlation between the two parameters is due to the unexpected lack of dependence of δq on the integrated vapour flux, as illustrated in Figure (1.2). Certainly, in part, this may arise from large-scale horizontal advection, but this cannot provide the whole explanation since Figure (1.1) shows that δT remains related in some way to the integrated sensible heat flux.

Rider and Robinson (1951) demonstrate that, in the lowest two metres of the boundary layer, the diurnal increase in temperature is affected by two comparable factors; the increase due to radiative flux convergence; and the decrease due to turbulent sensible heat flux divergence. Elliot (1964) also shows that, in the lowest ten metres, the calculated warming due to radiative divergence surpasses the observed warming. As a result of this, the turbulent sensible heat flux at a height of 10m is about 1°/o larger than the sensible heat flux at the ground. Thus the diurnal temperature increase

in a very shallow layer near the ground is controlled by the fine balance between the sensible heat flux in at the bottom, the sensible heat flux out at the top and the net absorption of radiation in the intervening layer. The magnitude of the heat flux out of the top of this shallow layer is affected by the temperature structure of the whole of the remainder of the boundary layer and this acts as the control on the increase in temperature near the ground. In effect, in a turbulent boundary layer, the temperature rise due to radiative convergence near the ground is mixed equally throughout the boundary layer. Deardorff (1974a) dismisses as insignificant the effect of radiative flux convergence on warming the planetary boundary layer and, additionally, if the boundary layer is of the order of 1000m deep, Elsasser diagrams (applicable only to cloudless conditions) will generally reveal that radiative divergence becomes a negligible term in the heat balance. For example, at both 00.00h and 12.00h on 2nd May 1971 at Crawley, the boundary layer is found to be cooling at a rate of $0.05^{o}C\ hr^{-1}$ due to radiative flux divergence.

It thus becomes unreasonable to attempt to obtain a better correlation between β and $(\frac{\gamma}{\Delta} \cdot \frac{\delta T}{\delta T_d})$ by elimination of the part of δT which is due solely to radiative heating or cooling and not due to the sensible heat flux; especially since comparison of Figures (1.1) and (1.2) shows that the lack of correlation is due to the apparently paradoxical behaviour of δq or δT_d.

The test cases of Chapter 4 reveal that, despite a large positive latent heat flux from the ground, the specific humidity of the air may drop during the day due to down-mixing of drier

air from above. Thus the vertical humidity and temperature structure of the atmosphere is of major importance in determining the value of δq (or of δT_d). In general, therefore, it may be stated that

$$\frac{\gamma}{\Delta} \cdot \frac{\delta T}{\delta T_d} = \beta \times f(e), \qquad (6.1)$$

where $f(e)$ may loosely be called a "function of the environment" and may be expected to be related in some way to the vertical structure of the lower troposphere.

In this chapter annual average values of β, δT and δT_d from throughout the world are used to determine the form of $f(e)$, which is then employed to predict regional values of β throughout Europe by using a comparatively dense network of stations reporting mean values of δT and δT_d - simple meteorological parameters of an almost universal availability. The use of annual average values hopefully eliminates the grosser effects of local advection.

6.1 Extended Entrainment Theory

If it is assumed that, on average and without advection,

$$\int (\text{total sensible heat flux}).dt = \rho c_p \, \delta T$$

$$\text{and } \int (\text{total latent heat flux}).dt = \rho \lambda \, \delta q,$$

where the integration is from dawn to the time of maximum temperature, then

$$\frac{\int(\text{total sensible heat flux}).dt}{\int(\text{total latent heat flux}).dt} = \frac{c_p}{\lambda} \cdot \frac{\delta T}{\delta q} = \frac{\gamma}{\Delta} \cdot \frac{\delta T}{\delta T_d} . \qquad (6.2)$$

The entrainment theory of Chapter 4 may be simplified,

for the purposes of this present investigation, by ignoring the phase lags between various fluxes and by ignoring subsidence which, itself, does not change either the temperature or the humidity at ground-level. Thus Equation (4.1) implies that, for a volume of air near the ground,

$$\text{(total sensible heat flux)} = H_o + H_h = H_o(1+A) \qquad (6.3)$$

and Equation (5.10) implies that, for a similar volume,

$$\text{(total latent heat flux)} = \lambda E_o + \lambda E_h$$
$$= \lambda E_o + A\frac{\lambda}{c_p}\frac{\Delta q}{\Delta\theta} H_o \qquad (6.4)$$

where Δq is a negative number and A is assigned the constant value of $0.25 = A'$.

Substitution of Equations (6.3) and (6.4) into Equation (6.2) gives

$$\frac{\int(1+A')H_o.dt}{\int(\lambda E_o + A'\frac{\lambda}{c_p}\frac{\Delta q}{\Delta\theta} H_o).dt} = \frac{\gamma}{\Delta}\cdot\frac{\delta T}{\delta T_d}, \qquad (6.5)$$

which, assuming a fairly constant value of Bowen ratio during the morning, may reasonably be simplified to

$$\beta\left(\frac{1+A'}{1+A'\frac{\lambda}{c_p}\frac{\Delta q}{\Delta\theta}\beta}\right) = \frac{\gamma}{\Delta}\cdot\frac{\delta T}{\delta T_d}. \qquad (6.6)$$

Strictly, this theory is only applicable to anti-cyclonic conditions with a subsidence inversion, in which case Δq and $\Delta\theta$ have fairly definite meanings. However, in cyclonic conditions, convection and turbulence still only penetrate as far as atmospheric stability allows and turbulence is dissipated in an equivalent way to the anti-cyclonic case by attempting to

thoroughly mix the boundary layer. Hence it is assumed in the following investigation that entrainment theory has validity in cyclonic conditions also, although the values of Δq and of $\Delta\theta$ or of their ratio may be very different from the anti-cyclonic cases. In effect, the factor in parenthesis in Equation (6.6) is the function of the environment introduced in Equation (6.1), the quantity $(\Delta q/\Delta\theta)$ being the appropriate parameter which describes the structure of the atmosphere.

6.2 Data Sources

Budyko (1956) uses the "relation equation" to determine annual evaporation from net radiation and rainfall. The empirical form of this equation is found using river basin data from several continents throughout the world; however it is not applicable to mountainous regions and, obviously, may not apply to very arid regions. Budyko further tested the empirical form of the relation equation (Budyko (1956) - Equation 107) by computing the run-off coefficients for 29 large European river basins and comparing them with the measured values. The mean relative error determined in this test was $\pm$ 13%.

The annual total of net radiation, the value of which is necessary not only for the relation equation but also to determine the annual sensible heat flux by the heat balance method, is found either from direct measurements, which are fairly common in Europe and N. America, or by the methods described in §3 of Budyko (1956). These methods take account of the latitude of a site, the local albedo at that site and its dependence upon the Sun's altitude, the difference

between local air temperature and local surface temperature, the transparency and average humidity of the atmosphere, the average cloudiness and its varying effect with the Sun's altitude, the cloud type and cloud height.

In this way Budyko has been able to construct the "Atlas Teplovogo Balansa Gidrometeorologicheskoe Iydatel'skoe" which gives values of annual average net radiation, evaporation and sensible heat flux throughout the world (except in mountainous regions) by interpolation between the isopleths. Using these maps, annual average Bowen ratios may be calculated at any sites throughout the world.

Budyko claims that his methods provide values of annual net radiation correct to within $\pm$ 10°/o, annual evaporation to within $\pm$ 5-10°/o and annual sensible heat flux, which is the difference between the two, to an accuracy of something worse than $\pm$10°/o. This implies that, at best, interpolation from Budyko's maps will give Bowen ratios correct to $\pm$ 20-30°/o. However, it should be remembered that interpolation often leads to a considerable increase in error, and this will be particularly true, for example, on the sensible heat flux map where there are only two isopleths in the whole of Europe, one running along the Mediterranean coast and the other passing through Finland. In addition, it must be remembered that the relation equation has only been tested on large river basins and when its predictions are applied to a particular site, which is assumed to be representative of a fairly small local region, then the errors involved may again be increased greatly.

Values of δT and of δT_d are obtainable from the "Tables of Temperature, Relative Humidity and Precipitation for

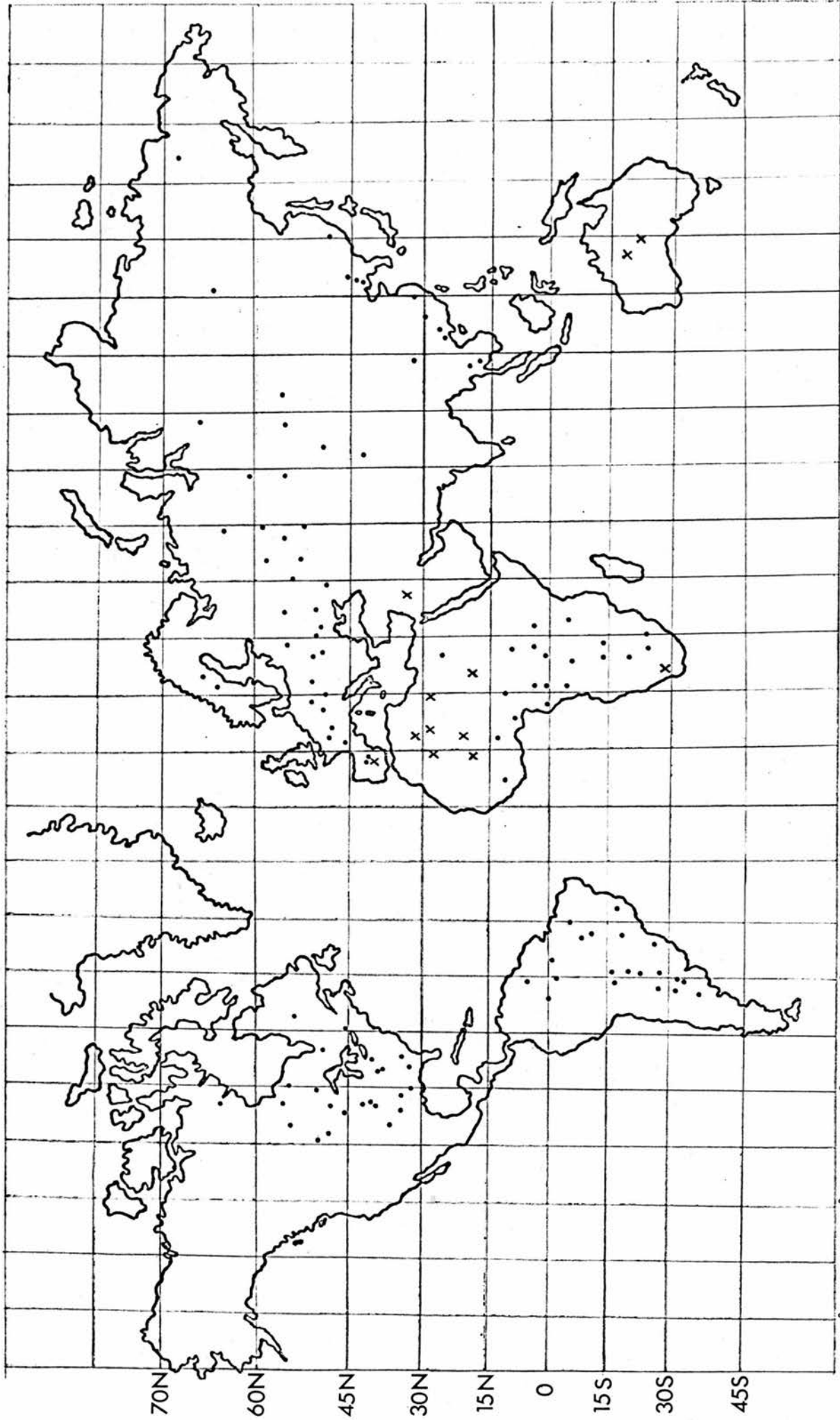

Figure (6.1) Meteorological stations throughout the world for which values of $(\Delta q/\Delta\theta)$ are computed (see also Appendix (1)).

x stations dealt with in §6.3(c).

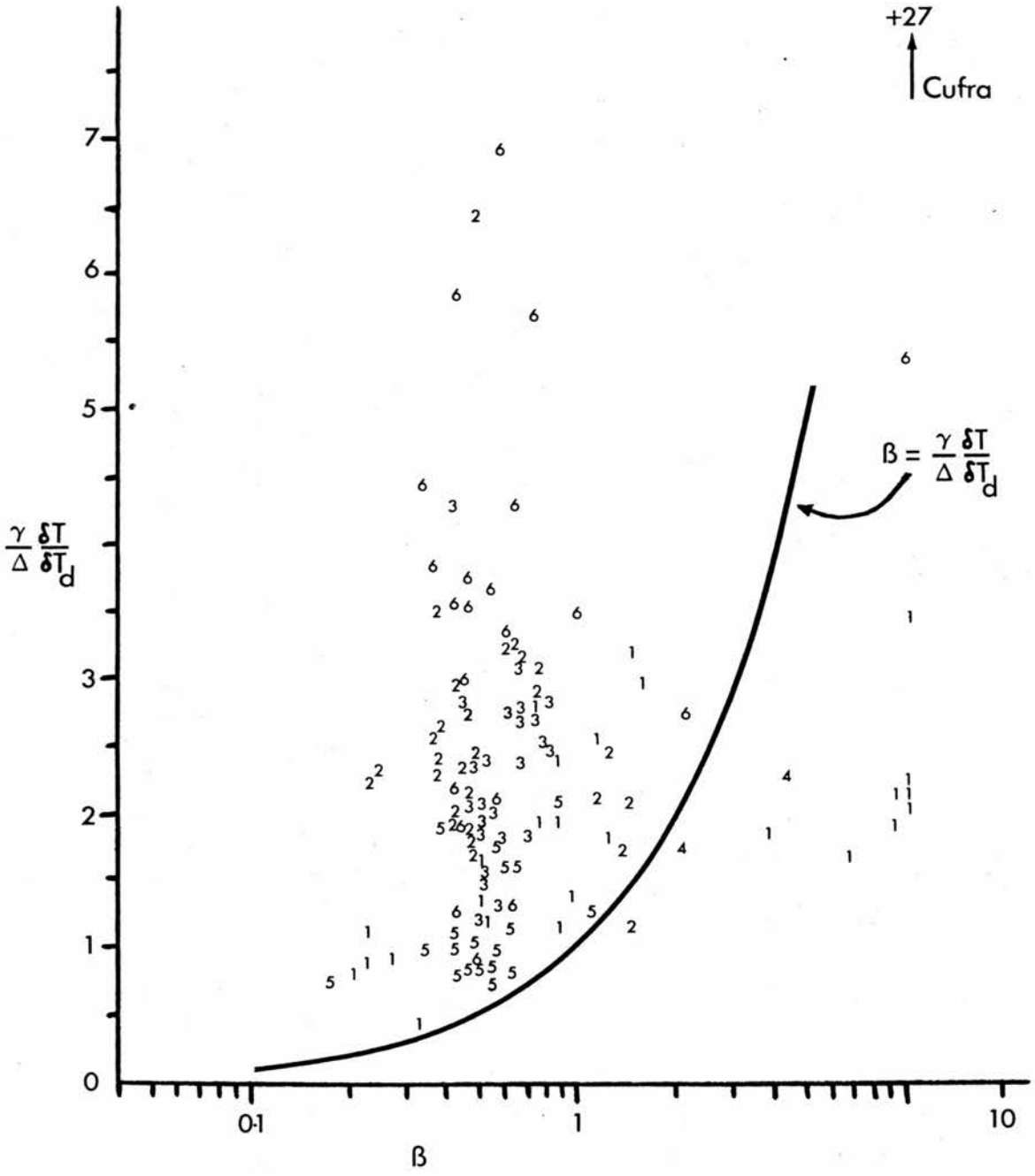

Figure (6.2) $(\frac{\gamma}{\Delta}\frac{\delta T}{\delta T_d})$ versus β for 122 stations throughout the

1 Africa, 3 N. America, 5 S. America,

2 Europe, 4 Australia, 6 Asia.

the World", Parts I - VI, compiled by the U.K. Meteorological Office. Only used are those stations which are greater than 100 km from the sea, since Nixon and Lawless (1968) show that coastal effects can greatly reduce evaporation in comparison to that found inland, and which report temperatures and relative humidities at a time between 05.30h and 08.00h and between 12.00h and 14.30h, (temperatures may alternatively be expressed as minimum and maximum values). The value of Δ is that corresponding to the temperature which is the average of the dawn and mid-day values of dew-point.

Figure (6.1) shows the 122 stations chosen, throughout the world, to give a reasonable cover of all the climatic regions and also to be in areas where Budyko's atlas provides relatively dependable information on the annual fluxes of latent and of sensible heat. These stations are listed by name and position in Appendix (1).

Figure (6.2) is a graph of $\frac{\gamma}{\Delta} \cdot \frac{\delta T}{\delta T_d}$ against β for these 122 stations and similarly to Figure (1.4) for Thetford Forest, there appears to be very little relation between the two parameters. Again, however, there is a preponderance of points lying to one side of the line $\beta = \frac{\gamma}{\Delta} \cdot \frac{\delta T}{\delta T_d}$, indicating that, for a given Bowen ratio, the diurnal increase in dew-point temperature is too small.

6.3 Test of Theory. Equation (6.6) implies that

$$\frac{\Delta q}{\Delta \theta} = \left[\frac{(1 + A')\beta}{\frac{\gamma}{\Delta} \cdot \frac{\delta T}{\delta T_d}} - 1 \right] \Big/ A' \frac{\lambda}{c_p} \beta \, . \qquad (6.7)$$

This is the part of the function of the environment which is

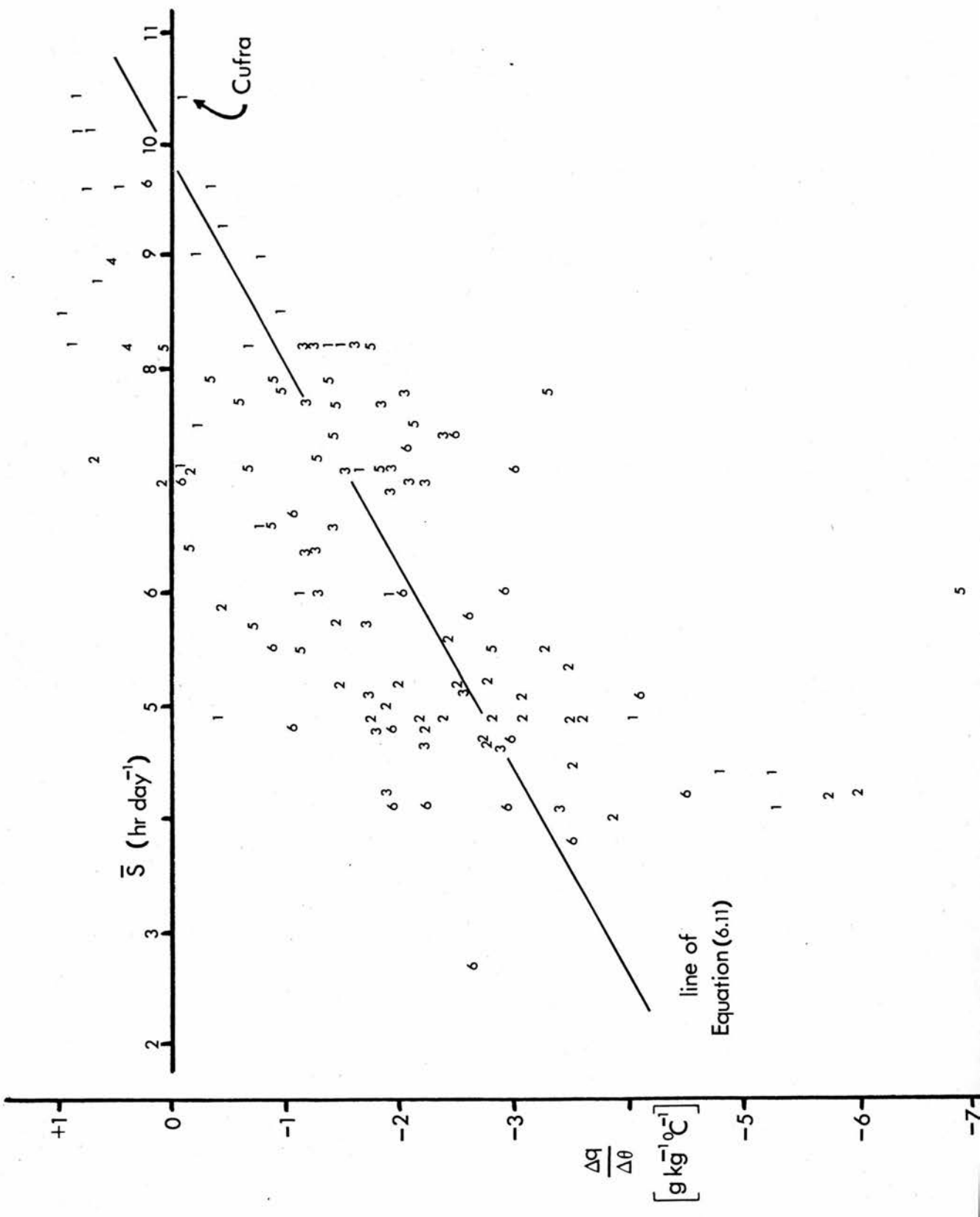

Figure (6.3) ($\Delta q/\Delta\theta$) versus $\bar{S}$ for 122 stations throughout the world.

1 Africa, 3 N. America, 5 S. America,
2 Europe, 4 Australia, 6 Asia.

dependent upon the average vertical structure of the atmosphere and, effectively, is an expression of the climate.

6.3(a) Average tropospheric structure and average sunshine

For the purposes of this test, the average vertical structure of temperature and humidity of the planetary boundary layer at each station might best be expressed in terms of the average isobaric curvature at each station. However, since that parameter is not easily determinable, it is preferable to use a commonly observed meteorological variable. The annual average number of hours per day of strong sunshine at each station is related to the average cloudiness which must, in turn, be dependent not only upon the stability of the boundary layer, and thereby upon its temperature structure, but also upon the humidity of the air near the ground and upon the gradient of humidity with height (as discussed for the particular case of convective cloud formation in Chapter 5). Therefore, it is reasonable to expect a correlation between the parameter $(\Delta q/\Delta\theta)$, evaluated at each station by Equation (6.7), and the average number of hours of sunshine at each station which is readily available, for example, by interpolation from the map in "Climate, Present, Past and Future, Vol. I" by H.H. Lamb (Methuen & Co., London (1972)).

Figure (6.3) shows $(\Delta q/\Delta\theta)$ plotted against $\overline{S}$ and indeed, a significant correlation is found.

6.3(b) Values of $(\Delta q/\Delta\theta)$

The values of $(\Delta q/\Delta\theta)$ in Figure (6.3) range from $-7\ gkg^{-1}K^{-1}$ to $+\ 1\ gkg^{-1}K^{-1}$. For an inversion-capped boundary layer, $(\Delta q/\Delta\theta)$ has a definite physical meaning as the ratio of the change in specific humidity across the inversion layer to the corresponding change in potential temperature and, for the cases studied in Chapters 3, 4 and 5, a typical value is $-0.5\ gkg^{-1}K^{-1}$ which lies towards the top end of the total range of values.

The most negative values of $(\Delta q/\ \Delta\theta)$ correspond to regions of little sunshine which are to be found in the predominantly cyclonic belts of Northern Europe, Northern N. America and the Equatorial Forests of Africa and S. America. Under cyclonic conditions of deep and vigorous convection, the planetary boundary layer has no strict limit and it is impossible to know up to which height effective mixing takes place. However, in general, the diurnal rise or fall in temperature and humidity can be separated into two distinct parts, that due to the fluxes of sensible and of latent heat at the ground and that due to the entrained fluxes either at the inversion or, in the cyclonic case, resulting from deep mixing in the unstable lower troposphere.

Employing the formulation of the anti-cyclonic case, the diurnal change in temperature due to the entrained flux, say $\delta_e T$, is given by

$$\rho\, c_p\, \delta_e T = \int (\text{entrained sensible heat flux}).dt$$

$$= \int (AH_o).dt \qquad (6.8)$$

and the diurnal change in specific humidity due solely to the

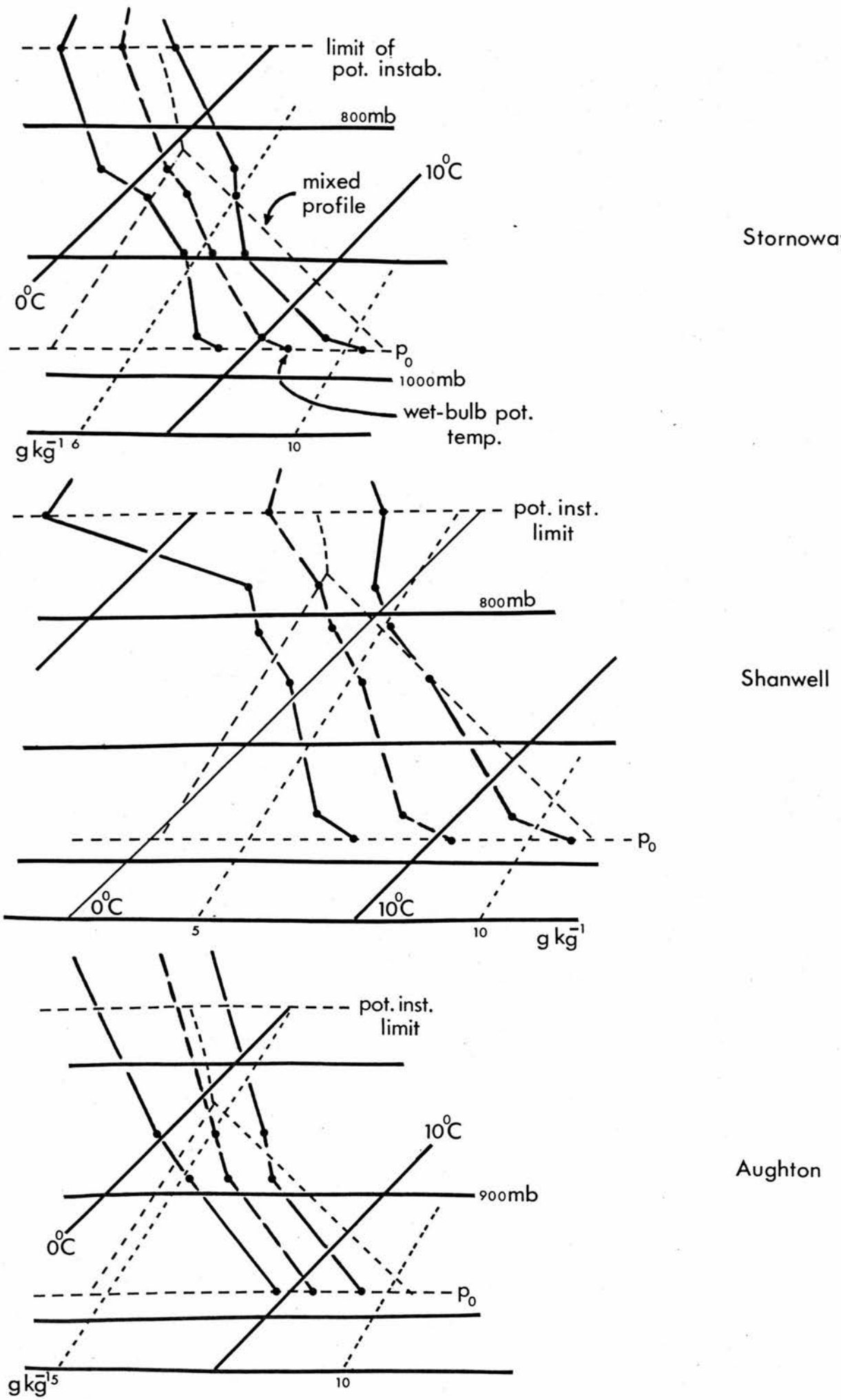

Figure (6.4) Temperature and humidity profiles at Stornoway, Shanwell & Aughton, 12.00h, 10th Sept. 1970.

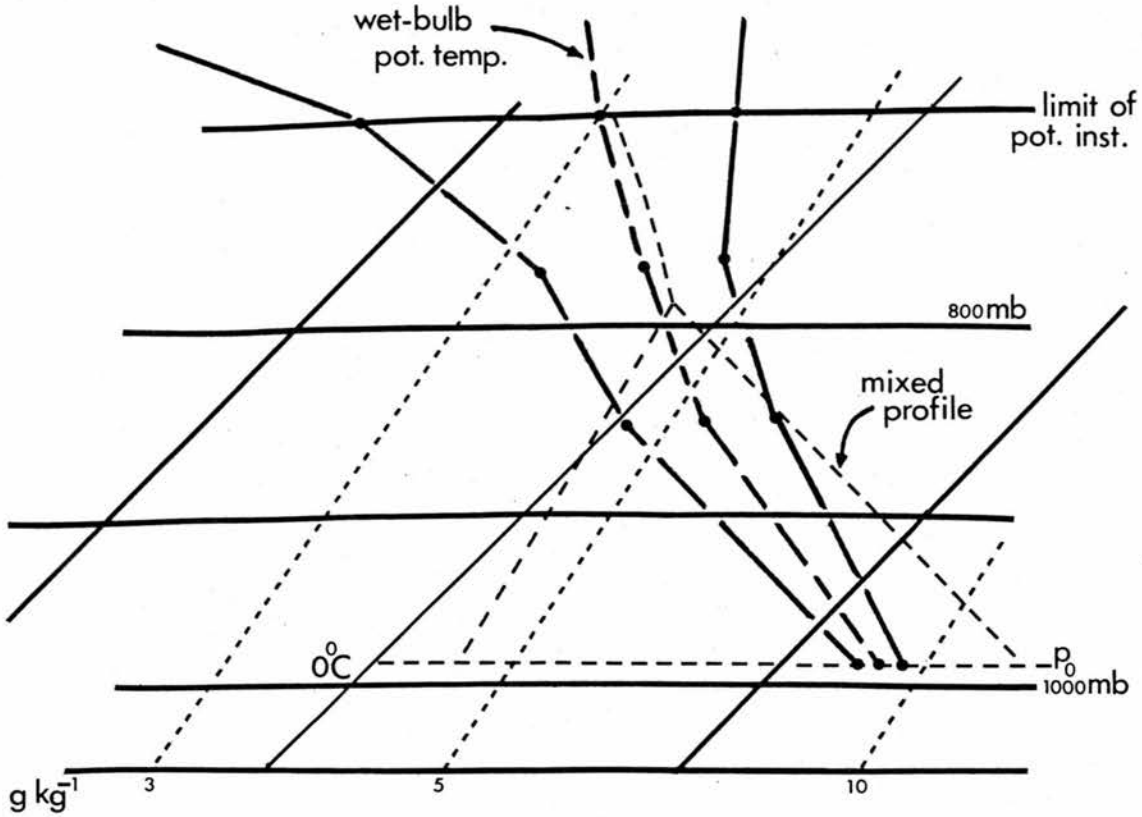

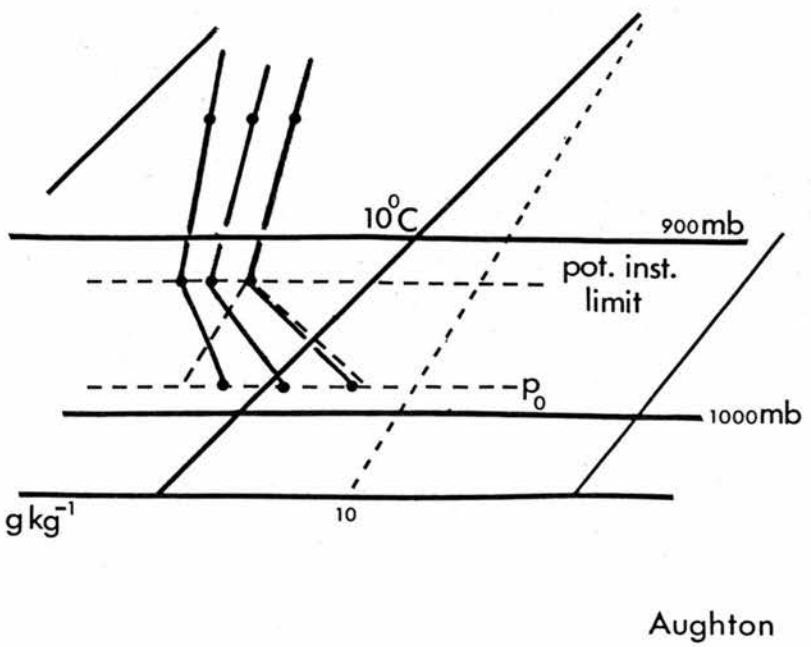

Figure (6.5) Temperature and humidity profiles at Shanwell, & Aughton, 12.00h, 16th Aug. 1970.

entrained flux, say $\delta_e q$, is given by

$$\rho\lambda\delta_e q = \int (\text{entrained latent heat flux}).dt$$

$$= \int (A \frac{\lambda}{c_p} \cdot \frac{\Delta q}{\Delta\theta} \cdot H_o).dt \quad , \qquad (6.9)$$

and so, from Equations (6.8) and (6.9),

$$\frac{\lambda}{c_p} \cdot \frac{\delta_e q}{\delta_e T} = \frac{\int (A \frac{\lambda}{c_p} \cdot \frac{\Delta q}{\Delta\theta} \cdot H_o).dt}{\int (A\, H_o).dt} = \frac{\lambda}{c_p} \cdot \frac{\Delta q}{\Delta\theta}$$

$$\Rightarrow \quad \frac{\delta_e q}{\delta_e T} = \frac{\Delta q}{\Delta\theta} \qquad (6.10)$$

Hence, in the cyclonic case, the "effective inversion strength", that is the value of $(\Delta q/\Delta\theta)$, may be estimated by determining the value of $(\delta_e q/\delta_e T)$ produced by thoroughly mixing the unstable layer and noting the relative changes in q and T which result at ground-level.

Figures (6.4) and (6.5), respectively, show the 12.00h temperature and humidity soundings on 10th Sept. 1970 at Stornoway, Shanwell and Aughton and on 16th Aug. 1970 at Shanwell and Aughton. Both these days were cyclonic but without any fronts in the vicinity of the radio-sonde stations. The nature of the lower tropospheric structure means that the choice of boundary layer is not critical and purely for consistency and objectivity the upper limit of the boundary layer has been defined as the upper limit of potential (or convective) instability on each of the soundings. On the Tøgram the boundary layer is then thoroughly mixed by the process of equalising areas between the humidity sounding and an iso-mixing ratio line and, if necessary, a saturated adiabatic and between the temperature sounding and a dry adiabatic and, if necessary, a

saturated adiabatic. The respective results for $(\delta_e q/\delta_e T)$, and equivalently for $(\Delta q/\Delta\theta)$, are $-2.9\ gkg^{-1}K^{-1}$, $-3.25\ gkg^{-1}K^{-1}$, $-1.85\ gkg^{-1}K^{-1}$, $-1.5\ gkg^{-1}K^{-1}$ and $-7.0\ gkg^{-1}K^{-1}$. These values of "effective inversion strength" are all considerably more negative than for anti-cyclonic conditions and strongly support the validity of the trend in Figure (6.3).

The highest values of $(\Delta q/\Delta\theta)$ occur in regions of great sunshine amounts and suggest that, in those locations, the atmosphere has an increasing specific humidity with increasing height. This is discussed in the following section.

6.3(c) Anomalies in Arid Regions

In Figure (6.2) there are 12 points lying to the right of the line $\beta = \frac{\gamma}{\Delta} \cdot \frac{\delta T}{\delta T_d}$ and, again, these 12 points lie significantly above the line $\Delta q/\Delta\theta = 0$ in Figure (6.3). These points represent the meteorological stations tabulated below along with their corresponding values of Bowen ratio from Budyko's maps (see Figure (6.1) and Appendix (1) for geographical locations).

Table (6.1)

Station	Bowen Ratio	Station	Bowen Ratio
Wave Hill	2.0	Pofadder	6.8
Alice Springs	4.3	Faya	9.3
Ciudad Real	1.5	Adrar	10.2
Rutba	9.9	Fort Flatters	10.2
Timbuktu	3.8	Tin-Zaouatene	9.3
El Golea	10.2	Sebha	10.2

All these stations lie in arid or semi-arid climatic regions for which it must be appreciated that Budyko's methods of determining the annual latent heat flux may be totally inappropriate.

His Saharan values in particular seem rather low for areas which may receive 0.1", or less, of rain per annum. On the other hand it is likely that most of the meteorological stations are sited at or near desert oases; respond to the local micro-climate; and do not give a diurnal variation of either temperature or dew-point which is representative of the open desert. This is because, in a well-irrigated oasis area, the regional Bowen ratio is likely to be considerably lower than 10, whereas, for parts of the open desert, it may be in the region of 100.

Maps, kindly made available by the Scottish National Library, and personal communications gratefully received from the Meteorological Offices of Libya, South Africa, Australia, Algeria and Spain give the following information on some of the afore-mentioned stations:

(a) WAVE HILL : Meteorological station is situated at the aerodrome. Prevailing wind is S.E. to E. Vegetation consists of open grass land, used for grazing, with scattered trees. A permanent stream is found at a distance of 3 miles to N.W. Occasional penetration of the monsoon brings a period of much above average rainfall.

(b) ALICE SPRINGS : Meteorological station is situated at the aerodrome just south of the town. Prevailing wind is S.E. to E. with very infrequent penetration of the monsoon. Vegetation consists of a variable grass cover

with scattered trees and some acres of cultivation.

(c) CIUDAD REAL : Prevailing wind is S.W. to W. The soil is of clay-type and the local vegetation is predominantly of cereal crops, horticultural crops, fruit trees and poplars. The River Guadiana is less than 10 km distant and the water table is at a depth of 2m.

(d) RUTBA : No information.

(e) TIMBUKTU : A belt of hills 300m high and covered with dense brushwood lies 3 miles to N. An extensive area of river, marsh and mangrove swamp lies 3 miles to S.

(f) EL-GOLEA : Prevailing wind is N. to E. with calm for 20°/o of time. Station is situated amidst palm trees with a 4 hectare lake at a distance of 800m to N.N.W. and a temporary water-course at 1½ km. Subterranean water lies just below the soil surface.

(g) POFADDER : Local topography is almost flat with some undulations and a range of hills 50m high lying 5-8 km to N.. No free-water surfaces locally but vegetation is of a low bushy type.

(h) FAYA : Station lies in a depression, locally surrounded by palm trees, steppe and several wells.

(i) ADRAR : Prevailing wind is N. to N.E. with calm for 5°/o of time. Station lies in a valley and a vast area of subterranean water, just below the surface, extends under the town and under the palm plantation.

(j) FORT FLATTERS : Prevailing wind is N. to E. with calm for 62°/o (sixty-two) of the year. Station lies outside the town and in a valley running E. to W. Soil is of sand and there is no water locally.

(k) TIN-ZAOUTENE : No information.

(ℓ) SEBHA : Prevailing wind is N. to E. with 8°/o of occasions being calm. Station is surrounded by hilly country and lies in a depression which is well-watered, having marshes and a palm plantation roughly 5 miles by 8 miles in extent.

All of these stations (except Fort Flatters) can not be regarded as being sited in representative desert regions and hence Budyko's values of β may well be totally inappropriate, thereby resulting in anomalous values of $(\Delta q/\Delta\theta)$. It is noteworthy that one Saharan station, namely Cufra, has a negative value of $(\Delta q/\Delta\theta)$ which is indicated on Figure (6.3). This is because the average diurnal change in dew-point at that station is + 0.6°C, whereas, for all other Saharan stations, it is near the value of + 6°C. However, from Budyko's maps, Cufra appears to have a Bowen ratio of 10.2. Now it is possible that local effects, such as a source of water vapour, the overnight deposition of dew or the formation of a strong overnight low-level inversion in a frost hollow, or indeed a combination of these, could greatly increase the diurnal variation of dew-point from the value experienced in the open desert; there is, however, no way in which that value can be reduced. So, although Cufra appears on maps as an oasis, it seems likely that its meteorological station is so sited as to give values representative of the desert, whereas all the others are unfortunately contaminated by their local environments.

In the following linear regression calculation the 12

arid-region stations are ignored because of the doubt in the validity of their assigned Bowen ratios.

6.3(d) Boundary layer structure in the Sahara desert

Helliwell and Mackenzie (1957) report the results of flights by an instrumented aircraft over the Saharan desert during a 10-day period in the early summer of 1956. Their Fig. 1 gives the mean profiles of temperature and frost point over that period. The temperature and specific humidity at the lowest level of 5,000 ft. are 24°C and 5.0 gkg^{-1} ; whereas the temperature and specific humidity at 18.000 ft, which is the height of the mean haze top and therefore the mean height of the boundary layer top, are respectively -11°C and 1.35 gkg^{-1}. So, relative to a dry adiabatic lapse rate, the temperature increases by 4.6°C and the specific humidity decreases by -3.65 gkg^{-1}, hence an estimate of $(\Delta q/\Delta\theta)$ for the boundary layer is -0.8 $gkg^{-1}K^{-1}$. The same result is found if the method of §6.3(b) is employed. This value further confirms the trend in the graph of Figure (6.3) since a small negative value of $(\Delta q/\Delta\theta)$ is obtained in a region of high sunshine.

6.3(e) Linear Regression and Correlation

Ignoring the 12 points with the most positive values of $(\Delta q/\Delta\theta)$ in Figure (6.3), for the reasons given in §6.3(c), the computed correlation coefficient for the remaining 110 points is 0.60 (with 95°/o confidence that the true value lies

between 0.47 and 0.71). This is a significant correlation ($P < 0.001$) and accounts for 36°/o of the variance; a reasonable percentage, since, for any point, the error in $\bar{S}$ is likely to be about ± 10°/o and the error in Bowen ratio, as stated in §6.2, is probably greater than ± 30°/o which leads to an absolute error in $(\Delta q/\Delta\theta)$ ranging from about ± 0.2 $gkg^{-1}K^{-1}$ for points with high sunshine to ± 5 $gkg^{-1}K^{-1}$ for points with low sunshine.

The regression equation for the 110 points is

$$\frac{\Delta q}{\Delta\theta} = 0.55\,\bar{S} - 5.42, \qquad (6.11)$$

which is shown in Figure (6.3).

6.3(f) Computation of Bowen Ratios from Simple Meteorological Measurements

For any station, if the annual average of hours per day of strong sunshine is known, then Equation (6.11) may be used to determine the annual average vertical structure of the boundary layer above that station in the form of $(\Delta q/\Delta\theta)$. Then, if the annual average diurnal increase of temperature and dew-point is known, Equation (6.6) may be rearranged to give

$$\beta = \left(\frac{\gamma}{\Delta} \cdot \frac{\delta T}{\delta T_d}\right)/\left(1 + A' - A' \frac{\lambda}{c_p} \cdot \frac{\gamma}{\Delta} \cdot \frac{\Delta q}{\Delta\theta} \cdot \frac{\delta T}{\delta T_d}\right) \qquad (6.12)$$

which is the annual average Bowen ratio of the region surrounding the station.

6.4 European Bowen Ratios

It is stated in §6.2 that Budyko's maps of annual sensible and latent heat fluxes are particularly difficult to interpret

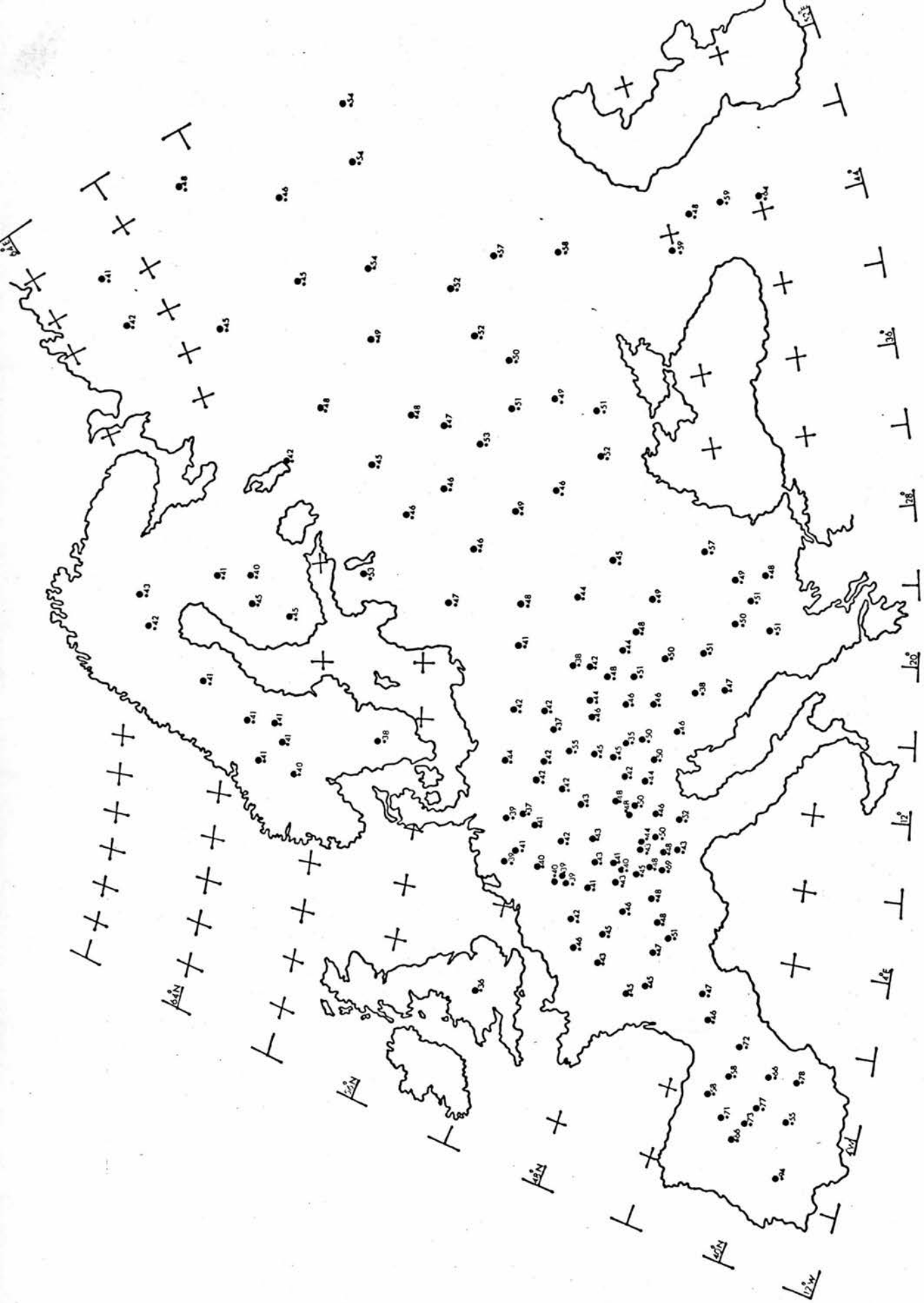

Figure (6.6) Distribution of stations in Europe, showing individual calculated values of β.

in Europe in order to obtain values of β. This is especially the case since the great geographical variations of climate and topography in Europe make interpolation a particularly hazardous procedure.

The latest edition of the previously entitled "Tables of Temperature, Relative Humidity and Precipitation for the World - Part III, Europe and the Atlantic Ocean North of 35°N", compiled by the U.K. Meteorological Office is the first to include information on annual average sunshine besides the data required to calculate δT and δT_d, and, as such, is perfectly suited for the calculation of Bowen ratios throughout Europe by means of Equations (6.11) and (6.12). The same criteria as described in § 6.2 result in 145 meteorological stations being used throughout Europe, Figure (6.6) giving their geographical locations and Appendix (2) listing them by name with position.

Figure (6.6) also gives the values of β at each of the 145 stations and isopleths of Bowen ratio at eleven stated values, ranging from 0.39 to 0.90, are presented in Figure (6.7). In the plotting of the isopleths no single station has been ignored and the consistency between adjacent stations is remarkably high over most of Europe, especially in the northern and eastern plains. Clearly, however, there is a general trend of increasing Bowen ratio from north to south and from west to east, the lowest value being 0.36 at Birmingham and the highest being 0.94 at Badajoz in Spain.

Figure (6.8) displays the corresponding values of $\alpha = \lambda E/R_n = \frac{1}{1+\beta}$ at each station and has isopleths at the eight listed values; again no station is ignored in the plotting of these isopleths.

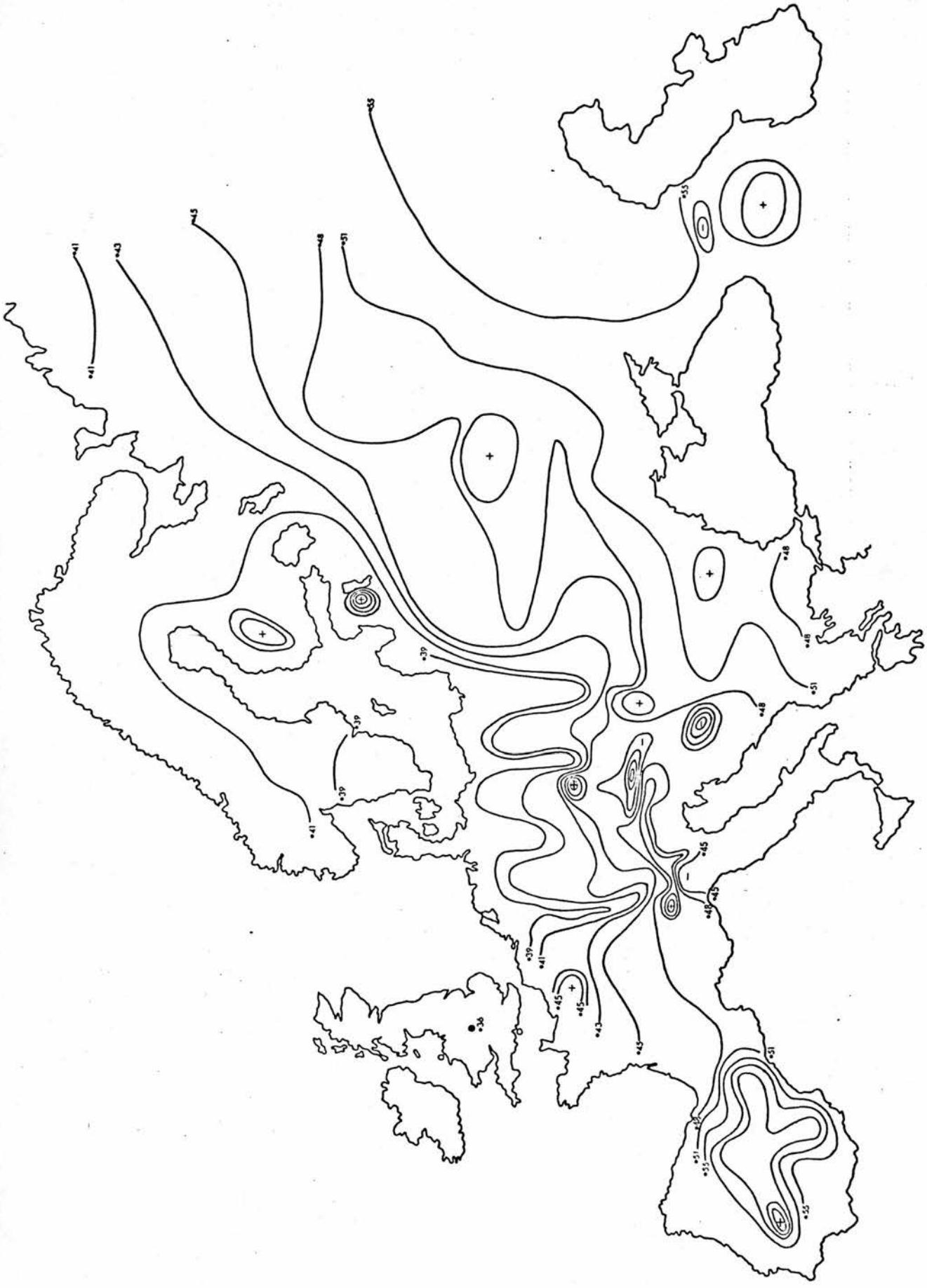

Figure (6.7) Isopleths of β in Europe (at values of 0.39, 0.41, 0.43, 0.45, 0.48, 0.51, 0.55, 0.6, 0.7, 0.8, 0.9.)

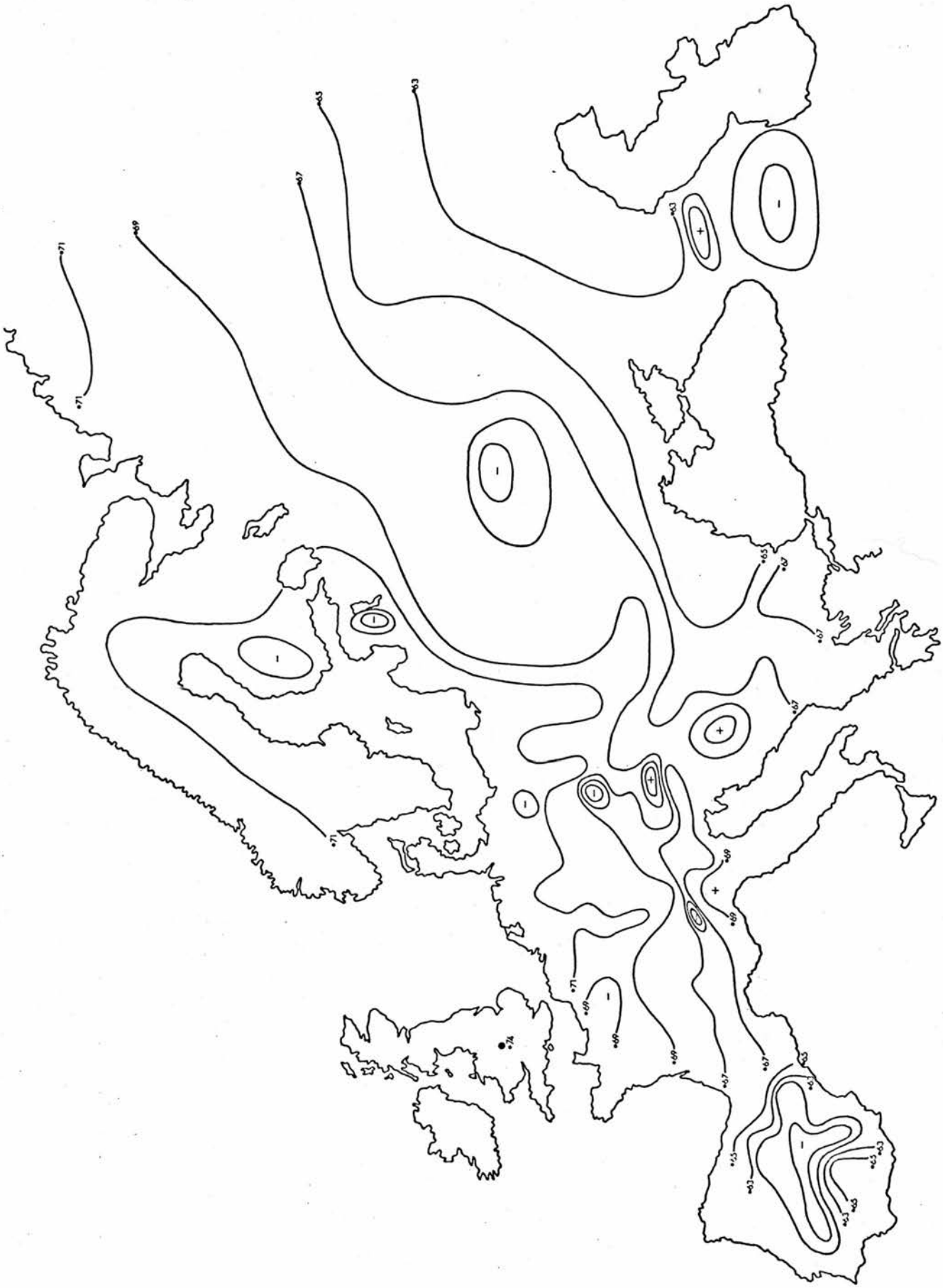

Figure (6.8) Isopleths of α in Europe (at values of 0.73, 0.71, 0.69, 0.67, 0.65, 0.63, 0.60, 0.56)

6.4(a) Physiological Control of Bowen Ratio

Equation (4.10) describes how the vapour flux from a vegetative cover is regulated by the surface (or canopy) resistance, r_s, which in turn is dependent upon the individual resistances of the stomata. In this way the vegetation exerts a physiological control over the vapour flux and hence over the value of Bowen ratio. Ludlow and Jarvis (1971) demonstrate in their Fig. 13 that, with all other variables held constant, the stomatal resistance of Sitka spruce remains unchanged for any irradiance greater than 20 Wm^{-2}. Hence, in general, during daylight hours the major influence on stomatal resistance, and consequently on canopy resistance, is soil water stress. Fig. 7 of Szeicz et al. (1973) illustrates the increase of canopy resistance with soil water stress and Davies (1972) observes that, over a period of four dry days, the canopy resistance of a bean crop increases and that α decreases from about 0.90 to 0.65 (correspondingly β increases from 0.11 to 0.54).

The build-up of soil water stress is dependent upon a number of factors such as the rate of evaporation, the amount and frequency of rainfall, the water-retentive properties of the soil and the efficiency of either surface or subterranean drainage of the soil. Additionally, regions that are not uncommonly subject to soil water stress normally only support vegetation which is suitably adapted to a xerophytic life, has an inherently high canopy resistance and therefore a low transpiration rate. Thus it is clear that the physiological control of Bowen ratio is a result of a wide variety of physiographical influences.

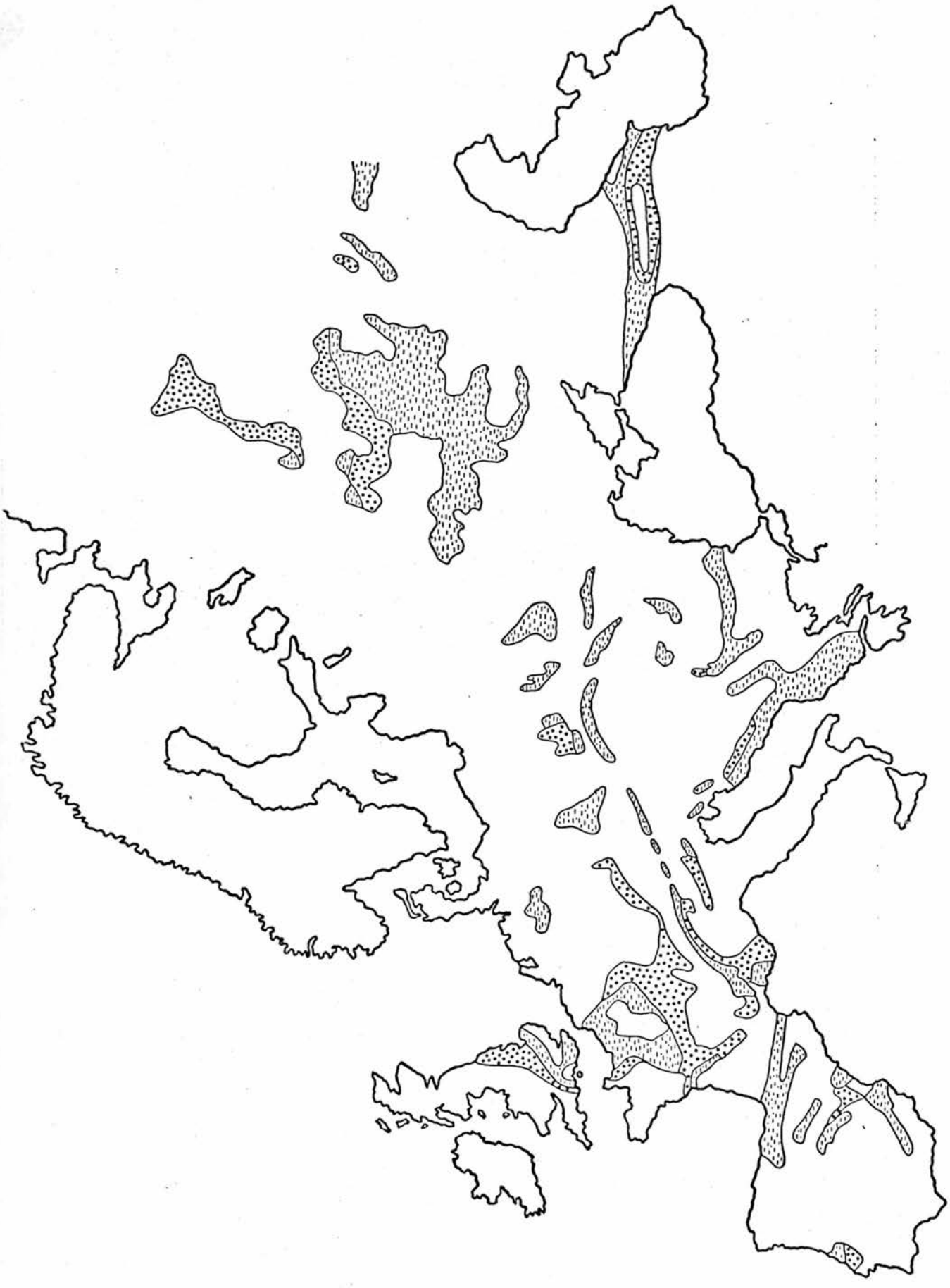

Figure (6.9) Geology of Europe

cretaceous jurassic

An overlay, identical to Figure (6.7), is placed in a pocket on the inside back cover of this thesis and may be used for comparison with Figures (6.9) to (6.13) which present, respectively, the most important features of European geology, pedology, rainfall, relief and drainage. The pedological map is by H.E. Stremme (Kiel, 1969) and is to be found in the "Atlas of the Cereal-growing Areas in Europe" (Pudoc, Centre for Agricultural Publishing and Documentation, Wageningen (1969); Elsevier Publishing Co.) and the details on the rainfall map are extracted from the "Climatic Atlas of Europe, I" (W.M.O. and Unesco (1970), printed by Cartographia, Budapest).

Detailed comparison of all these maps with Figure (6.7) is left to the reader although the following six sub-sections discuss some of the more striking features.

6.4(b) Geology and Bowen Ratio

Some of the areas of locally high Bowen ratio lie in areas of Jurassic or cretaceous bed-rock, both of which are porous and thereby provide good drainage for the overlying soil, resulting in a comparatively low annual evaporation. A particularly outstanding example is that of Praha (50° 05'N, 14° 25'E) which lies in a basin of cretaceous rock surrounded by a ring of hills. Other examples are provided by the areas around Paris (48° 49'N, 2° 29'E), Münster (51° 58'N, 7° 38'E), Zakopane (49° 17'N, 19° 58'E) and Bryansk (53° 15'N, 34° 22'E). The Alps and Caucasus are partly composed of porous rocks and also produce high values of Bowen ratio.

Key to Figure (6.10)

Code letter	Soil Type
F	tundra
P	podzols
P_o	podzols and organic soils
B	grey-brown podzdic soils
M	brown Mediterranean soils
R	red Mediterranean and reddish brown soils
T	chernozems
C	chestnut soils
S	desert soils (sierozems) and dunes
A	alluvial soils, gleys, saline and alkaline
o	organic soils
K/V	soils from limestone (K) marl and clay (V)
L	soils of mountains - lithosols, rankers, shallow rendzines (and terra rossa)
L_o	soils of mountains and organic soils

Any letter followed by 1 indicates that the soil is shallow stony.

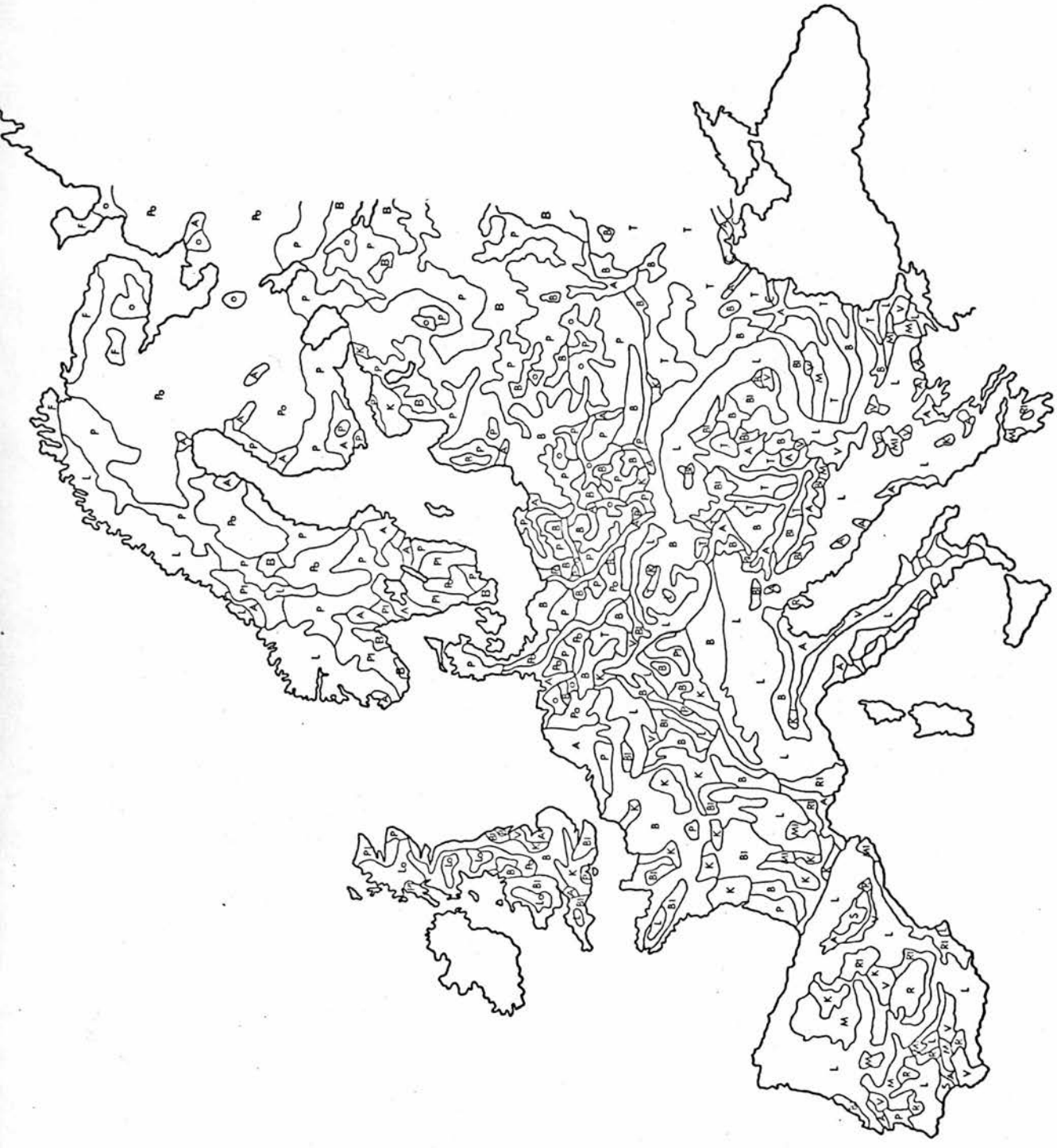

Figure (6.10) Pedology of Europe (key on previous page)

6.4(c) Pedology and Bowen Ratio

Soils which do not retain moisture and are therefore predominantly dry are those derived from limestone, the lithosols, rankers and shallow rendzines, the desert soils and any soil which is shallow and stony (on Figure (6.10) these correspond to the code letters K, L, L_o, S and any letter with subscript $_1$). Areas of these soil types are found in Central Spain, in the Alps, throughout the Carpathian Mountains, in Western Jugoslavia, in a belt running north-south from Reims (49° 18'N, 4° 02'E) to Dijon (47° 16'N, 5° 05'E), in an area between Münster (51° 58'N, 7° 38'E) and Frankfurt (50° 07'N, 8° 40'E) and also to the west of Tartu (58° 23'N, 26° 43'E). All of these, except the Carpathians, are regions in which the Bowen ratio is anomalously high. The lack of meteorological stations in the Carpathians unfortunately means that, in this area, the isopleths, as drawn in Figure (6.7), may mask a fine structure.

Soils which are comparatively damp, due to moisture retention, are those of marl, of clay and of alluvium (code letters V and A on Figure (6.10)). These may be found extensively in Holland, at Luxembourg (49° 37'N, 6° 03'E) and Echternach (49° 49'N, 6° 25'E), in the Po Valley, around Slavonski Brod (45° 09'N, 18° 01'E), between Budapest (47° 31'N, 19° 02'E) and Eisenerz (47° 33'N, 14° 53'E), and also in Southern and North-western Finland. All of these either relate to specific areas of anomalously low Bowen ratio or surround areas of anomalously high Bowen ratio.

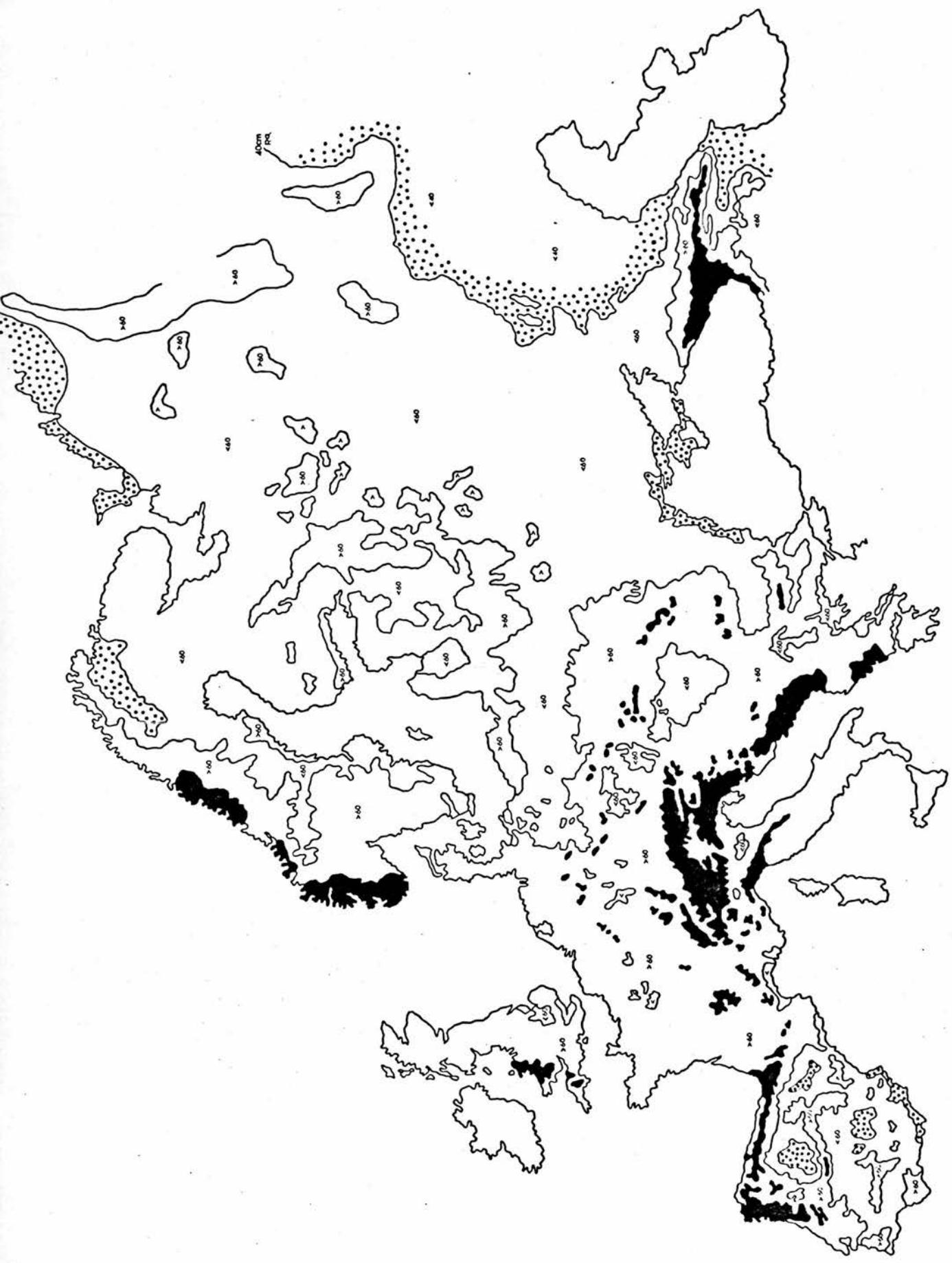
40cm
Rainfall of Europe
< 40 cm p.a.
40-60 cm p.a.
60-120 cm p.a.
> 120 cm p.a.

Figure (6.11)

Figure (6.12) Relief of Europe (contours at 200 and 1000m)

>1000m

6.4(d) Rainfall and Bowen ratio

It is rainfall that predominantly accounts for the general trend of increasing Bowen ratio towards the east and south. Indeed, in Eastern Europe, the isopleth of $\beta = 0.55$ very closely follows the isohyet of 40 cm p.a. and, in Central Spain, the distribution of a generally low rainfall appears to account largely for the distribution of generally high values of Bowen ratio. On a more localised scale, there is low rainfall to the west of Paris and there are distinct rain shadow areas around Budapest (47° 31'N, 19° 02'E), Praha (50° 05'N, 14° 25'E) and along the middle Rhine Valley, especially between Frankfurt (50° 07'N, 8° 40'E) and Echternach (49° 49'N, 6° 25'E); within all these areas are to be found anomalously high values of Bowen ratio.

On the other hand, high rainfall tends to produce a low Bowen ratio and this is exemplified by the region around Eisenerz (47° 33'N, 14° 53'E), Innsbruck (47° 16'N, 11° 24'E) and Salzburg (47° 48'N, 13° 00'E).

6.4(e) Relief and Bowen Ratio

Areas of high relief are likely to be areas of comparatively steep gradients, hence good drainage and dry soils with, perhaps, also some bare rock surfaces. The mountainous or hilly regions of Spain, Scandinavia, the High Tatras of Southern Poland, the Alps, Western Jugoslavia, the Caucasus and the Central Russian Uplands are all areas of locally high Bowen ratio.

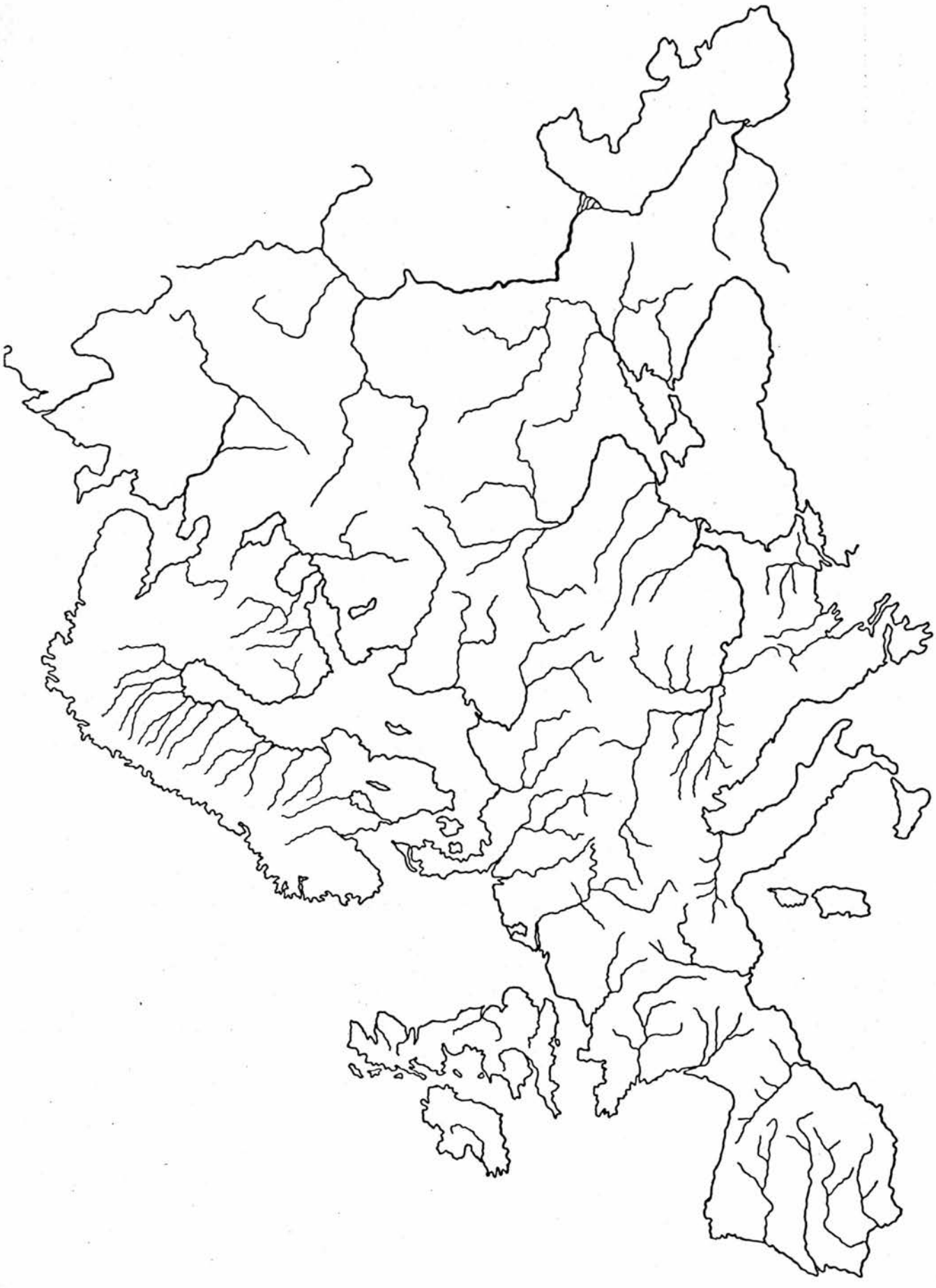

Figure (6.13) Drainage of Europe.

6.4(f) Drainage and Bowen ratio

A large river basin is usually an area within which the water table is close to the surface and gradients are generally slight, thus providing a liberal supply of ground water to vegetation, reducing the likelihood of soil water stress and resulting in a low value of Bowen ratio, This is noticeable in the Upper Rhine Valley near Basel (47° 33'N, 7° 35'E), in the valley of the River Moselle near Echternach (49° 49'N, 6° 25'E), in the Po Valley, and in the valley of the Sava, a tributary of the Danube which runs through Eastern Jugoslavia.

6.4(g) General Comments

The previous five sub-sections have dealt with each influence upon plant physiology and upon Bowen ratio separately whereas, for any particular location, the gamut of physiographic influences must be considered and each element balanced against the others in order to estimate the overall effect. For example, it may be thought that the high precipitation of the Alps would produce a low value of Bowen ratio but this appears to be outweighed by the combined effects of good drainage, of thin soil, of porous rock and of lack of vegetation, all of which tend to increase the Bowen ratio. Similarly, Frankfurt (50° 07'N, 8° 40'E) lies in the Main Valley and also in a rain shadow area which is sheltered by the hills to the west of the Rhine. Apparently this latter effect prevails in giving it a Bowen ratio higher than that found in the higher rainfall and clay-soil region of Clervaux (50° 03'N, 6° 01'E), Luxembourg (49° 37'N, 6° 03'E) and Echternach (49° 49'N, 6° 25'E)

which are on or near the River Moselle just to the west of the Rhine.

The physiographic influences upon Bowen ratio are of such a fine scale, especially in Western and Southern Europe, that it is perhaps surprising that good agreement is often found between the values determined at and assigned to the widely separated meteorological stations of Figure (6.6) and one or more of the parameters mapped in Figures (6.9) to (6.13). This suggests that a value of β assigned to a particular station is, in fact, representative of a surrounding area which is dimensionally of roughly the same size as the areas of continuity of geology, pedology, rainfall, relief and drainage as mapped in Figures (6.9) to (6.13).

6.5 Application to Thetford Forest Data

Chapter 3 demonstrates that, despite a vapour flux from the forest, the humidity of the air above the trees may drop during the day due to the predominant influence of the down-mixing from above of dry air which is supplied by entrainment across an inversion. Figure (6.3) shows that this effect is enhanced in generally more cloudy or cyclonic weather and that the humidity may be expected to drop even more under these circumstances. It is not surprising, therefore, that, of the 40 days at Thetford Forest plotted in Figure (1.3), no less than 27 exhibit a decrease in specific humidity between dawn and 13.30 GMT.

Over the 40 days, the average values of δT and of δq are + 6.18^{o}C and - 0.168 gkg^{-1}, respectively, while the

average number of hours per day of strong sunshine at the nearby meteorological station of Honington is 4.91 hr day^{-1}. Assuming that these days provide a large enough sample for the net effect of synoptic-scale advection to be negligible and for Equations (6.11) and (6.12) to be applicable, the calculated value of the average Bowen ratio, from Thetford Forest data, is 0.63. The average of all the twenty-minute-average measured values of Bowen ratio between dawn and 13.30 GMT on each of the 40 days is 0.90. (The corresponding values of α are 0.61 and 0.53 which implies a difference between them of 15°/o.)

The difference between the calculated value of β and the measured value is in the expected sense since the average values of δT and of δq over Thetford Forest cannot be controlled entirely by the forest itself but must be influenced to a certain extent by advection from the surrounding arable land for which β would be much less than 0.9.

CHAPTER 7

CONCLUSIONS

The initial intention of this thesis was to explain the unexpected behaviour during the day of humidity over Thetford Forest by constructing a simple physical model of the forest/atmosphere system. As Holmes and Dingle (1965) recommend, the model is designed purposely to avoid numerical methods and excessive refinement. In this way, demands on time and on data are reduced, the analysis is simplified and any real relationships are less likely to be obscured.

The simple model of humidity variation under anti-cyclonic conditions presented here is expedited by the formulation of an entirely new theory of entrainment. Some of the assumptions basic to this theory are contrary to contemporary thought, but the test employed in §3.1(a) provides an encouraging degree of support. Undoubtedly, however, further experimentation is essential to remove any doubt. Preferably such work would comprise the accurate determination of the diurnal development of the inversion layer on several strongly convective days. Since the inversion layer is convoluted and is quickly changing in both shape and position, the task is formidable, but may be made tractable by using several Cardington-style tethered balloons in conjunction and resorting to considerable spatial and temporal averaging.

The simple model, constructed in Chapter 4, predicts diurnal humidity variation under anti-cyclonic conditions and is straight-forward enough to be used by anyone without the aid of calculators. The seven test-cases of § 4.3(c)

are, unfortunately, bedevilled by synoptic scale advection and poor data on inversion structure. However, the model appears to be capable of accurate predictions under suitable conditions and it would be valuable to further test the predictive equations in relatively unchanging, strongly anti-cyclonic conditions and at an inland location which is surrounded by several radio-sonde stations which, preferably, provide ascents more often than at mid-night and mid-day.

The model of Chapter 4 demands a knowledge of the likely maximum net radiation during the day and this requirement instigated the development of the theory of Chapter 5. It has long been a major problem in general day-to-day forecasting to predict whether or not cumulus cloud will develop and to what extent it will grow. Hopefully, the theory and predictive parameter of Chapter 4 may become a useful forecasting tool but, again, further rigorous testing is required. An interesting experiment would be to measure, on a standard horizontal flight path, the average radius of rising convective plumes under varying extents of cumulus cloud cover and to determine if, as postulated, the radius decreases as the cloud cover increases. Although the parameter D is statistically tested in §5.3(c) for its effectiveness in distinguishing between days of different cloud cover, it still remains to be seen how valuable it is, in a statistical sense, as a tool for the prediction of the number of oktas of cloud cover at any time of day.

Finally the diurnal humidity variations in non-anti-cyclonic weather conditions are treated climatically in Chapter 6. The theory of this chapter also raises several

interesting points which may be investigated in greater detail. It would be useful, from the radio-sonde records of several diverse locations in the world, to determine the annual average values of $(\Delta q/\Delta\theta)$, using some criterion for its evaluation such as that of § 6.3(b), and to find whether or not these values are related to the annual average hours per day of sunshine at those locations, as suggested by Figure (6.3). Additionally, it would be valuable to compare values of Bowen ratio calculated by Equations (6.11) and (6.12) with those determined by the methods of Budyko and others, and, further, to construct a map of Bowen ratios for a much smaller region than Europe and to make a far more detailed comparison of it with the physiographical influences on plant physiology.

Rodda (1971) emphasises the importance to the modern world of monitoring, understanding, predicting and controlling the movement of water through the environment and fundamental to this movement is the controlling influence of evaporation from ground-surface and vegetation. The rate of evaporation depends not only upon physiological factors which affect the Bowen ratio but also upon meteorological factors which affect the ambient atmospheric humidity. Hopefully, this thesis has made a contribution towards the understanding of the vegetation/planetary boundary layer system which will help in the eventual improvement of our hydrological techniques. On the other hand, the preceding remarks make it clear that much of the work presented here should be regarded as a starting point and requires further experimentation and verification.

APPENDIX (1)

AFRICA

ADRAR (27° 52'N, 0° 17'W)
EL GOLEA (30° 35'N, 2° 53'E)
FORT FLATTERS (28° 06'N, 6° 42'E)
TIN-ZAOUATENE (19° 57'N, 2° 55'E)
CUFRA (24° 12'N, 23° 21'E)
SEBHA (27° 01'N, 14° 26'E)
TIMBUKTU (16° 46'N, 3° 01'W)
NIAMEY (13° 31'N, 2° 06'E)
FAYA (18° 00'N, 19° 10'E)
MAROUA (10° 36'N, 14° 19'E)
MITSIG (0° 47'N, 11° 34'E)
BERBERATI (4° 15'N, 15° 48'E)
OUESSO (1° 37'N, 16° 04'E)
RAGA (8° 28'N, 25° 41'E)
ENUGU (6° 27'N, 7° 29'E),
LEOPOLDVILLE (4° 20'S, 15° 18'E)
BARUMBA (1° 15'N, 23° 29'E)
KOUROUSSA (10° 39'N, 9° 53'W)
LULUABOURG (5° 43'S, 22° 25'E)
MAUN (19° 59'S, 23° 25'E)
BALOVALE (13° 34'S, 23° 06'E)
KASEMPA (13° 27'S, 25° 50'E)
TABORA (5° 02'S, 32° 49'E)
MAFEKING (25° 51'S, 25° 39'E)

ASIA

SURGUT (61° 17'N, 73° 20'E)
OMSK (54° 58'N, 73° 20'E)
SEMI-PALATINSK (50° 24'N, 80° 13'E)
KRASNOYARSK (56° 01'N, 92° 52'E)
VILYUYSK (63° 45'N, 121° 35'E)
TOMSK (56° 30'N, 84° 58'E)
TURUKHANSK (65° 55'N, 87° 38'E)
SREDNE-KOLYMSK (65° 55'N, 87° 38'E)
KHABOROUSK (48° 28'N, 135° 03'E)
HARBIN (45° 43'N, 126° 40'E)
CH'ANG-CH'UN (43° 55'N, 125° 18'E)
MUKDEN (41° 48'N, 123° 23'E)
HENG CHOW (26° 56'N, 112° 25'E)
HANKOW (30° 35'N, 114° 17'E)
NANKING (32° 03'N, 118° 47'E)
WUCHOW (23° 38'N, 111° 17'E)
NAKORN RAJASIMA (14° 58'N, 102° 07'E)
CHIENGMAI (18° 47'N, 98° 59'E)
ALMA-ATA (43° 16'N, 76° 53'E)
CH'ENG-TU (30° 41'N, 104°, 12'E)
RUTBA (33° 02'N, 40° 17'E)

APPENDIX (1) (Contd.)

AFRICA (Contd.)

POFADDER (29° 08'S, 19° 23'E)
PIETERSBURG (23° 56'S, 29° 29'E)
MPIKA (11° 51'S, 31° 27'E)
MWINILUNGA (11° 45'S, 24° 26'E)

EUROPE

CIUDAD REAL (38° 59'N, 3° 55'W)
MADRID (40° 25'N, 3° 41'W)
SALAMANCA (40° 58'N, 5° 40'W)
LIMOGES (45° 52'N, 1° 17'E)
ORLEANS (47° 56'N, 1° 53'E)
BELFORT (47° 38'N, 6° 52'E)
BERLIN (52° 27'N, 13° 18'E)
STUTTGART (48° 47'N, 9° 10'E)
PRAHA (50° 05'N, 14° 25'E)
POZNAN (52° 25'N, 16° 56'E)
BREST (52° 05'N, 23° 40'E)
L'VOV (49° 50'N, 24° 01'E)
KIROVOGRAD (48° 31'N, 32° 17'E)
KIYEV (50° 27'N, 30° 30'E)
MINSK (53° 54'N, 27° 33'E)

AUSTRALIA

WAVE HILL (17° 30'S, 130° 57'E)
ALICE SPRINGS (23° 38'S, 133° 35'E)

N. AMERICA

BAKER LAKE (64° 18'N, 96° 05'W)
TROUT LAKE (53° 50'N, 89° 52'W)
NITCHEQUON (53° 12'N, 70° 35'W)
GILLAM (56° 21'N, 94° 46'W)
THE PAS (53° 49'N, 101° 15'W)
KAPUSKASING (49° 25'N, 82° 25'W)
WINNIPEG (49° 54'N, 97° 14'W)
OTTAWA (45° 20'N, 75° 41'W)
ELLENDALE (46° 00'N, 98° 31'W)
COLUMBUS (39° 58'N, 83° 00'W)
DES MOINES (41° 35'N, 93° 37'W)
DODGE CITY (37° 46'N, 99° 58'W)
KANSAS CITY (39° 07'N, 94° 35'W)
INDIANAPOLIS (39° 46'N, 86° 10'W)
ASHEVILLE (35° 36'N, 82° 32'W)

APPENDIX (1) (Contd.)

EUROPE (Contd.)

KHAR'KOV (50° 00'N, 36°14'E)
KALUGA (54° 31'N, 36° 16'E)
STALINGRAD (48° 42'N, 44° 31'E)
PENZA (53° 11'N, 45° 01'E)
KIROV (58° 36'N, 49° 41'E)
UFY (54° 43'N, 55° 56'E)
VOLOGDA (59° 14'N, 39° 53'E)
UST' SHCHUGOR (64° 16'N, 57° 34'E)
ZLATOUST (55° 10'N, 59° 41'E)
KAZAN (55° 47'N, 49° 08'E)
OSTERSUND (63° 11'N, 14° 39'E)
STENSELE (65° 04'N, 17° 10'E)

S. AMERICA

CORDOBA (31° 22'S, 64° 15'W)
CORRIENTES (27° 28'S, 58° 50'W)
PARANA (31° 44'S, 60° 31'W)
ROSARIO (32° 58'S, 60° 40'W)
VICTORICA (36° 13'S, 65° 26'W)
CONCEPTION (16° 15'S, 62° 03'W)
BARRA DO CORDA (5° 35'S, 45° 28'W)
CACERES (16° 04's, 57° 41'W)
CATALAO (18° 10'S, 47° 52'W)
CORUMBA (19° 00'S, 57° 39'W)

N. AMERICA (Contd.)

ATLANTA (33° 45'N, 84° 23'W)
OKLAHOMA (35° 29'N, 97° 32'W)
VICKSBURG (32° 22'N, 90° 53'W)
LITTLE ROCK (34° 45'N, 92° 16'W)
WILLISTON (48° 09'N, 103° 35'W)
REGINA (50° 26'N, 104° 39'W)
REGINA (50° 26'N, 104° 39'W)
SIOUX LOOKOUT (50° 07'N, 91° 54'W)
SIOUX CITY (42° 23'N, 96° 23'W)
LOUISVILLE (38° 15'N, 85° 45'W)

S. AMERICA (Contd.)

GUARAPUAVA (25° 16'S, 51° 30'W)
MANAUS (3° 08'S, 60° 01'W)
PARANA (12° 26'S, 48° 06'W)
SANTAREM (2° 30'S, 54° 42'W)
UAUPES (0° 08'S, 67° 05'W)
MISION INGLESA (23° 23'S, 58° 25'W)
TEOFILO OTONI(17° 45'S, 41° 26'W)
SANTA ELENA (4° 36'N, 61° 07'W)
SANTIAGO DEL ESTERO (27° 46'S, 64° 18'W)
CONCEICAO DO ARAGUAIA (8° 15'S, 49° 12'W)

APPENDIX (2)

LILLEHAMMER (61° 06'N, 10° 29'E)
OSTERSUND (63° 11'N, 14° 39'E)
STENSELE (65° 04'N, 17° 10'E)
UST' SHCHUGOR (64° 16'N, 57° 34'E)
YARENSK (62° 10'N, 49° 05'E)
BIRMINGHAM (52° 29'N, 1° 56'W)
LE PUY (45° 03'N, 3° 54'E)
LYON (45° 42'N, 4° 47'E)
PARIS (48° 49'N, 2° 29'E)
REIMS (49° 18'N, 4° 02'E)
BELFORT (47° 38'N, 6° 52'E)
BERN (46° 57'N, 7° 26'E)
BRNO (49° 11'N, 16° 33'E)
BUDAPEST (47° 31'N, 19° 02'E)
DIJON (47° 16'N, 5° 05'E)
ECHTERNACH (49° 49'N, 6° 25'E)
FELDKIRCH (47° 15'N, 9° 35'E)
FREIBURG (47° 59'N, 7° 51'E)
GRAZ (47° 04'N, 15° 28'E)
HOF (50° 19'N, 11° 55'E)
KASSEL (51° 19'N, 9° 29'E)
KLAGENFURT (46° 38'N, 14° 19'E)
KRAKOW (50° 04'N, 19° 57'E)
ROROS (62° 34'N, 11° 23'E)
SARNA (61° 41'N, 13° 07'E)
TAMPERE (61° 30'N, 23° 46'E)
UST'TSIL'MA (65° 27'N, 52° 10'E)
AUXERRE (47° 49'N, 3° 34'E)
CLERMONT-FERRAND (45° 46'N, 3° 05'E)
LIMOGES (45° 52'N, 1° 17'E)
ORLEANS (47° 56'N, 1° 53'E)
POITIERS (46° 35'N, 0° 21'E)
BASEL (47° 33'N, 7° 35'E)
BERLIN (52° 27'N, 13° 18'E)
BOLZANO (46° 28'N, 11° 19'E)
BROCKEN (51° 48'N, 10° 37'E)
CLERVAUX (50° 03'N, 6° 01'E)
DRESDEN (51° 01'N, 13° 46'E)
EISENERZ (47° 33'N, 14° 53'E)
FRANKFURT (50° 07'N, 8° 40'E)
GENEVE (46° 12'N, 6° 09'E)
HANOVER (52° 24'N, 9° 40'E)
INNSBRUCK (47° 16'N, 11° 24'E)
KESZTHELY (46° 46'N, 17° 14'E)
KOLN (50° 56'N, 6° 57'E)
LEIPZIG (51° 18'N, 12° 23'E)

LINZ (48° 18'N, 14° 16'E)
LUGANO (46° 00'N, 8° 57'E)
MILANO (45° 27'N, 9° 17'E)
NANCY (48° 42'N, 6° 14'E)
POZNAN (52° 25'N, 16° 56'E)
PREROV (49° 27'N, 17° 27'E)
ST. MORITZ (46° 33'N, 9° 53'E)
SNIEZKA (50° 44'N, 15° 44'E)
STRASBOURG (48° 35'N, 7° 46'E)
VERONA (45° 24'N, 10° 53'E)
WROCLAW (51° 07'N, 17° 05'E)
ZAKOPANE (49° 17'N, 19° 58'E)
ZUGSPITZE (47° 25'N, 10° 59'E)
BREST (52° 05'N, 23° 40'E)
CLUJ (46° 47'N, 23° 40'E)
DEBRECEN (47° 36'N, 21° 39'E)
KAUNUS (54° 54'N, 23° 53'E)
KIYEV (50° 27'N, 30° 30'E)
MINSK (53° 54'N, 27° 33'E)
SZEGED (46° 15'N, 20° 09'E)
VELIKIYE-LUKI (56° 21'N, 30° 31'E)
WARSZAWA (52° 13'N, 21° 02'E)
GOR'KIY (56° 20'N, 44° 00'E)
KAZAN (55° 47'N, 49° 08'E)
KHAR'KOV (50° 00'N, 36° 14'E)
MUNCHEN (48° 09'N, 11° 34'E)
LITVINOVICE (48° 58'N, 14° 28'E)
LUXEMBOURG (49° 37'N, 6° 03'E)
MOSONMAGYAROVAR (47° 53'N, 17° 16'E)
NURNBERG (49° 27'N, 11° 03'E)
PRAHA (50° 05'N, 14° 25'E)
SALZBURG (47° 48'N, 13° 00' E)
SLAVONSKI BROD (45° 09'N, 18° 01'E)
SONNBLICK (47° 03'N, 12° 57'E)
STUTTGART (48° 47'N, 9° 10'E)
WINTERSWIJK (51° 58'N, 6° 43'E)
ZAGREB (45° 49'N, 15° 58'E)
ZERMATT (46° 01'N, 7° 45'E)
ZVOLEN (48° 35'N, 19° 08'E)
BRYANSK (53° 15'N, 34° 22'E)
CHERNOVTSY (48° 17'N, 25° 56'E)
EGER (47° 53'N, 20° 23'E)
KIROVOGRAD (48° 31'N, 32° 17'E)
L'VOV (49° 50'N, 24° 01'E)
SMOLENSK (54° 47'N, 32° 04'E)
VASILEVICE (52° 16'N, 29° 48'E)
VISHNIY VOLOCHEK (57° 35'N, 34° 34'E)
BOGOLOVSK (59° 45'N, 59° 01'E)
KALUGA (54° 31'N, 36° 16'E)
KIROV (58° 36'N, 49° 41'E)
KURSK (51° 45'N, 36° 12'E)
MUNSTER, (51° 58'N, 7° 38°E)

MOSKVA (55° 46'N, 37° 40'E)
PERM (58° 01'N, 56° 16'E)
STALINGRAD (48° 42'N, 44° 31'E)
TAMBOV (52° 44'N, 41° 28'E)
VOLOGDA (59° 14'N, 39° 53'E)
ZLATOUST (55° 10'N, 59° 41'E)
AVILA (40° 39'N, 4° 42'W)
DNEPROPETROVSK (48° 27'N, 35° 04'E)
BAGNERES DE BIGORRE (43° 04'N, 0° 09'E)
CIUDAD REAL (38° 59'N, 3° 55'W)
SALAMANCA (40° 58'N, 5° 40'W)
TOULOUSE (43° 33'N, 1° 23'E)
ZARAGOZA (41° 38'N, 0° 53'W)
BEOGRAD (44° 48'N, 20° 28'E)
NIS (43° 20'N, 21° 54'E)
PLOVDIV (42° 09'N, 24° 45'E)
SOFIYA (42° 42'N, 23° 20'E)
TBILISI (41° 43'N, 44° 48'E)
AHTARI (62° 33'N, 24° 09'E)
KUOPIO (62° 54'N, 27° 41'E)
SVEG (62° 02'N, 14° 25'E)
JUNGFRAUJOCH (46° 33'N, 7° 59'E)
JONKOPING (57° 46'N, 14° 11'E)
VYTEGRA (61° 00'N, 36° 27'E)
PENZA (53° 11'N, 45° 01'E)
SARATOV (51° 32'N, 46° 03'E)
STAVROPOL (45° 02'N, 41° 58'E)
UFY (54° 43'N, 55° 56'E)
VORONEZH (51° 40'N, 39° 13'E)
ALBACETE (39° 00'N, 1° 49'W)
BADAJOZ (38° 54'N, 6° 58'W)
BURGOS (42° 20'N, 3° 42'W)
CUENCA (40° 05'N, 2° 08'W)
MADRID (40° 25'N, 3° 41'W)
SORIA (41° 46'N, 2° 29'W)
VALLADOLID (41° 38'N, 4° 44'W)
SARAJEVO (43° 52'N, 18° 26'E)
BUCURESTI (44° 25'N, 26° 06'E)
PLEVEN (43° 25'N, 24° 37'E)
SKOPJE (41° 59'N, 21° 28'E)
ORDZHONIKIDZE (43° 02'N, 44° 41'E)
YERIVAN (40° 10'N, 44° 30'E)
KAJAANI (64° 17'N, 27° 41'E)
SODANKYLA (67° 22'N, 26° 39'E)
PAJALA (67° 12'N, 23° 25'E)
SANTIS (47° 15'N, 9° 20'E)
TARTU (58° 23'N, 26° 43'E)

REFERENCES

1. Ball, F.K. (1960) "Control of inversion height by surface heating", Quart. J.R. Met. Soc., 86, p. 483.

2. Best, A.C.; Knighting, E; Pedlow, R.H. and Stormonth, K. (1952) "Temperature and humidity gradients in the first 100m over S.E. England", Geophys. Mem., No. 89, (Met. Off.).

3. Betts, A.K. (1973) "Non-precipitating cumulus convection and its parameterization", Quart. J.R. Met. Soc., 99, p. 178.

4. Bilham, E.G. (1938) "The Climate of the British Isles", Macmillan & Co. Ltd., London.

5. Budyko, M.I. (1958) "The Heat Balance of the Earth's Surface", Dept. of Commerce (Weather Bureau), U.S.A.

6. Carson, D.J. (1973) "The development of a dry inversion-capped convectively unstable boundary layer", Quart. J.R. Met. Soc., 99, p. 450.

7. Carson, D.J. and Smith, F.B. (1973) "A thermodynamic model for the development of a convectively unstable boundary layer", Turb. and Diff. Note, 34, (Met. Off.)

8. Cattle, H. and Weston, K.J. (1975) "Budget studies of heat flux profiles in the convective boundary layer over land", Quart. J.R. Met. Soc., 101, p.353.

9. Clarke, R.H. (1970) "Observational studies in the atmospheric boundary layer", Quart. J.R. Met. Soc., 96, p. 91.

10. Cornford, S.G. (1966) "Strato-cumulus, a review of some physical aspects", Met. Mag., 95, p. 292.

11. Davies, J.A. (1972) "Actual, potential and equilibrium evaporation for a beanfield in S. Ontario", Agric. Met., 10, p. 331.

REFERENCES (Contd.)

12. Deardorff, J.W. (1974a) "Three-dimensional numerical study of the height and mean structure of a heated planetary boundary layer", Boun. Layer Met., 7, p.81.

13. Deardorff, J.W. (1974b) "Three-dimensional study of turbulence", Boun. Layer Met., 7, p. 199.

14. Elliot, W.P. (1964) "The height variation of vertical heat flux near the ground", Quart. J.R. Met. Soc., 90, p. 260.

15. Geiger, R. (1966) "The Climate near the ground", Harvard Univ. Press, Cambridge, Mass.

16. Green, F.W.H. (1956) "Another remarkable low humidity", Weather, 11, p. 300.

17. Green, F.H.W. (1965) "The incidence of low relative humidity in the British Isles", Met. Mag., 94, p.81.

18. Green, F.H.W.; Watson, A. and Piccozi, N. (1964) "Very Low humidity in the East of Scotland in December 1962", Met. Mag., 93, p. 225.

19. Hawke, E.L. (1944) "The incidence of extremely low relative humidity in Southern England", Quart. J.R. Met. Soc., 70, p. 274.

20. Hawke, E.L. (1946) "A near approach to zero relative humidity at ground-level in England", Quart. J.R. Met. Soc., 72, p. 173.

21. Helliwell, N.C. and Mackenzie, J.K. (1957) "Observations of humidity, temperature and wind at Idris 23rd May - 2nd June, 1956" Met. Res. Paper, 1024, (Met. Off.).

22. Holmes, R.M. and Dingle, A. Nelson (1965) "The relationship between the macro- and micro-climate", Agric. Met., 2, p. 127.

23. James, D.G. (1957) "Observations from aircraft of temperatures and humidities near stratocumulus cloud", Met. Res. Paper, 1055, (Met. Off.).

REFERENCES (Contd.)

24. Johnston, D.W. (1958) "The estimation of maximum day temperature from the tephigram", Met. Mag. 87, p. 265.

25. Kaimal, J.C. (1974) "Translation speed of convective plumes in the atmospheric surface layer", Quart. J.R. Met. Soc., 100, p. 46.

26. Lenschow, D.H. and Johnson, W.B. (1968) "Concurrent airplane and balloon measurements of atmospheric boundary-layer structure over a forest", J. App. Met., 7, p. 79.

27. Lilly, D.K. (1968) "Models of cloud-topped mixed layers under a strong inversion", Quart. J.R. Met. Soc., 94, p. 292.

28. Ludlow, M.M. and Jarvis, P.G. (1971) "Photosynthesis in Sitka Spruce, I. General characteristics", J. App. Ecol. 8, p. 925.

29. Lumb, F.E. (1964) "Cloud and solar radiation at the sea surface", Quart. J.R. Met. Soc., 90, p. 43.

30. McCarthy, J. (1974) "Field verification of the relationship between entrainment rate and cumulus cloud diameter", J. Atmos. Sci., 31, p. 1028.

31. McNaughton, K.G. and Black, T.A. (1973) "A study of evapotranspiration from a Douglas Fir forest using the energy balance approach", Water Res. Res., 9, p. 1579.

32. Monteith, J.L. (1965) "Evaporation and environment", Symp. Soc. expl. Biol., xix, p. 205.

33. Monteith, J.L. (1973) "Principles of Environmental Physics", Edward Arnold (Publishers) Ltd., London.

34. Nixon, P.R. and Lawless, G.P. (1968) "Advective influences on the reduction of evapotranspiration in a coastal environment", Water Res. Res., 4, p. 39.

REFERENCES (Contd.)

35. Pasquill, F. (1972) "Some aspects of boundary layer description", Quart. J.R. Met. Soc., 98, p. 469.

36. Rayment, R. and Readings, C.J. (1974) "A case study of the structure and energetics of an inversion", Quart. J.R. Met. Soc., 100, p. 221.

37. Read, R.S. (1934) "Exceptionally dry air, July 10th 1934", Met. Mag., 69, p. 181.

38. Readings, C.J.; Golton, E. and Browning, K.A. (1973) "Fine-scale structure and mixing within an inversion", Boun. Layer Met., 4, p. 275.

39. Richardson, L.F. (1920) "Rate of production of eddy-energy by convection", Proc. Roy. Soc., A, 97, p.373.

40. Rider, N.E. and Robinson, G.D. (1951) "A study of the transfer of heat and water vapour above a surface of short grass", Quart. J.R. Met. Soc., 77, p. 375.

41. Rodda, J.C. (1971) "Why hydrology?", Nature, 232, p. 301.

42. Scorer, R.S. and Ludlam, F.H. (1953) "Bubble theory of penetrative convection", Quart. J.R. Met. Soc., 79, p. 94.

43. Sellers, W.D. (1965) "Physical Climatology", The Univ. of Chicago Press, Chicago and London.

44. Smith. F.B.; Carson, D.J. and Oliver, H.R. (1972) "Mean wind-direction shear through a forest canopy", Boun. Layer Met., 3, p. 178.

45. Smith, M.F. (1974) "A short note on a sea-breeze crossing E. Anglia", Met. Mag., 103, p. 115.

46. Smith, R.C. (1958) "Abnormally low humidity in Scotland", Met. Mag., 87, p. 35.

47. Stewart, J.B. and Thom, A.S. (1973) "Energy budgets in pine forest", Quart. J.R. Met. Soc., 99, p. 154.

48. Szeicz, G; Van Bavel, C.H.M. and Takami, S. (1973) "Stomatal factor in the water use and dry matter matter production by Sorghum", Agric. Met., 12, p. 361.

REFERENCES (Contd.)

49. Tennekes, H. (1973) "A model for the dynamics of the inversion above a convective boundary layer", J. Atmos. Sci., 30, p. 558.

50. Tunnell, G.A. (1958) "World distribution of atmospheric water vapour pressure", Geophys. Mem., No. 100, (Met. Off.).

51. Turner, J.S. (1963) "The motion of buoyant elements in turbulent surroundings", J. Fluid Mech., 16, p.1.

52. Vandenplas, A. (1947) "La température au Congo Belge", Institut Royal Météorologique de Belgique Memoires, Vol. XXIV.

53. Vandenplas, A. (1949) "L'humidité atmosphérique et l'évaporation au Congo Belge", Publication de la direction de l'Agriculture, de l'Elevage et de la Colonisation, Bruxelles.

54. Warner, J. (1963) "Observations relating to theoretical models of a thermal", J. Atmos. Sci., 20, p. 546.

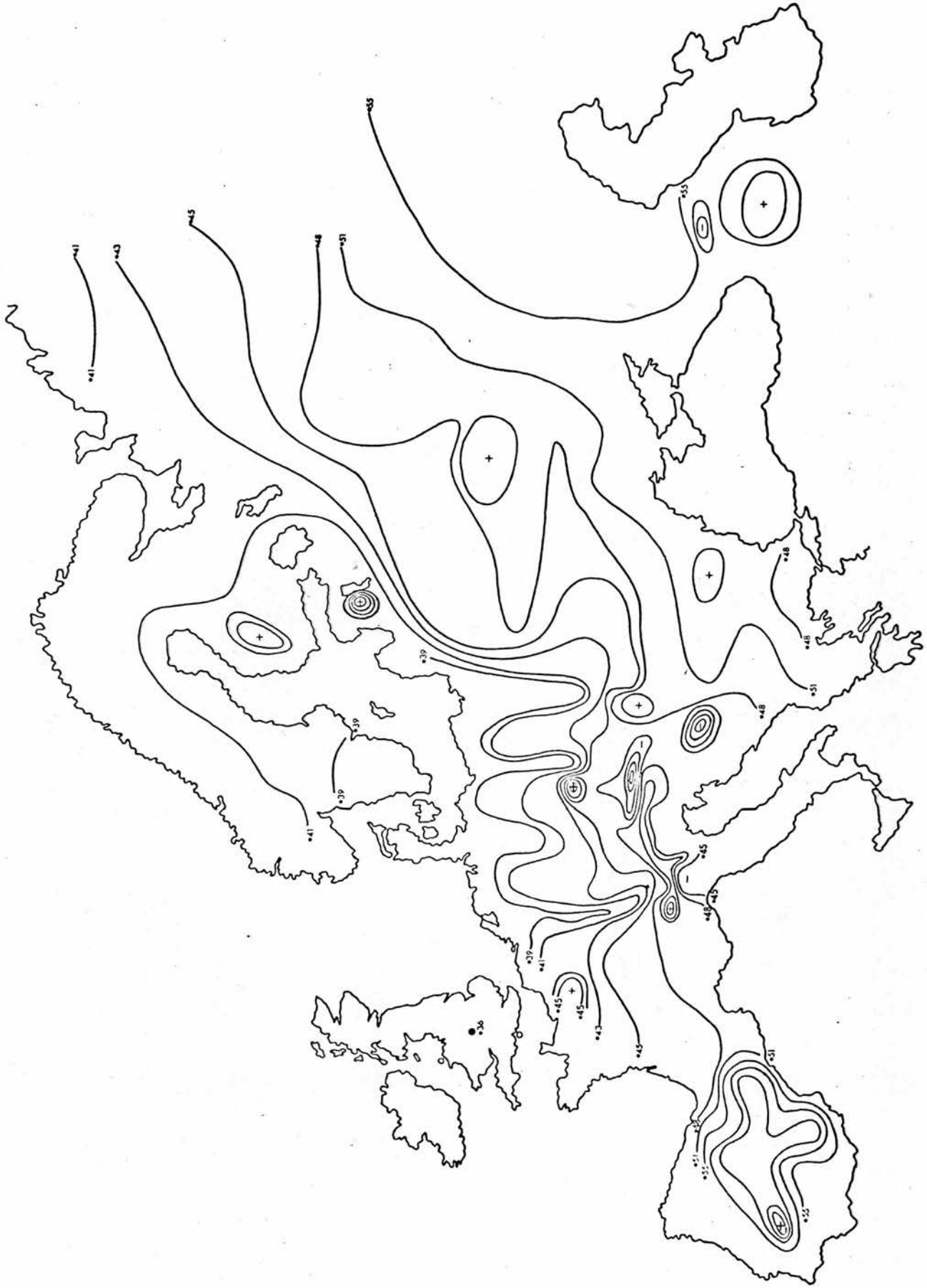

Figure (6.7) Isopleths of β in Europe (at values of 0.39, 0.41, 0.43, 0.45, 0.48, 0.51, 0.55, 0.6, 0.7, 0.8, 0.9.)